The Shifted Boundary Method:
A Framework for Immersed Computational Mechanics

Guglielmo Scovazzi
Civil & Environmental Engineering Department
Duke University (USA)

Seminar: FEM Seminar Series

Lawrence Livermore National Laboratory

Thursday, January 20, 2021

Duke UNIVERSITY

Acknowledgments

Collaborators on the work presented here (present and past):

Alex Main (former Postdoc, now Research Scientist at Ansys)

Ting Song (former Ph.D. now Research Scientist at ExxonMobil)

Oriol Colomés (former Postdoc, now Faculty at TU Delft in The Netherlands)

Léo Nouveau (former Postdoc, now Faculty at U. Rennes in France)

Nabil Atallah (former Ph.D. student, now Postdoc at LLNL)

Kangan Li (Ph.D. student, just graduated, *looking for jobs*)

Sponsors:

U.S. DEPARTMENT OF ENERGY | Office of Science

Lawrence Livermore National Laboratory

Science to Shape the Future of the Army — Army Research Office — 1951

Office of Naval Research — USN — ONR — Science & Technology

ExxonMobil Upstream Research

Motivation I

Complex geometry is still a key challenge in engineering simulations

- Engineering designs are often characterized by geometric complexity
- The merging of topology optimization and advanced manufacturing (e.g., *additive manufacturing*) may exacerbate this trend

Structural joint (welded)

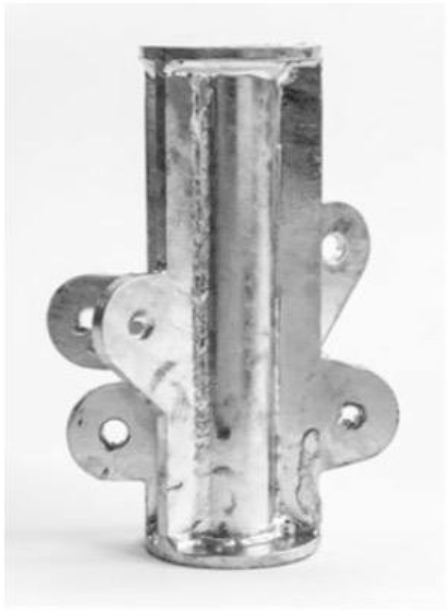

Structural joint (3D-printed)

Geometric model of a vascular stent

Motivation II

Reality/Drawing/CT images

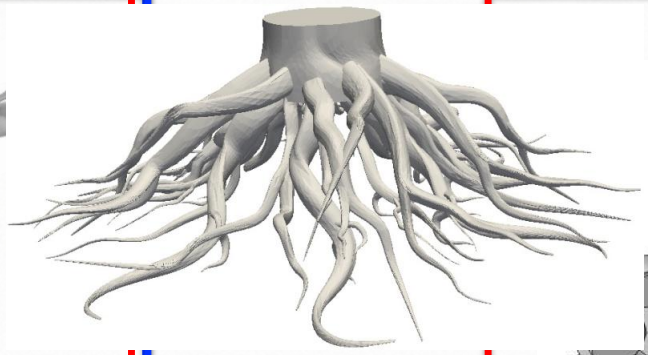

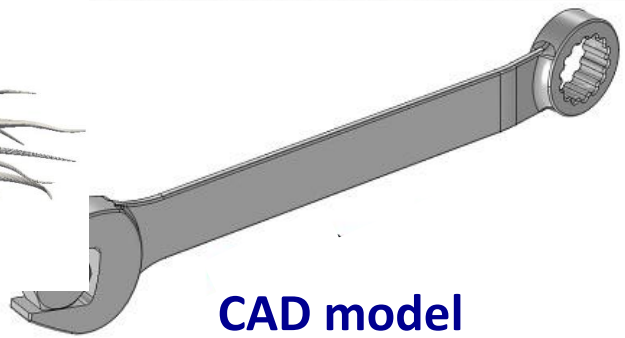

CAD model

mesh refinement

Sometimes 90% FEA workflow

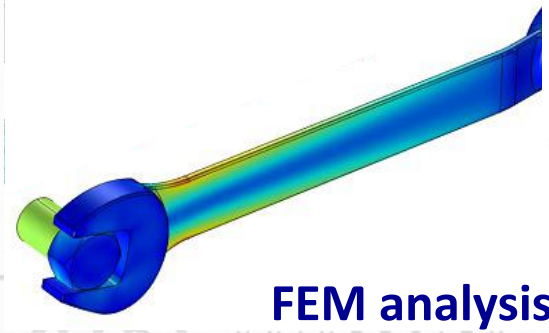

FEM analysis

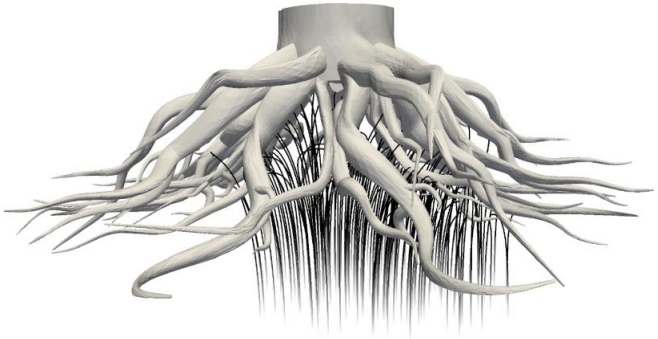

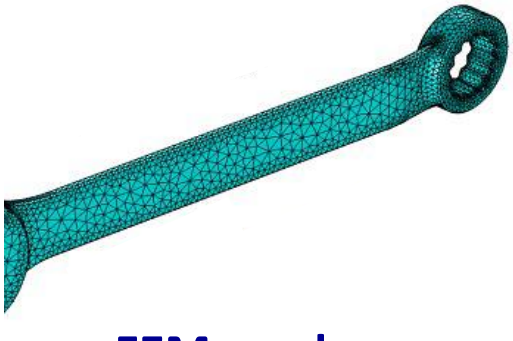

FEM mesh

Motivation III

Imaging-to-computing, an *emerging* field:

An efficient transition from geometries reconstructed from images to computation may impact and transform many fields of application:

- *Biomedical engineering*: CT-scans are given as pixilated data or STL format (collections of triangular facets and their nodal coordinates). Body-fitted meshing can be quite hard to perform.
- *Subsurface imaging and computing* (meshing requires considerable effort in reservoir engineering applications)
- *Additive manufacturing simulations* (e.g., 3D-printing). The typical file format for 3D-printers is again STL

In these examples the geometric information is not very precise and/or consistent (surfaces with *gaps* and *overlaps*, typical of computer graphics, STL = set of *disconnected* triangular faces)

Duke UNIVERSITY

Overview

Two commonly used computational strategies:

1. *Body-fitted grids.* The grid conforms to the boundary geometry of the shape to be simulated.
   - *Advantages*: Easier treatment of the boundary conditions (and boundary layers)
   - *Limitations*: Requires more advanced meshing for complex geometry, or re-meshing in problems with large deformations

2. *Embedded/immersed grids*. The shape to be simulated is fully or partially embedded (or immersed) into a regular background grid.
   - *Advantages*: Generality of the method, especially if coupling heterogeneous computational frameworks, rapid prototyping
   - *Limitations*: More complex enforcement of boundary conditions

Duke UNIVERSITY

Existing Embedded Boundary Methods

Unfitted Finite Element Methods (excluding GFEM-XFEM)

- Embedded methods of finite element type (a.k.a. *cutFEMs*, *unfitted FEMs, Finite Cell Method, Embedded Splines, IGA-Immersogeometric etc.*) often rely on XFEM methodologies to integrate on cut cells, *Inverse Lax-Wendroff procedure* (DG) [Burman, Hansbo, Larson, Massing, Cirak, Kamenski, Schillinger, Yan, Parvizian, Düster, Rank, Wall, Annavarapu, Dolbow, Harari, Badia, Rossi, C-W. Shu, Masud, *et. al.*, etc.]
- Unfitted/embedded FEMs typically utilize *Lagrange multipliers* or *Nitsche* variational formulations
- CutFEMs/unfitted FEMs require data structures and special quadratures to integrate on geometrically complex cut cells
- *The small cut-cell problem*: Integration over cut cells introduces additional interface degrees of freedom that may yield stability problems, very small time-steps or poor matrix conditioning. [Burman & Hansbo *Appl. Num. Math.* (2012)]. Solution: *ghost penalty*, and related methods

Overview of the Shifted Boundary Method

Key ideas: [with Alex Main at Duke University: the origins of the method]

- Use a *purely* embedded approach

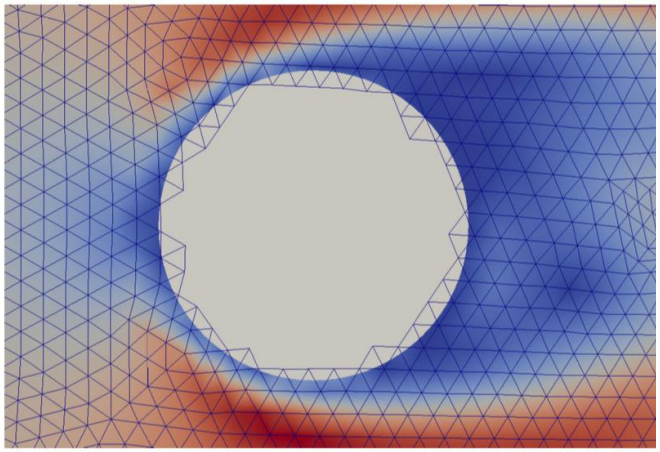

Duke UNIVERSITY

Overview of the Shifted Boundary Method

Key ideas: [with Alex Main at Duke University: the origins of the method]

- Use a *purely* embedded approach
- Use the Nitsche framework to impose boundary conditions weakly

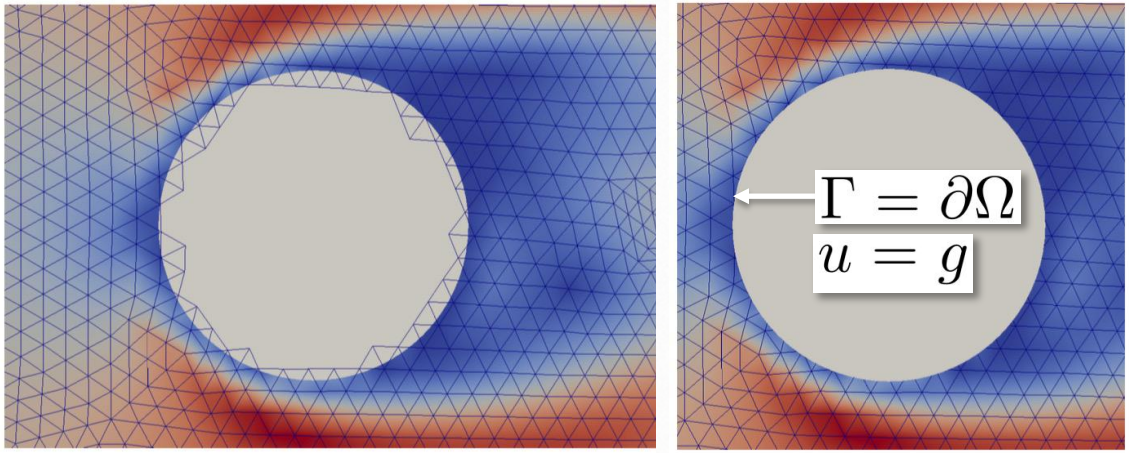

Duke UNIVERSITY

Overview of the Shifted Boundary Method

Key ideas: [with Alex Main at Duke University: the origins of the method]

- Use a *purely* embedded approach
- Use the Nitsche framework to impose boundary conditions weakly
- Apply boundary conditions on a surrogate boundary, near the true boundary

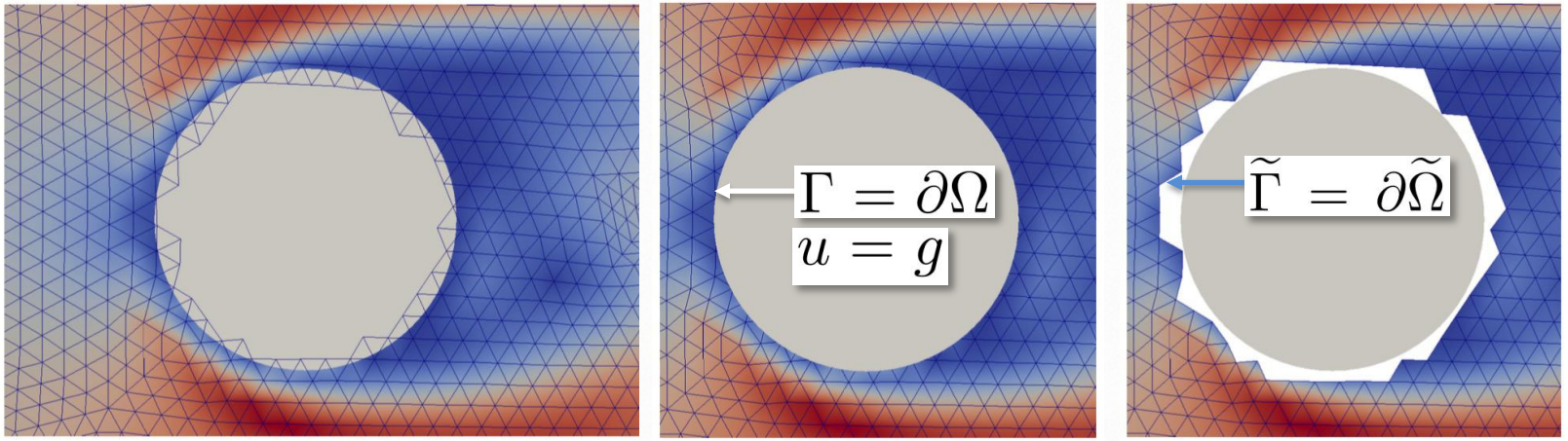

Duke UNIVERSITY

Overview of the Shifted Boundary Method

Key ideas: [with Alex Main at Duke University: the origins of the method]

- Use a *purely* embedded approach
- Use the Nitsche framework to impose boundary conditions weakly
- Apply boundary conditions on a surrogate boundary, near the true boundary
- Appropriately modify the boundary condition to account for the discrepancy between surrogate and true boundary

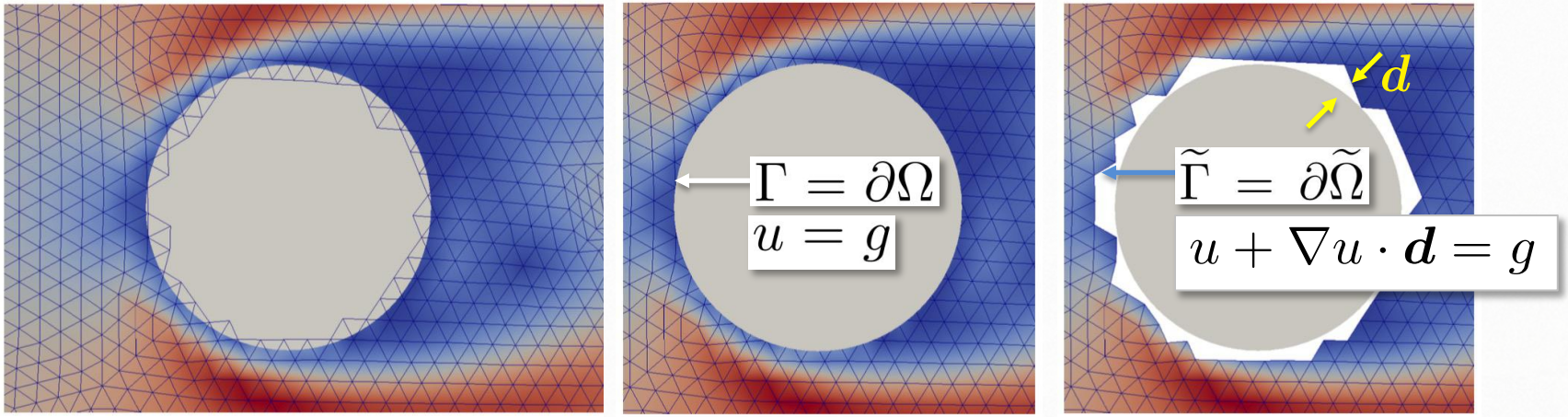

Overview of the Shifted Boundary Method

Key ideas: [with Alex Main at Duke University: the origins of the method]

- Use a *purely* embedded approach
- Use the Nitsche framework to impose boundary conditions weakly
- Apply boundary conditions on a surrogate boundary, near the true boundary
- Appropriately modify the boundary condition to account for the discrepancy between surrogate and true boundary

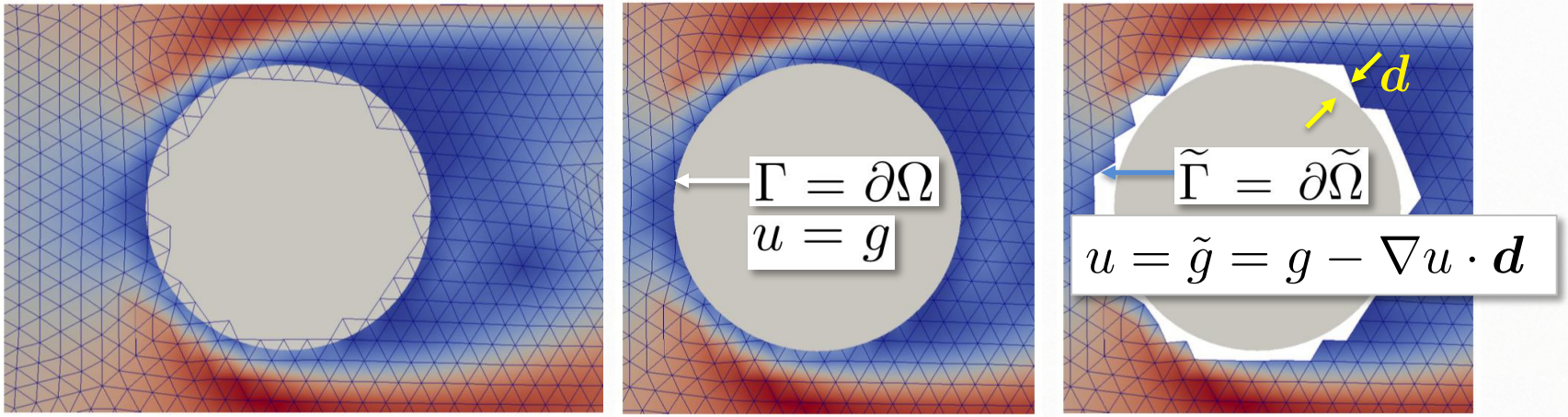

The Shifted Boundary Method (SBM)

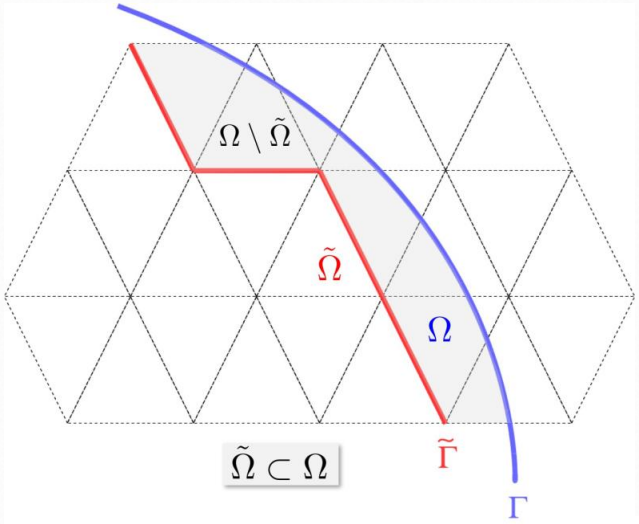

The extension map $\boldsymbol{M}$ & a distance vector function $\boldsymbol{d}$

$$\boldsymbol{M} : \tilde{\Gamma} \to \Gamma$$

$$\tilde{\boldsymbol{x}} \mapsto \boldsymbol{x}$$

$$\boldsymbol{d}_{\boldsymbol{M}}(\tilde{\boldsymbol{x}}) = \boldsymbol{x} - \tilde{\boldsymbol{x}} = [\boldsymbol{M} - \boldsymbol{I}](\tilde{\boldsymbol{x}})$$

Extension of functions defined on boundaries:

$$\bar{\psi}(\tilde{\boldsymbol{x}}) \equiv \psi(\boldsymbol{M}(\tilde{\boldsymbol{x}}))$$

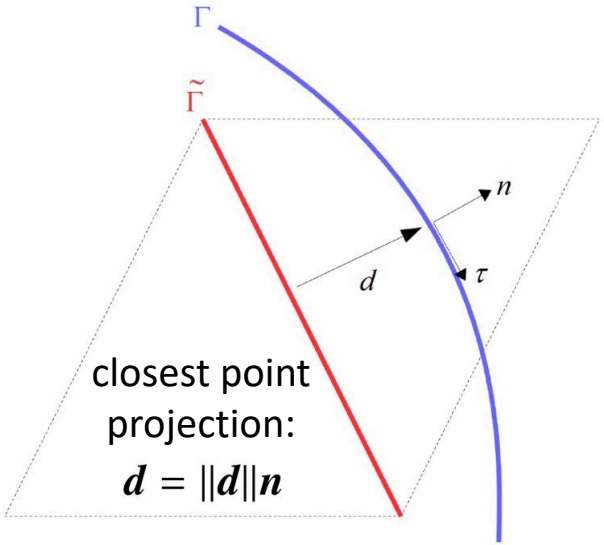

[with Alex Main at Duke University: the origins of the method]

The (Base) Nitsche Method

A prototypical example: The Poisson problem

Strong form of the equation

$$\begin{aligned} \Delta u + f &= 0 && \text{on } \Omega \\ u &= g && \text{on } \Gamma = \partial\Omega \end{aligned}$$

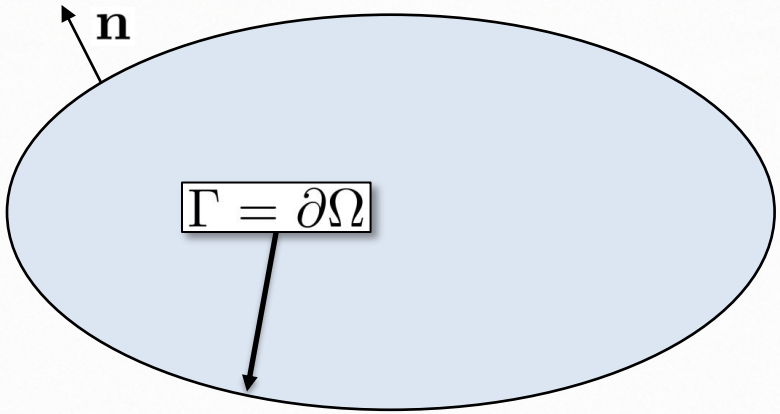

Augmented Lagrangian formulation

$$\int_\Omega \nabla w \cdot \nabla u = \int_\Omega w\, f$$

Nitsche's formulation

$$\int_\Omega \nabla w \cdot \nabla u - \int_\Gamma w \frac{\partial u}{\partial n} - \int_\Gamma \frac{\partial w}{\partial n}(u-g) + \int_\Gamma \alpha\, w\,(u-g) = \int_\Omega w\, f$$

Duke UNIVERSITY

[with Alex Main at Duke University: the origins of the method]

The Shifted Nitsche Method

A prototypical example: The Poisson problem

Weak form of the equation with weak boundary conditions (Nitsche method):

$$\int_{\Omega} \nabla w \cdot \nabla u - \int_{\Gamma} w \frac{\partial u}{\partial n} - \int_{\Gamma} \frac{\partial w}{\partial n} (u - g) + \int_{\Gamma} \alpha\, w\, (u - g) = \int_{\Omega} w\, f$$

Shifted Nitsche method:

$$\int_{\tilde{\Omega}} \nabla w \cdot \nabla u - \int_{\tilde{\Gamma}} w \frac{\partial u}{\partial n} - \int_{\tilde{\Gamma}} \frac{\partial w}{\partial n} (u - \tilde{g}) + \int_{\tilde{\Gamma}} \alpha\, w\, (u - \tilde{g}) = \int_{\tilde{\Omega}} w\, f$$

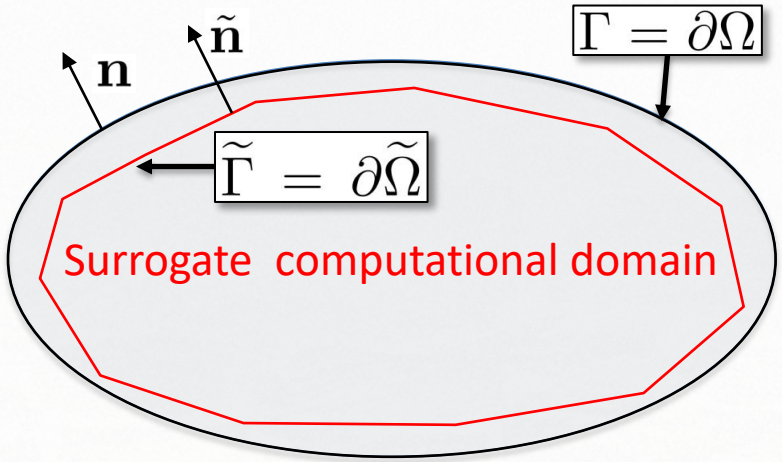

[with Alex Main at Duke University: the origins of the method]

The Shifted Nitsche Method

A prototypical example: The Poisson problem

Weak form of the equation with weak boundary conditions (Nitsche method):

$$\int_{\tilde{\Omega}} \nabla w \cdot \nabla u - \int_{\tilde{\Gamma}} w \frac{\partial u}{\partial n} - \int_{\tilde{\Gamma}} \frac{\partial w}{\partial n} (u - \tilde{g}) + \int_{\tilde{\Gamma}} \alpha\, w\, (u - \tilde{g}) = \int_{\tilde{\Omega}} w\, f$$

$$\int_{\tilde{\Omega}} \nabla w \cdot \nabla u - \int_{\tilde{\Gamma}} w \frac{\partial u}{\partial n} - \int_{\tilde{\Gamma}} \frac{\partial w}{\partial n} (u + \nabla u \cdot \boldsymbol{d} - g) + \int_{\tilde{\Gamma}} \alpha\, w\, (u + \nabla u \cdot \boldsymbol{d} - g) = \int_{\tilde{\Omega}} w\, f$$

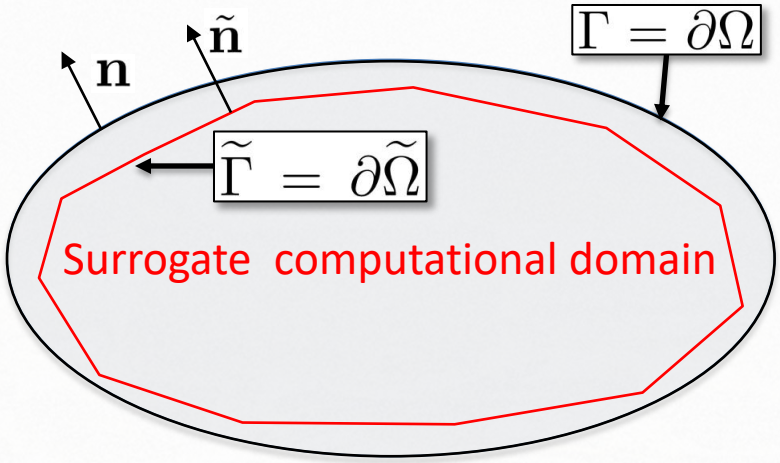

[with Alex Main at Duke University: the origins of the method]

Numerical Results: Poisson Problem

Numerical convergence test with an exact solution on a circular domain

$$\Delta u + 1 = 0 \quad on\ \Omega$$
$$u|_\Gamma = 0$$

Exact solution: $u = \frac{1}{4}(R^2 - r^2)$

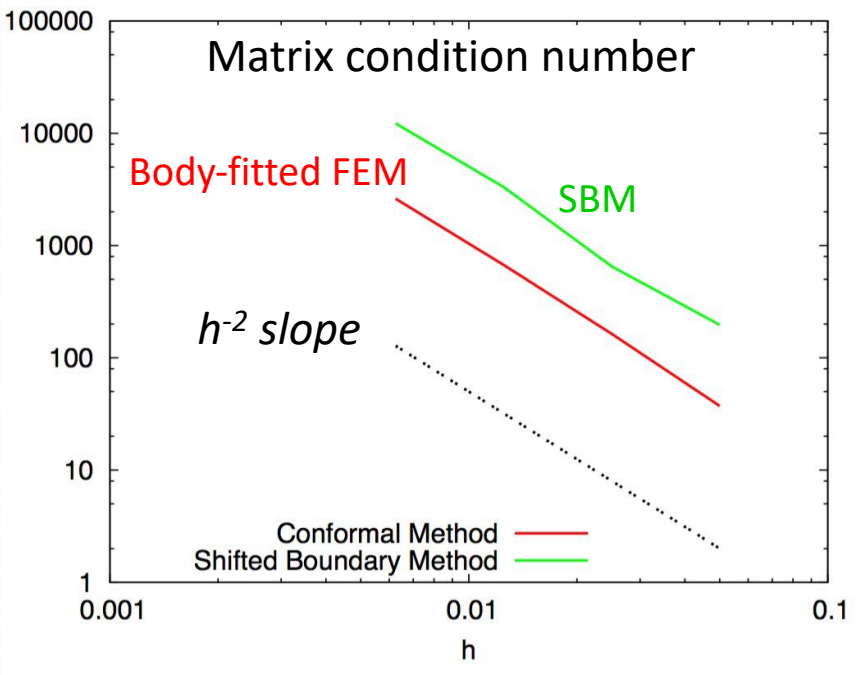

L² norm of the error (linear FEMs)

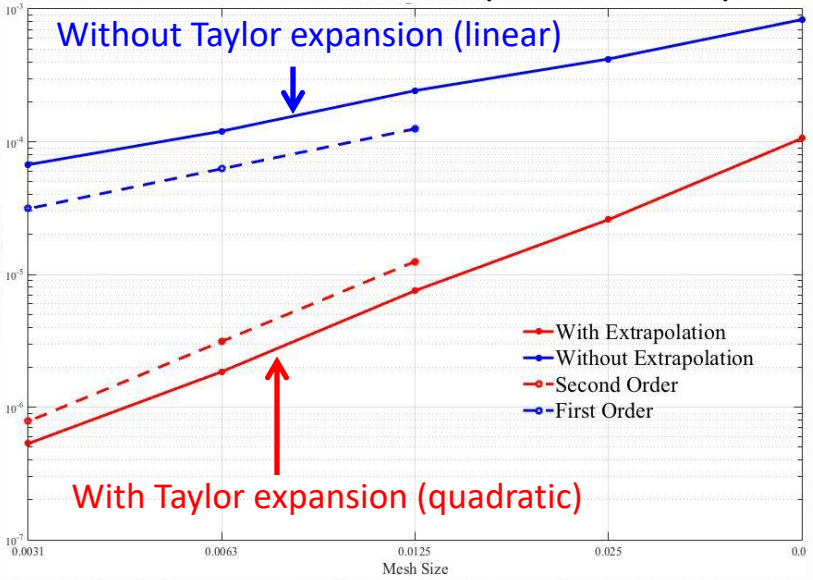

Condition number (*estimated!*):

- About 3 times larger than for the body-fitted method
- Same scaling with h^{-2} has for the body-fitted method

Duke UNIVERSITY

[with Alex Main at Duke University: the origins of the method]

Numerical Results: Poisson Problem

[with Nabil Atallah (at Duke) & Claudio Canuto, Math. Dept., Politecnico di Torino]

Exact solution (manufactured):

$$u(x, y) = y \sin(2\pi x) - x \cos(2\pi y)$$

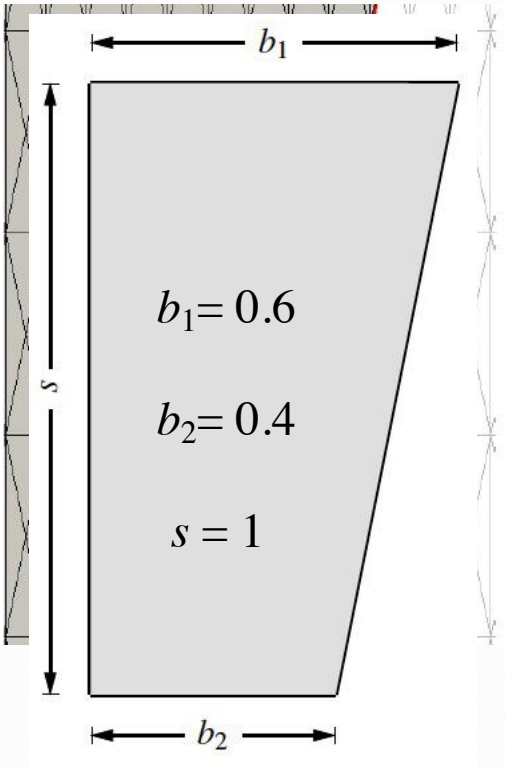

Piecewise-linear triangular finite elements

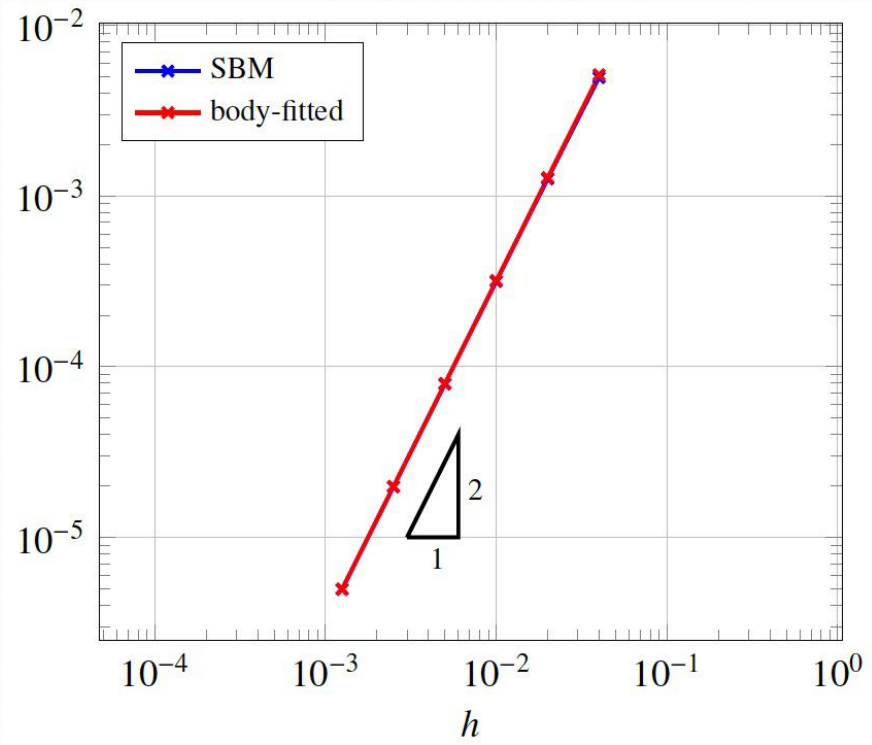

Mesh Size	No. of surrogate edges with $\boldsymbol{\nu} \cdot \boldsymbol{n} \leq 0$	% of total surrogate edges
4.00E-02	1	4.35%
2.00E-02	1	2.33%
1.00E-02	5	5.43%
5.00E-03	9	5.06%
2.50E-03	23	6.35%
1.25E-03	38	5.38%

Duke UNIVERSITY

The SBM for Domains with Corners

[with Nabil Atallah (at Duke) & Claudio Canuto, Math. Dept., Politecnico di Torino]

Solution: Consider a surrogate edge $\tilde{E}$ with $\tilde{n}$ as its unit normal.

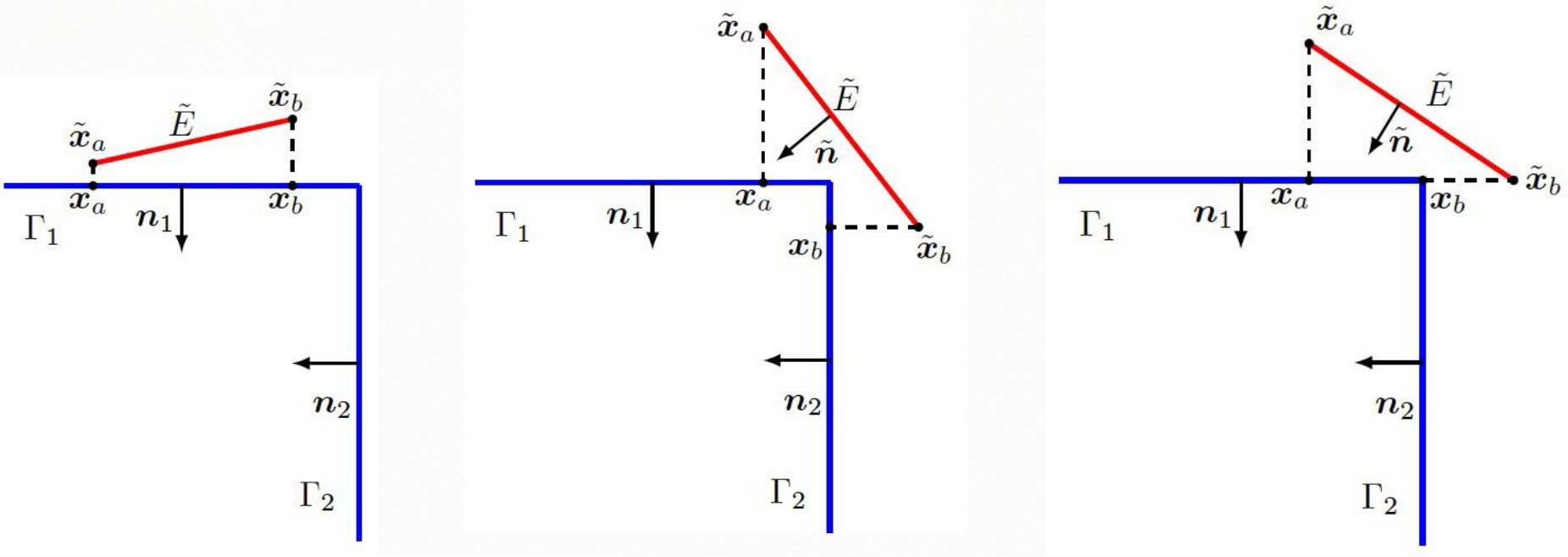

$$\Gamma_m = \arg\max_{\Gamma_s \in L} f(\Gamma_s) \quad \text{where } f(\Gamma_s) = \sum_{i=a,b} \tilde{\boldsymbol{n}} \cdot \boldsymbol{n}_{\Gamma_s}(\boldsymbol{x}_i).$$

The three-dimensional case is similar

N. Atallah, C. Canuto, G. Scovazzi, "Analysis of the Shifted Boundary Method for the Poisson problem in domains with corners," Mathematics of Computation

Duke UNIVERSITY

Numerical Analysis: Poisson Problem

Coercivity of the SBM variational form

We have a coercivity estimate:

$$a_u^h(u^h, u^h) \geq C_a \|u^h\|_a^2 , \qquad \forall u^h \in V^h(\tilde{\Omega}) ,$$

where

$$\|u^h\|_a^2 = \|\nabla u^h\|_{0;\tilde{\Omega}}^2 + \|\sqrt{1/h}\,(u^h + \nabla u^h \cdot \boldsymbol{d})\|_{0;\tilde{\Gamma}_D}^2$$

Duke UNIVERSITY

Numerical Analysis: Poisson Problem

Coercivity of the SBM variational form

We have a coercivity estimate:

$$a_u^h(u^h, u^h) \geq C_a \, \| u^h \|_a^2 \, , \qquad \forall u^h \in V^h(\tilde{\Omega}) \, ,$$

where

$$\| u^h \|_a^2 = \| \nabla u^h \|_{0;\tilde{\Omega}}^2 + \| \sqrt{1/h} \, (u^h + \nabla u^h \cdot \boldsymbol{d}) \|_{0;\tilde{\Gamma}_D}^2$$

Boundedness (Continuity)

We can also prove continuity (boundedness): $V(\tilde{\Omega}; h) = V^h(\tilde{\Omega}) + V(\tilde{\Omega}) \subset H^2(\tilde{\Omega}; \tilde{\mathscr{T}}^h)$

$$a_u^h(u, w^h) \leq C_{\mathscr{A}} \, \| \, w^h \, \|_a \, \| \, u \, \|_{V(\tilde{\Omega};h)} \, , \qquad \| \, v \, \|_{V(\tilde{\Omega};h)}^2 = \| \, v \, \|_a^2 + | \, h \, w |_{2;\tilde{\Omega};\tilde{\mathscr{T}}^h}^2$$

for all $u \in V(\tilde{\Omega}; h)$ *and for all* $w^h \in V^h(\tilde{\Omega})$.

Duke UNIVERSITY

Numerical Analysis: Poisson Problem

Consistency error due to the Taylor expansions:

$$
\begin{aligned}
a_u^h(u, w^h) - l_u^h(w^h) = & -(w^h, \underbrace{\Delta u + f}_{0})_{\tilde{\Omega}} - \langle \sqrt{h}\, \nabla w^h \cdot \tilde{\boldsymbol{n}}\,, \sqrt{1/h} \rangle_{\tilde{\Gamma}_D} \\
& + \langle \alpha \sqrt{1/h}\, (w^h + \nabla w^h \cdot \boldsymbol{d}), \sqrt{1/h}\, \rangle_{\tilde{\Gamma}_D} \\
\leq & \; C_{PBL}\, ||w^h||_a h_{\tilde{\Gamma}_D}\, \hat{h}_{\tilde{\Gamma}_D}^{3/2}\, \|\nabla(\nabla u)\|_{0,\Omega}\,.
\end{aligned}
$$

Duke UNIVERSITY

Numerical Analysis: Poisson Problem

Consistency error due to the Taylor expansions:

$$
\begin{aligned}
a_u^h(u, w^h) - l_u^h(w^h) = & -(w^h, \underbrace{\Delta u + f}_{0})_{\tilde{\Omega}} - \langle \sqrt{h}\, \nabla w^h \cdot \tilde{\boldsymbol{n}}\,, \sqrt{1/h} \rangle_{\tilde{\Gamma}_D} \\
& + \langle \alpha \sqrt{1/h}\, (w^h + \nabla w^h \cdot \boldsymbol{d}), \sqrt{1/h}\, \rangle_{\tilde{\Gamma}_D} \\
\leq & \; C_{PBL}\, ||w^h||_{a h_{\tilde{\Gamma}_D}}\, \hat{h}_{\tilde{\Gamma}_D}^{3/2}\, \|\nabla(\nabla u)\|_{0,\Omega}\,.
\end{aligned}
$$

Optimal convergence estimate in the energy norm (using Strang's second lemma)

$$
\begin{aligned}
\| u - u^h \|_{V(\tilde{\Omega};h)} \leq & \left(1 + \frac{\|a_u^h\|_{V(h)\times V^h(\tilde{\Omega})}}{C_a} \right) \inf_{w^h \in V^h(\tilde{\Omega})} \| u - w^h \|_{V(\tilde{\Omega};h)} \\
& + \frac{1}{C_a} \sup_{w^h \in V^h(\tilde{\Omega})} \frac{|l^h(w^h) - a_u^h(u, w^h)|}{\|w^h\|_{V(\tilde{\Omega};h)}}\,. \\
\leq & \; C\, h_{\tilde{\Omega}}\, (\|\nabla(\nabla u)\|_{0,\Omega})
\end{aligned}
$$

Duke UNIVERSITY

Numerical Analysis: Poisson Problem

Consistency error due to the Taylor expansions:

$$
\begin{aligned}
a_u^h(u,w^h) - l_u^h(w^h) = & -(w^h, \underbrace{\Delta u + f}_{0})_{\tilde{\Omega}} - \langle \sqrt{h}\,\nabla w^h \cdot \tilde{\boldsymbol{n}}\,, \sqrt{1/h}\rangle_{\tilde{\Gamma}_D} \\
& + \langle \alpha\sqrt{1/h}\,(w^h + \nabla w^h \cdot \boldsymbol{d}), \sqrt{1/h}\,\rangle_{\tilde{\Gamma}_D} \\
\leq & \; C_{PBL}\,||w^h||_a h_{\tilde{\Gamma}_D}\,\hat{h}_{\tilde{\Gamma}_D}^{3/2}\,\|\nabla(\nabla u)\|_{0,\Omega}\,.
\end{aligned}
$$

Optimal convergence estimate in the energy norm (using Strang's second lemma)

$$
\begin{aligned}
\|\,u - u^h\,\|_{V(\tilde{\Omega};h)} \leq & \left(1 + \frac{\|a_u^h\|_{V(h)\times V^h(\tilde{\Omega})}}{C_a}\right) \inf_{w^h \in V^h(\tilde{\Omega})} \|\,u - w^h\,\|_{V(\tilde{\Omega};h)} \\
& + \frac{1}{C_a} \sup_{w^h \in V^h(\tilde{\Omega})} \frac{|l^h(w^h) - a_u^h(u,w^h)|}{\|w^h\|_{V(\tilde{\Omega};h)}}\,. \\
\leq & \; C\,h_{\tilde{\Omega}}\,(\|\nabla(\nabla u)\|_{0,\Omega})
\end{aligned}
$$

Suboptimal (<u>not in practice!</u>) duality (L^2) estimate: $\|u - u^h\|_{0;\tilde{\Omega}} \leq C_0\,h_{\tilde{\Omega}}^{3/2}\,\|\nabla(\nabla u)\|_{0,\tilde{\Omega}}$

Duke UNIVERSITY

Numerical Analysis: Stokes Flow Problem

[with Nabil Atallah (at Duke) & Claudio Canuto, Math. Dept., Politecnico di Torino]

Stability (LBB)

$$\mathscr{B}([\boldsymbol{u}^h, p^h]; [\boldsymbol{w}^h, q^h]) \geq \alpha_{LBB} \, |||[\boldsymbol{u}^h, p^h]|||_{\mathscr{B}} \, |||[\boldsymbol{w}^h, q^h]|||_{\mathscr{B}}$$

An LBB *inf-sup* condition can be derived in the case of the Stokes' operator

Convergence (in natural norm)

$$|||\,[\boldsymbol{u}, p] - [\boldsymbol{u}^h, p^h]\,|||_{W(\tilde{\Omega};h)} \leq C\, h_{\tilde{\Omega}} \left(\|\nabla(\nabla \boldsymbol{u})\|_{0,\Omega} + \|\nabla p\|_{0,\tilde{\Omega}} \right)$$

The proof is analogous to the one for the Poisson problem, using the *inf-sup* LBB condition and Strang's second lemma.

Duality estimates (L^2-estimates for the velocity field)

$$\|\boldsymbol{u} - \boldsymbol{u}^h\|_{0;\tilde{\Omega}} \leq C_0\, h_{\tilde{\Omega}}^{3/2} \left(\|\nabla(\nabla \boldsymbol{u})\|_{0,\tilde{\Omega}} + \|\nabla p\|_{0,\tilde{\Omega}} \right)$$

Analogous but more complicated proof than in the Poisson case. We observe quadratic convergence for the velocity, in practical calculations

Similar results hold for the Darcy flow equations (mixed-Poisson)

Duke UNIVERSITY

Numerical Analysis: Linear Elasticity

[with Nabil Atallah (at Duke) & Claudio Canuto, Math. Dept., Politecnico di Torino]

Stability (coercivity by Korn's inequality)

$$\mathscr{B}^{[\tilde{\Omega}]}_{\mathrm{SBM}}([\boldsymbol{u}^h,\boldsymbol{\varepsilon}^h];[\boldsymbol{u}^h,\boldsymbol{\varepsilon}^h]) \geq c_{\mathrm{SBM}} \,|||\,[\boldsymbol{u}^h,\boldsymbol{\varepsilon}^h]\,|||^2_{\mathrm{SBM};\tilde{\Omega}}$$

$$|||\,[\boldsymbol{u}^h,\boldsymbol{\varepsilon}^h]\,|||^2_{\mathrm{SBM}} = \left(1-\tau_\varepsilon/2\right)\,\|\mathbf{C}^{1/2}\,\nabla^s\boldsymbol{u}^h\|^2_{0;\tilde{\Omega}_h\setminus\tilde{\Omega}^\ell_h} + \tau_\varepsilon\,\|\mathbf{C}^{1/2}\,\nabla^s\boldsymbol{u}^h\|^2_{0;\tilde{\Omega}^\ell_h} + \tau_\varepsilon\,\rho_{\min}\left(l(\tilde{\Omega})^{-2}\,\|\boldsymbol{u}^h\|^2_{H^1(\tilde{\Omega}_h)} + \|\,h^{1/2}\,\nabla\boldsymbol{u}^h\|^2_{0;\tilde{\Gamma}_{D,h}}\right)$$
$$+\left(1-\tau_\varepsilon\right)\left(\|\mathbf{C}^{1/2}\,\boldsymbol{\varepsilon}^h\|^2_{0;\tilde{\Omega}^\ell_h} + \|h^{1/2}\,(\mathbf{C}^{1/2}\,\boldsymbol{\varepsilon}^h)\|^2_{0;\tilde{\Gamma}_{D,h}}\right) + \|\rho_{\mathsf{C}}^{-1/2}\,\tau_{\boldsymbol{u}}^{1/2}\,\nabla\cdot(\mathbf{C}\,\boldsymbol{\varepsilon}^h)\|^2_{0;\tilde{\Omega}^\ell_h} + \|\rho_{\mathsf{C}}^{1/2}h^{-1/2}\boldsymbol{S}_{D,h}\,\boldsymbol{u}^h\|^2_{0;\tilde{\Gamma}_{D,h}}$$

Convergence (energy norm)

$$|||\,[\boldsymbol{e}_{\boldsymbol{u}},\boldsymbol{e}_{\boldsymbol{\varepsilon}}]\,|||_{\mathrm{SBM}} \lesssim \rho^{1/2}_{\max}\left(h_{\tilde{\Omega}_h}|\boldsymbol{u}|_{2;\tilde{\Omega}_h} + h_{\tilde{\Gamma}_{D,h}}\,|\boldsymbol{u}|_{2;\Omega\setminus\tilde{\Omega}_h} + h^{3/2}_{\tilde{\Gamma}_{D,h}}\,l(\tilde{\Omega}_h)^{1/2}\;|\boldsymbol{\varepsilon}|_{2;\tilde{\Omega}^\ell_h}\right)$$

Optimal convergence is achieved.

Convergence (L2-estimates for the displacement field)

$$\|\boldsymbol{e}_{\boldsymbol{u}}\|_{0;\tilde{\Omega}_h} \lesssim \rho^{1/2}_{\max}\,\rho^{-1/2}_{\min}\,h^{3/2}_{\tilde{\Omega}_h}\,l(\tilde{\Omega}_h)^{1/2}(|\boldsymbol{u}|_{2;\Omega} + |\boldsymbol{\varepsilon}|_{2;\tilde{\Omega}^\ell_h})$$

We observe quadratic convergence for the displacement, in practical calculations

Duke UNIVERSITY

Porous Media Flow (Mixed Formulation)

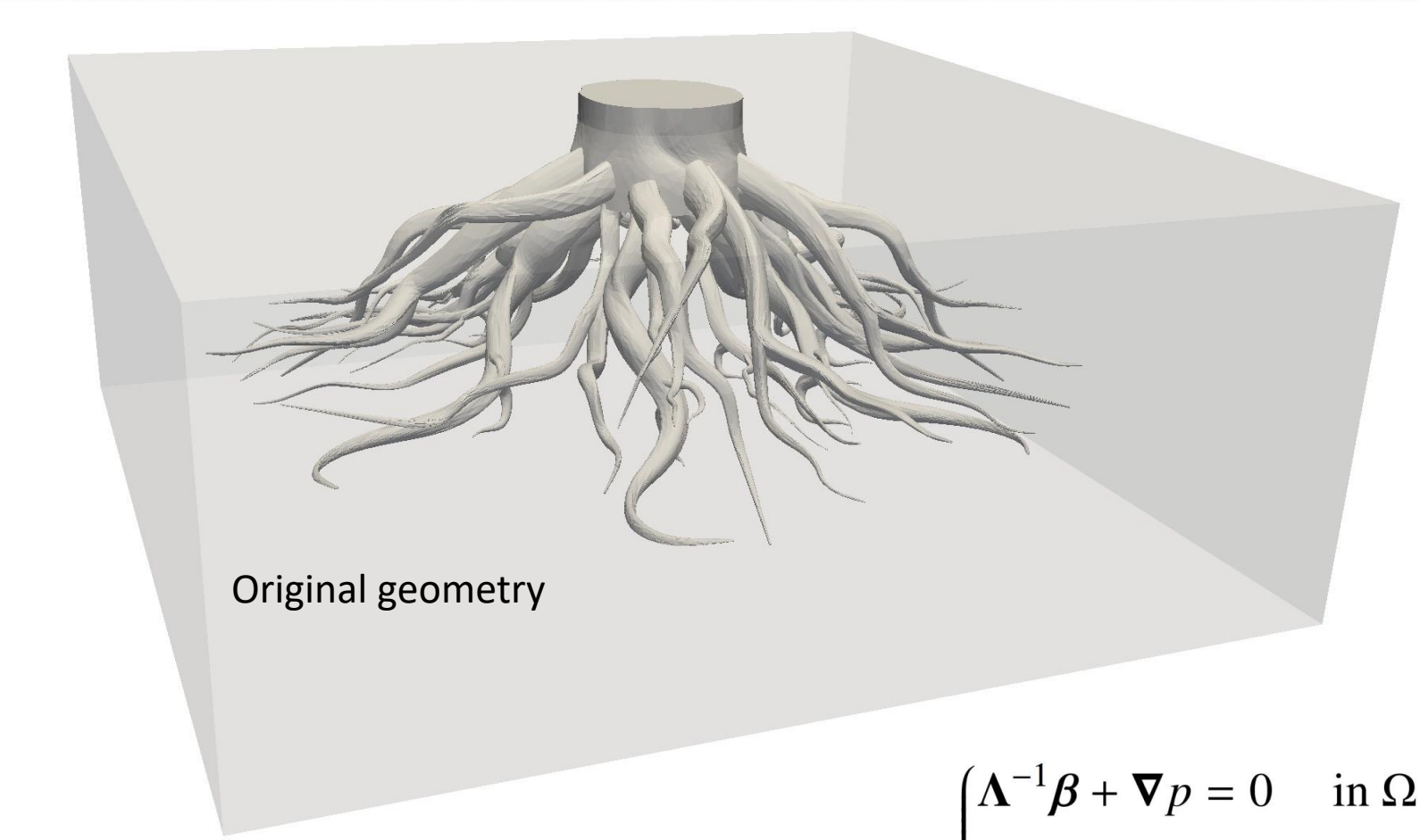

Original geometry

[with Nabil Atallah and in collaboration with G. Katul, CEE, Duke University]

$$\begin{cases} \boldsymbol{\Lambda}^{-1}\boldsymbol{\beta} + \boldsymbol{\nabla} p = 0 & \text{in } \Omega \\ \boldsymbol{\nabla} \cdot \boldsymbol{\beta} = \phi & \text{in } \Omega \\ p = p_D & \text{on } \Gamma_D \\ \boldsymbol{\beta} \cdot \boldsymbol{n} = h_N & \text{on } \Gamma_N \end{cases}$$

Duke UNIVERSITY

Porous Media Flow (Mixed Formulation)

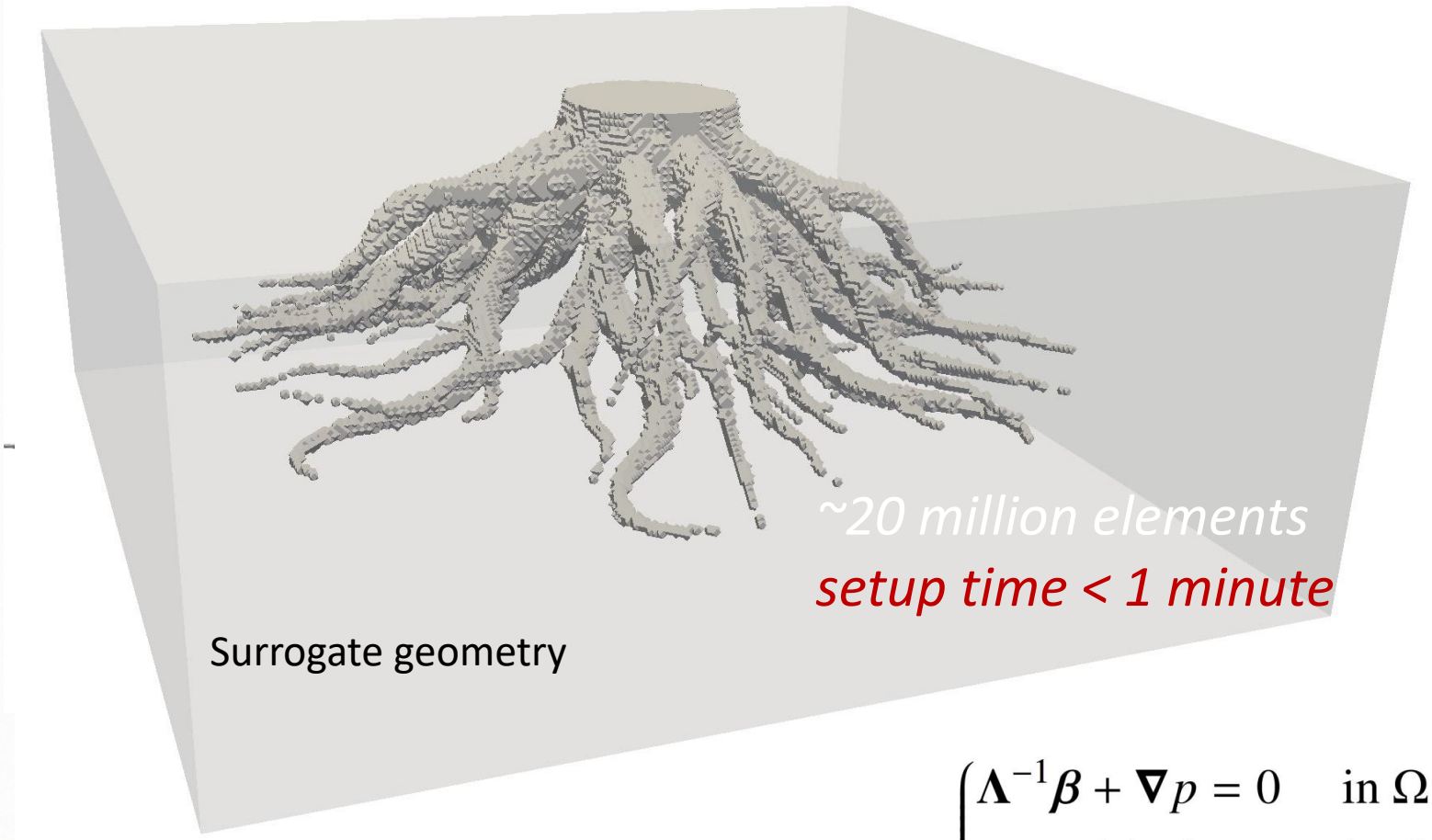

[with Nabil Atallah and in collaboration with G. Katul, CEE, Duke University]

$$\begin{cases} \boldsymbol{\Lambda}^{-1}\boldsymbol{\beta} + \boldsymbol{\nabla} p = 0 & \text{in } \Omega \\ \boldsymbol{\nabla} \cdot \boldsymbol{\beta} = \phi & \text{in } \Omega \\ p = p_D & \text{on } \Gamma_D \\ \boldsymbol{\beta} \cdot \boldsymbol{n} = h_N & \text{on } \Gamma_N \end{cases}$$

Duke UNIVERSITY

Porous Media Flow (Mixed Formulation)

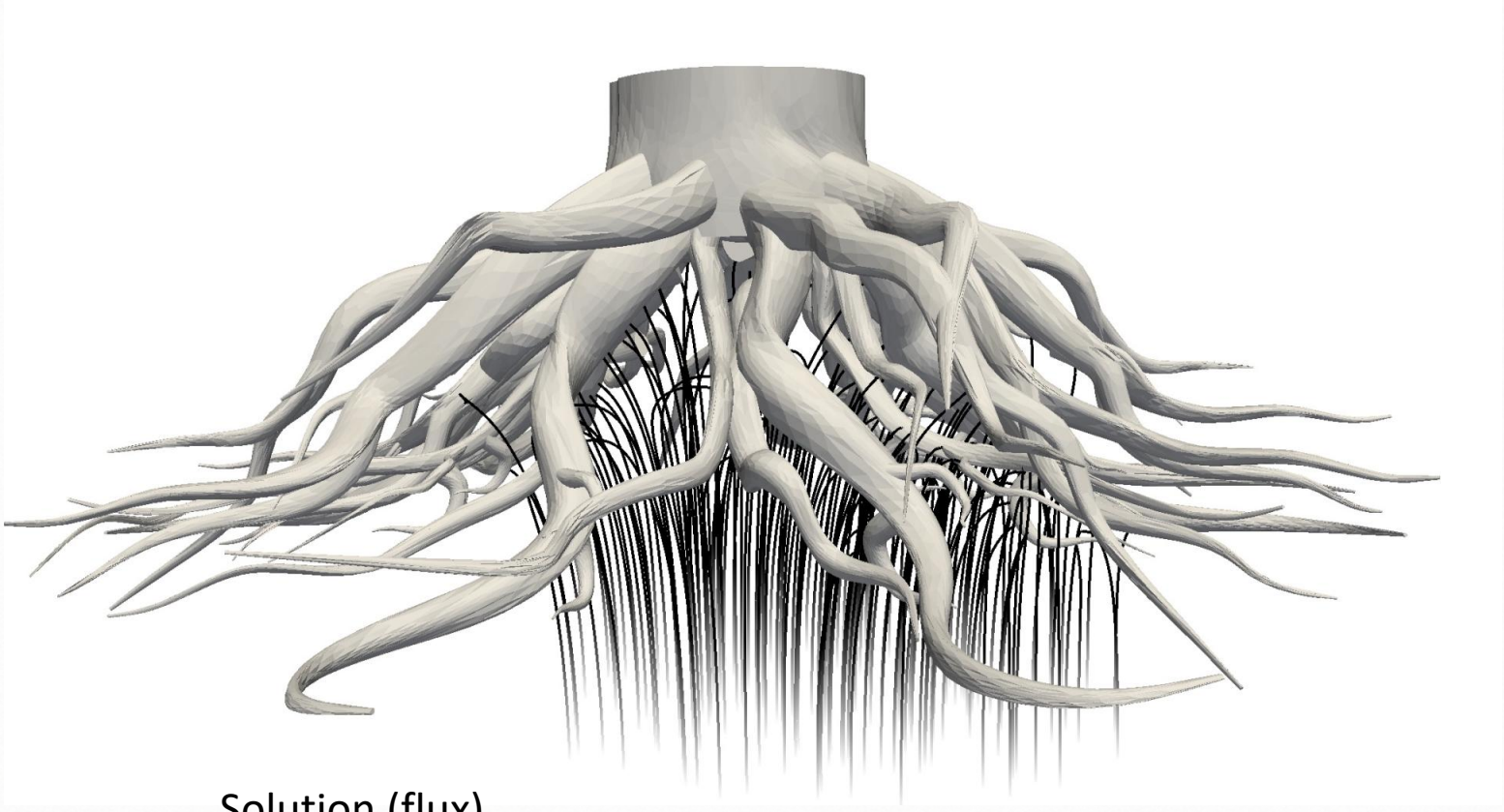

Solution (flux)

[with Nabil Atallah and in collaboration with G. Katul, CEE, Duke University]

$$\begin{cases} \boldsymbol{\Lambda}^{-1}\boldsymbol{\beta} + \boldsymbol{\nabla} p = 0 & \text{in } \Omega \\ \boldsymbol{\nabla} \cdot \boldsymbol{\beta} = \phi & \text{in } \Omega \\ p = p_D & \text{on } \Gamma_D \\ \boldsymbol{\beta} \cdot \boldsymbol{n} = h_N & \text{on } \Gamma_N \end{cases}$$

Duke UNIVERSITY

The Shifted Boundary Method

Convergence test (Navier-Stokes): Decelerating cylinder test

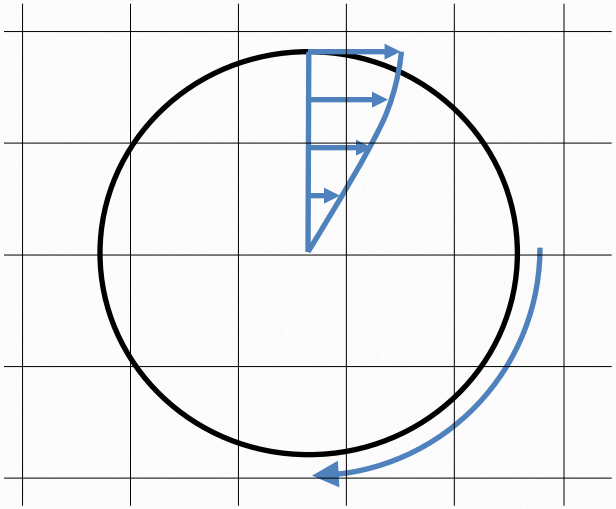

Exact solution:

$$u_\phi(r,t) = \frac{C}{J_1\left(\sqrt{\frac{i\omega\rho}{\mu}}R\right)} J_1\left(\sqrt{\frac{i\omega\rho}{\mu}}r\right) e^{(-i\omega t)}$$

Mesh Size	With Extrapolation: 2nd order	Without Extrap.: 1st order
0.05	0.1338	2.548
0.025	4.143 * 10^-2	0.9565
0.0125	1.067 * 10^-2	0.4761
0.00625	3.422 * 10^-3	0.265
0.003125	9.576 *10^-4	0.1404
K	**1.78**	**1**

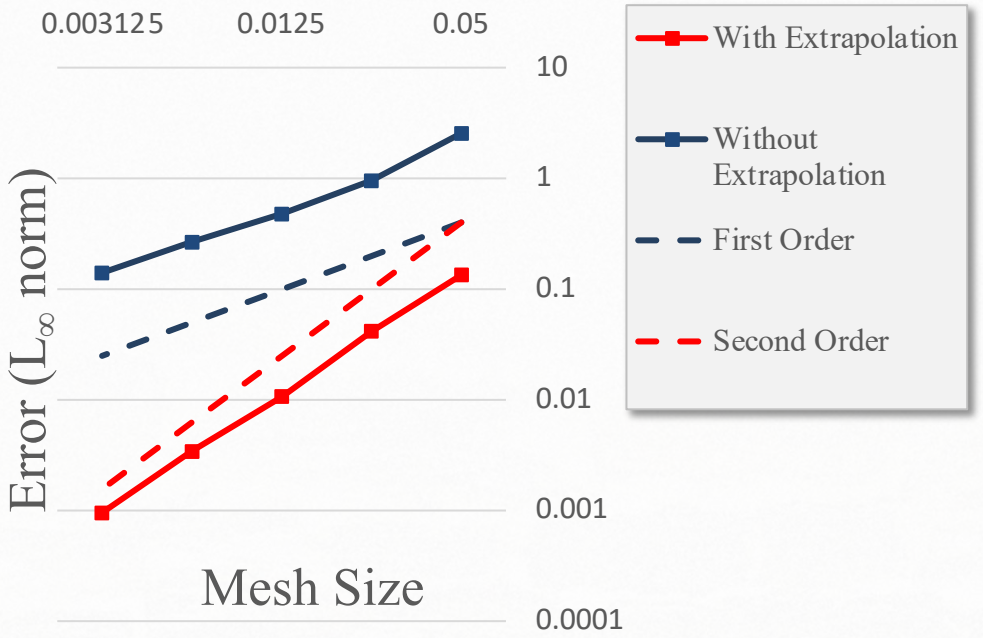

[with Alex Main at Duke University: the origins of the method]

Turbulent Flows

Formulations based on turbulent viscosities:

$$\textit{Find } \boldsymbol{u} \in \boldsymbol{V}^h(\tilde{\Omega}) \textit{ and } p \in Q^h(\tilde{\Omega}) \textit{ such that, } \forall \boldsymbol{u} \in \boldsymbol{V}^h(\tilde{\Omega}) \textit{ and } \forall q \in Q^h(\tilde{\Omega}),$$

$$0 = \mathbb{NS}[\mu + \mu_T](\boldsymbol{u}, p; \boldsymbol{w}, q) + \mathbb{STAB}[\mu + \mu_T](\boldsymbol{u}, p; \boldsymbol{w}, q)$$

- Spalart-Allmaras (SA) model with the Shifted Boundary Method are very similar to the Navier-Stokes equations
- Implicit LES is performed through the VMS stabilization/modeling approach

Wall model for the velocity boundary conditions:

$$\boldsymbol{u} = \boldsymbol{g} - \nabla \boldsymbol{u} \cdot \boldsymbol{d} \qquad \Rightarrow \qquad \boldsymbol{u} = \boldsymbol{g} - \boldsymbol{u}_{wall}(\boldsymbol{d}, \nabla \boldsymbol{u}, \ldots)$$

$$u^+ = \frac{1}{\kappa} \log y^+ + C^+$$

$$u_\tau = \sqrt{\frac{\tau_w}{\rho}}\,,$$

$$y^+ = \frac{u_\tau y}{\nu}\,,$$

$$u^+ = \frac{u}{u_\tau}\,,$$

[with Alex Main at Duke University: the origins of the method]

Flow Over a Circular Cylinder

A classical test to validate algorithms for laminar/turbulent flow

Re	St (vs. reference)	C_D (vs. reference)	Reference source
20	-	2.09 (1.99)	[7]
100	0.167 (0.164,0.157)	1.35 (1.34)	[7, 39]
300	0.211 (0.203, 0.215)	1.38 (1.37)	[39]
3900	0.203 (0.203)	1.04 (1.00)	[7]

[7] Beaudan & Moin (1995)

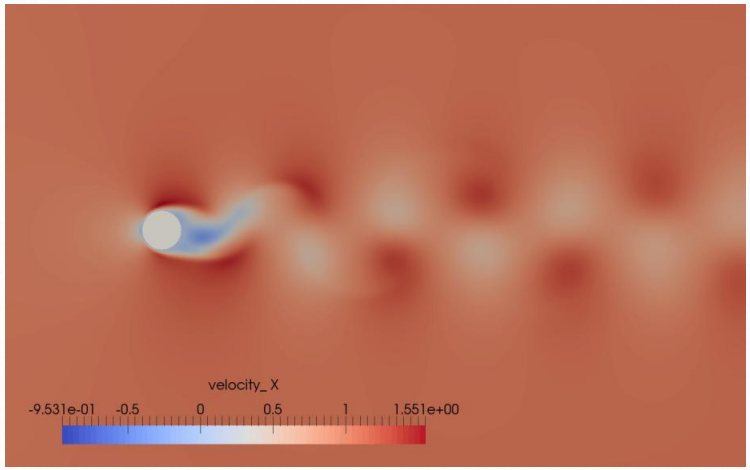

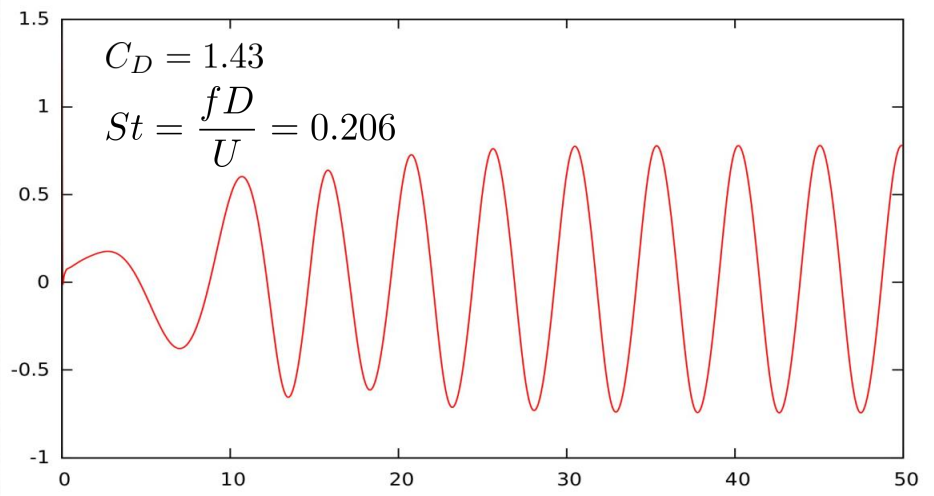

Lift coefficient, Re = 250

Duke UNIVERSITY

Flow Over a Circular Cylinder at Re=3,900

A classical test to validate algorithms for turbulent flow simulation

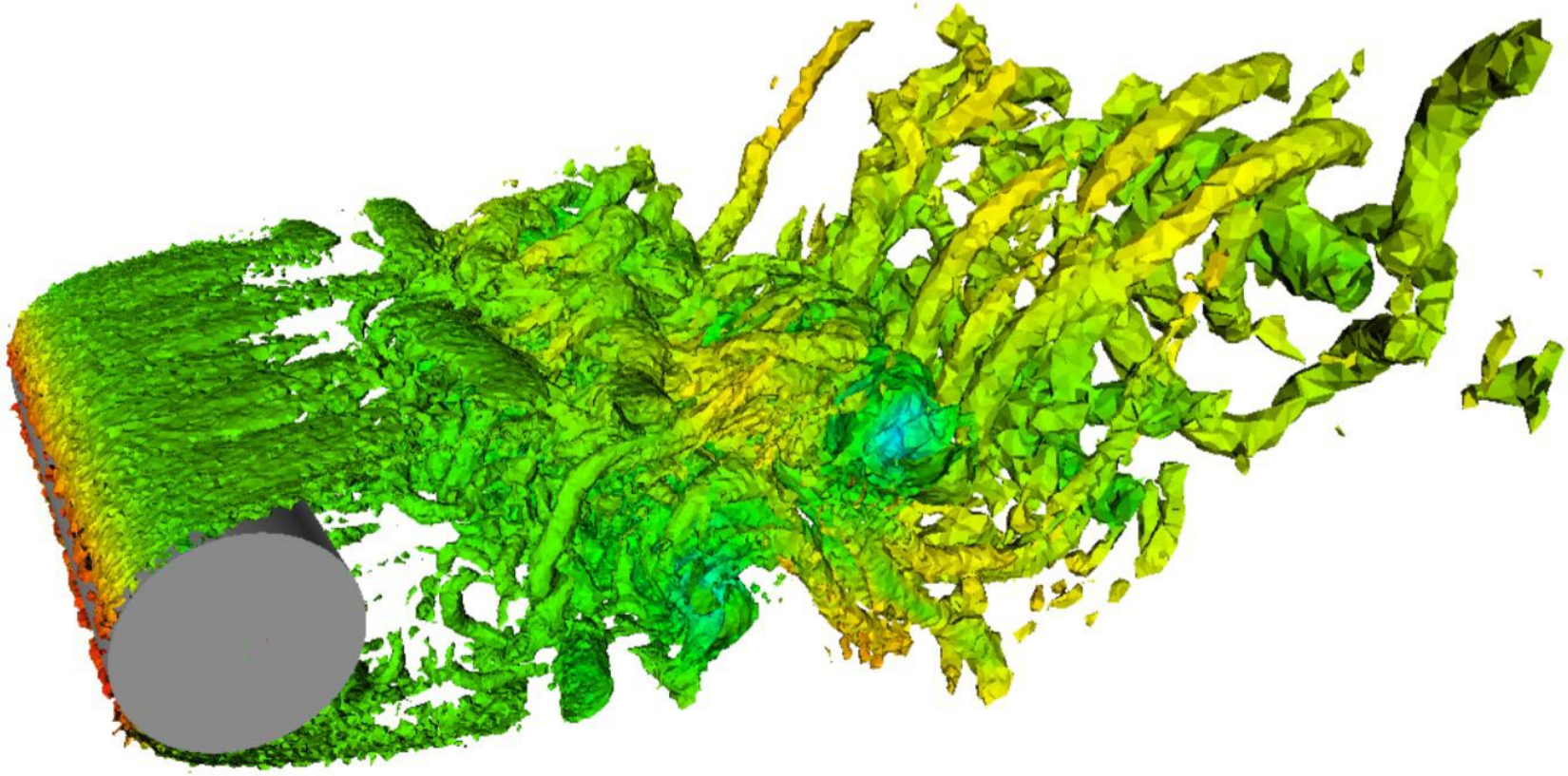

Q-criterion isosurfaces (used to visualize vortex structures)

Duke UNIVERSITY

[with Alex Main at Duke University: the origins of the method]

Flow Over a Circular Cylinder at Re=3,900

A classical test to validate algorithms for turbulent flow simulation

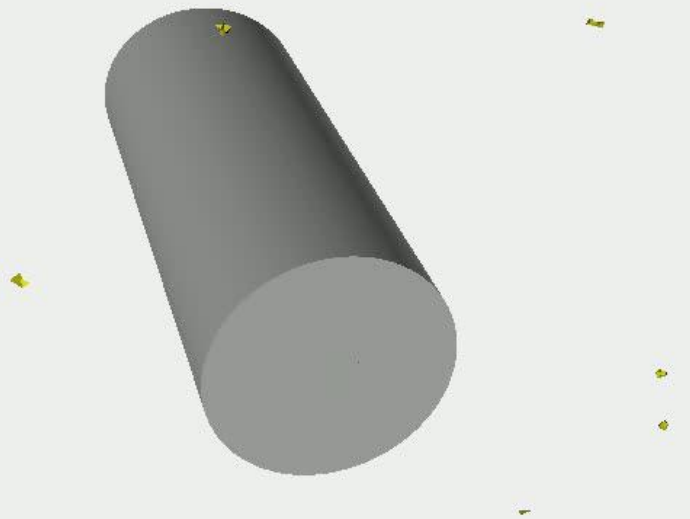

Q-criterion isosurfaces (used to visualize vortical structures)

Rendered by LiveViz

Duke UNIVERSITY

[with Alex Main at Duke University: the origins of the method]

A More Complicated Shape at Re=3,900

A differential geometry monster (the Monkey Trefoil)

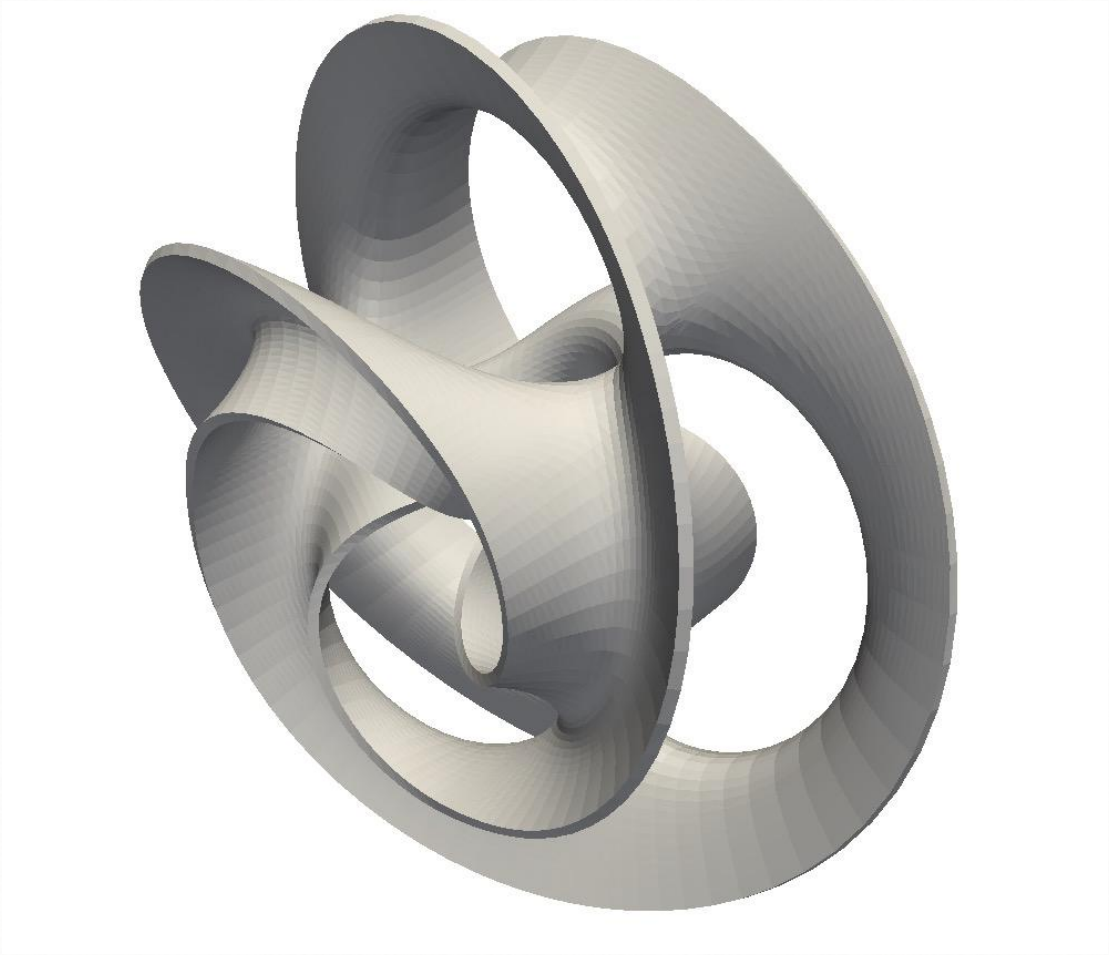

[with Alex Main at Duke University: the origins of the method]

A More Complicated Shape at Re=3,900

A differential geometry monster (the Monkey Trefoil)

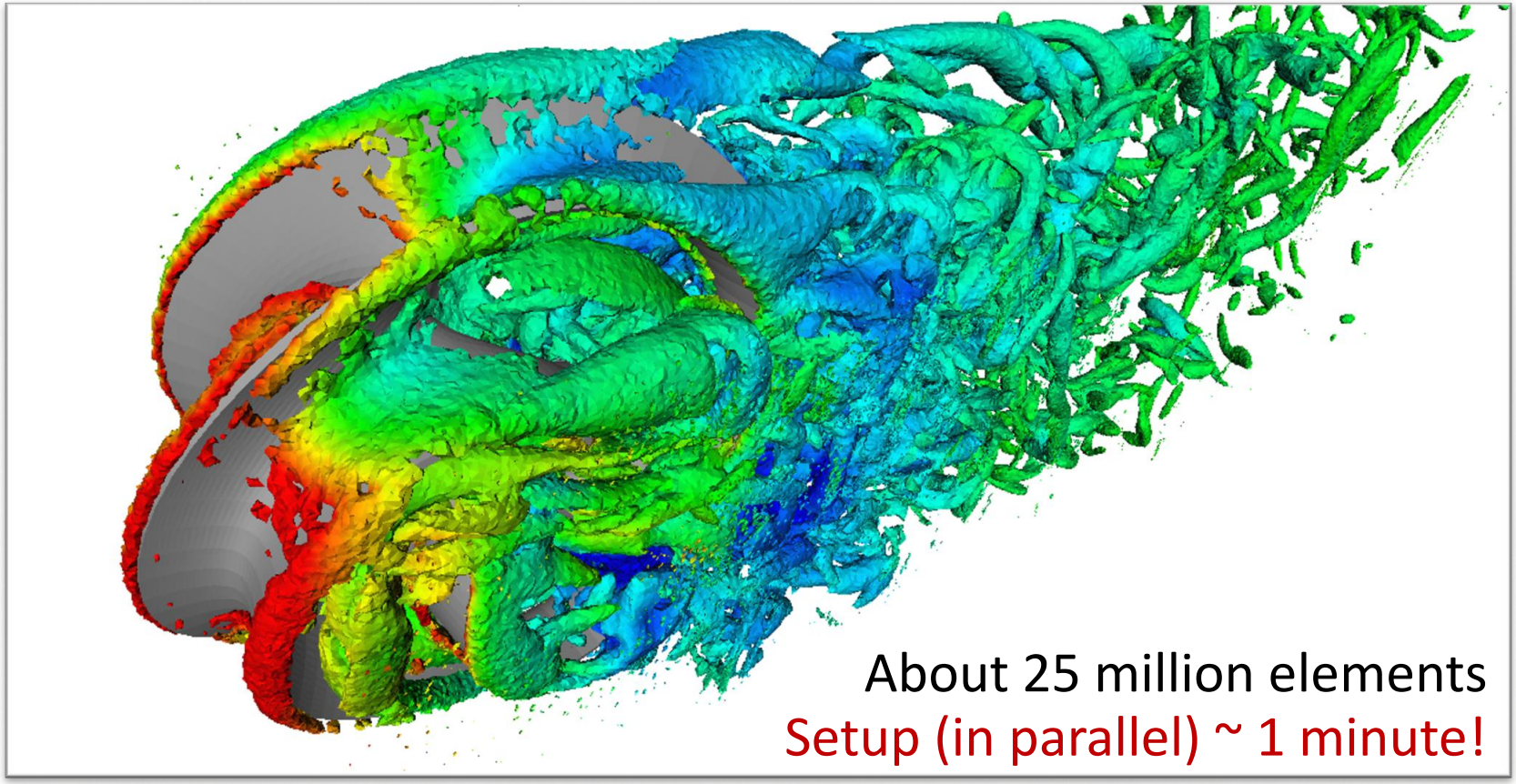

Q-criterion isosurfaces (used to visualize vortical structures)

Duke UNIVERSITY

[with Alex Main at Duke University: the origins of the method]

The SBM for Solid Mechanics

An alternative cycle to CAD-Meshing-Computing

Original geometry

The SBM for Solid Mechanics

An alternative cycle to CAD-Meshing-Computing

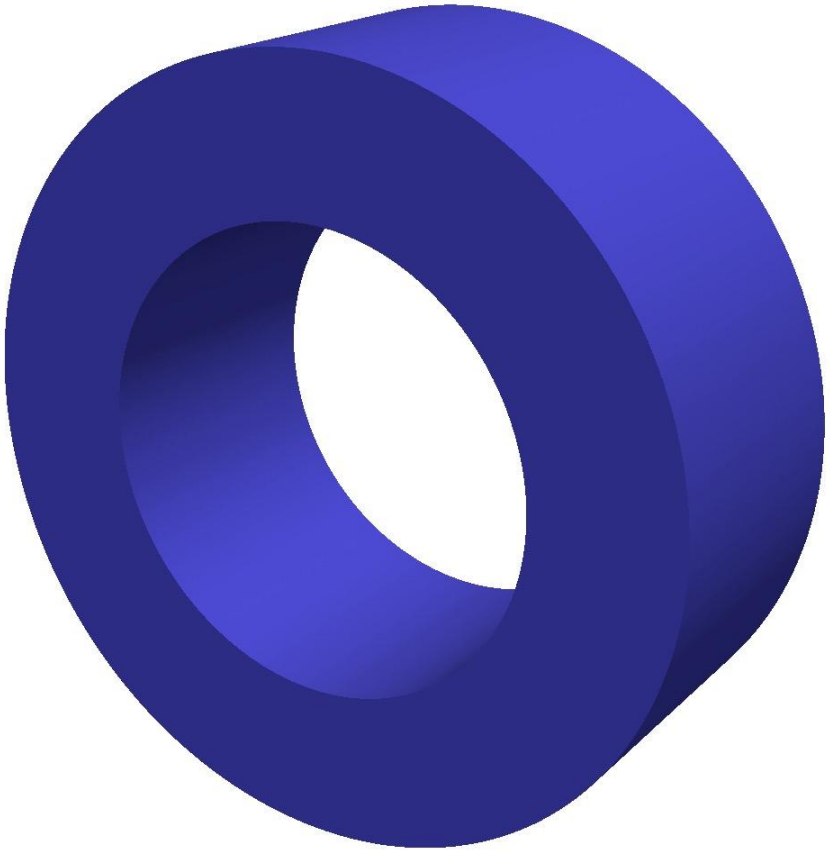

The background domain

Duke UNIVERSITY

The SBM for Solid Mechanics

An alternative cycle to CAD-Meshing-Computing

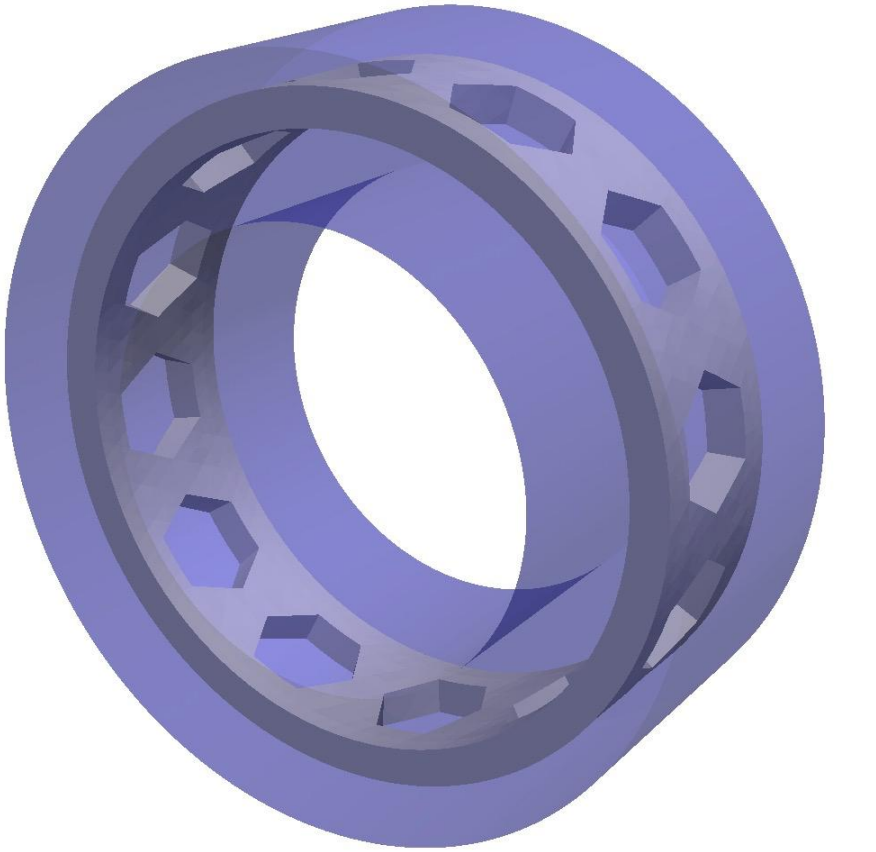

The background domain and the immersed original geometry

Duke UNIVERSITY

The SBM for Solid Mechanics

An alternative cycle to CAD-Meshing-Computing

The initial set of active elements (with boundary conditions sidesets)

Duke UNIVERSITY

The SBM for Solid Mechanics

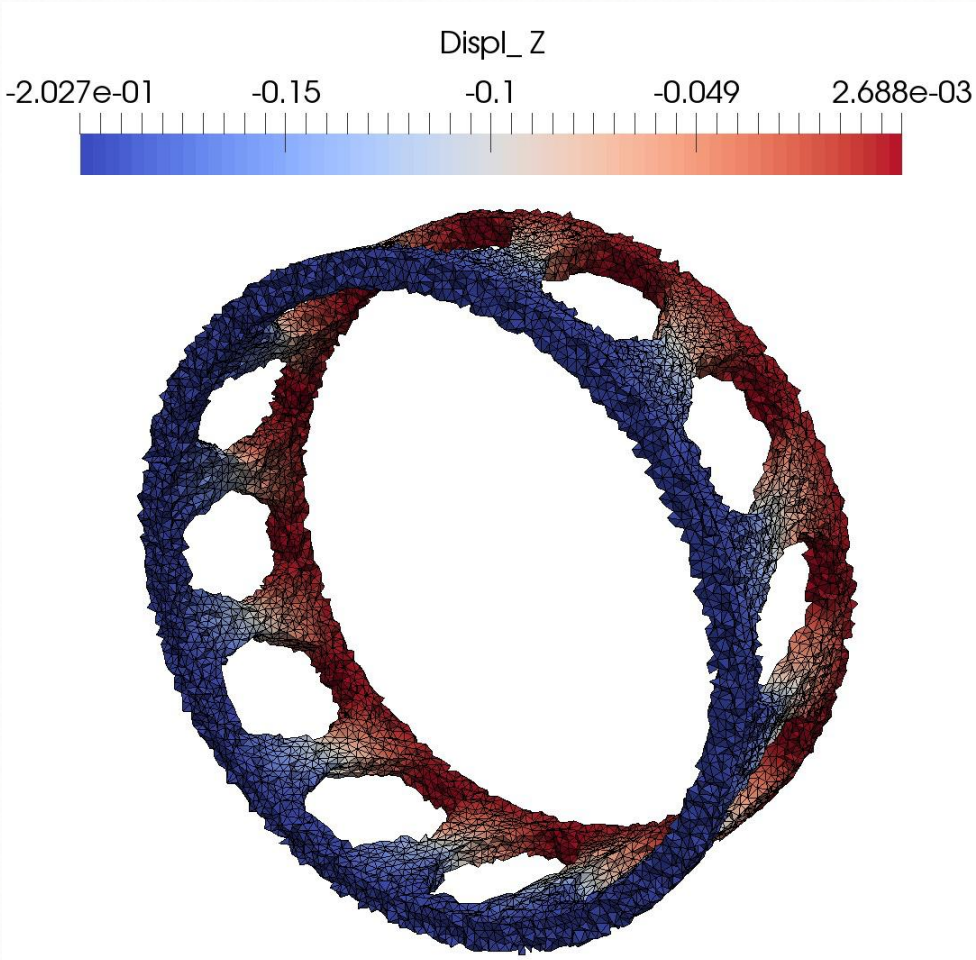

Deformed configuration of the set of active elements

Duke UNIVERSITY

The SBM for Solid Mechanics

An alternative cycle to CAD-Meshing-Computing

The intersection of the immersed geometry with the grid

The SBM for Solid Mechanics

An alternative cycle to CAD-Meshing-Computing

Deformation of the intersected immersed geometry

Duke UNIVERSITY

Credit of SBM for Solid Mechanics

Ph.D. thesis of Nabil M. Atallah

Duke UNIVERSITY

The SBM for Solid Mechanics

Key challenges:

- Imposition of traction (Neumann) boundary conditions
- Numerical stability of Neumann conditions
- Effect of geometric complexity (edges/corners, etc.) on numerical stability
- Computational cost vs. standard Finite Element Method

The SBM for Solid Mechanics

Static linear elasticity problem

$$0 = \boldsymbol{b} + \nabla \cdot \boldsymbol{\sigma}(\nabla^s \boldsymbol{u}) \quad \text{(governing eq.)}$$

$$\boldsymbol{u} = \boldsymbol{u}_D \quad \text{(displacement BCs)}$$

$$\boldsymbol{\sigma}(\nabla^s \boldsymbol{u})\boldsymbol{n} = \boldsymbol{t}_N \quad \text{(traction BCs)}$$

= 0 for piecewise linear fcn.s

$$\boldsymbol{\sigma}(\boldsymbol{\varepsilon}) = \mathbf{C}\,\boldsymbol{\varepsilon} \qquad \nabla^s \boldsymbol{u} = 1/2\left(\nabla \boldsymbol{u} + \nabla^t \boldsymbol{u}\right)$$

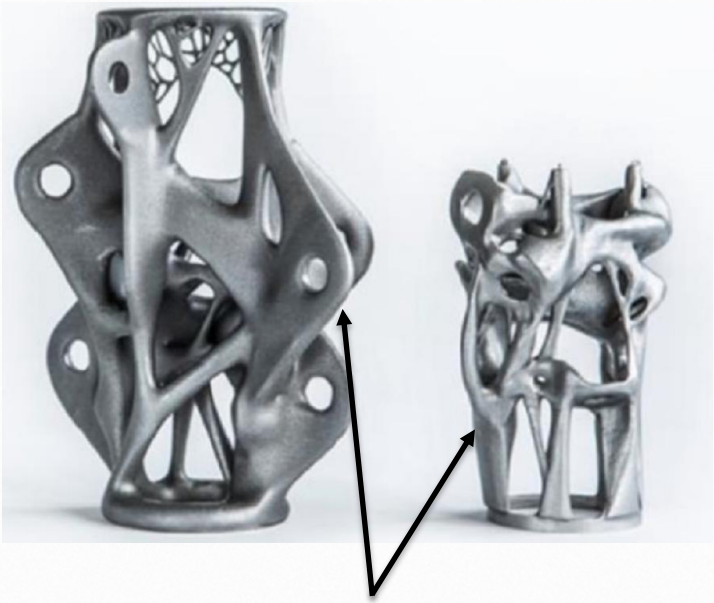

Neumann [Traction] BC

Idea: Recast the linear elasticity problem in mixed form:

$$0 = \boldsymbol{b} + \nabla \cdot \boldsymbol{\sigma}(\boldsymbol{\varepsilon}) \quad \text{(governing eq.)}$$

$$\boldsymbol{\varepsilon} = \nabla^s \boldsymbol{u} \quad \text{(strain eq.)}$$

$$\boldsymbol{u} + (\nabla \boldsymbol{u})\boldsymbol{d} = \boldsymbol{u}_D \quad \text{(displacement BCs)}$$

$$(\boldsymbol{\sigma} + \nabla \boldsymbol{\sigma}\, \boldsymbol{d})\,\boldsymbol{n} = (\mathbf{C}\,\boldsymbol{\varepsilon} + \nabla(\mathbf{C}\,\boldsymbol{\varepsilon})\,\boldsymbol{d})\,\boldsymbol{n} = \boldsymbol{t}_N \quad \text{(traction BCs)}$$

$\neq 0$

Duke UNIVERSITY

Efficient Implementation of SBM for Solid Mechanics

Apply the mixed formulation *only* on a layer one-element thick

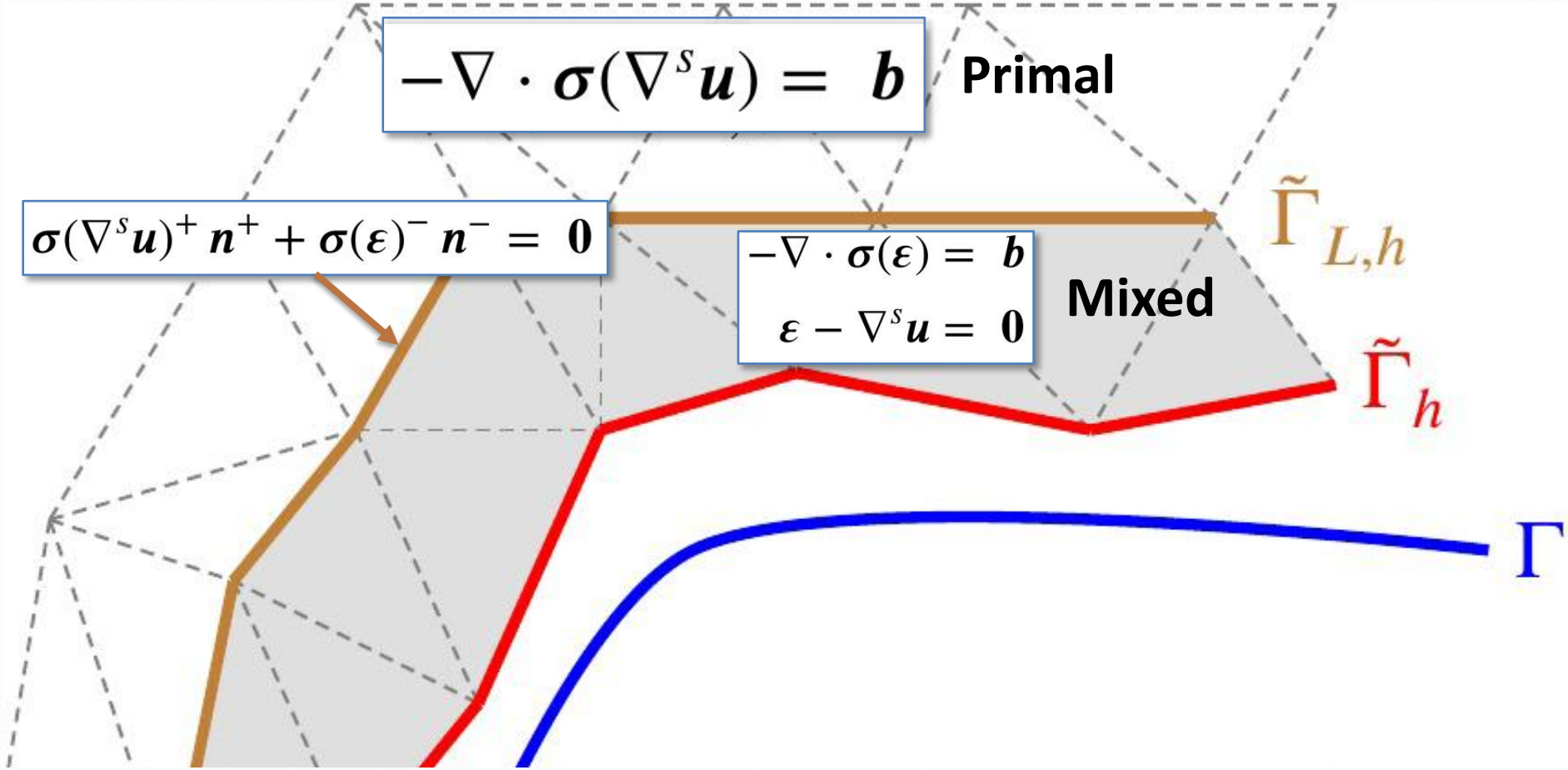

Duke UNIVERSITY

The SBM for Domains with Corners

How to handle multiple boundary conditions near corners/edges?

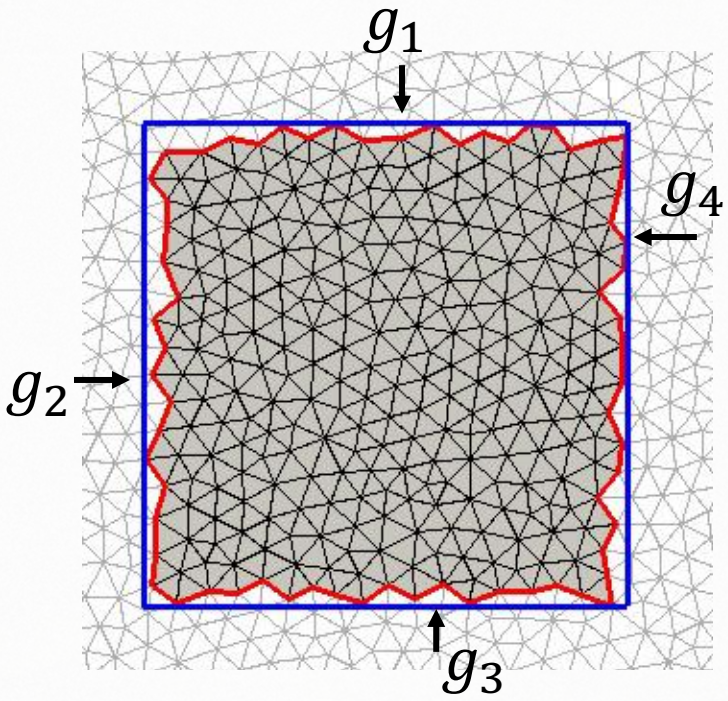

True domain and boundary

?

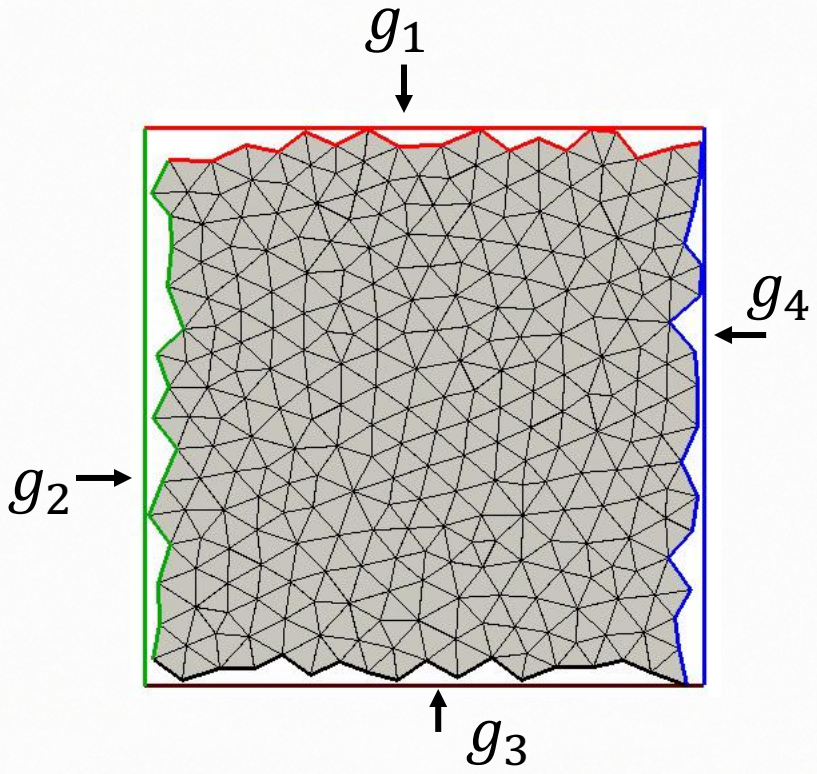

Mapping boundary conditions

Duke UNIVERSITY

Cook's Membrane (Compressible Elasticity)

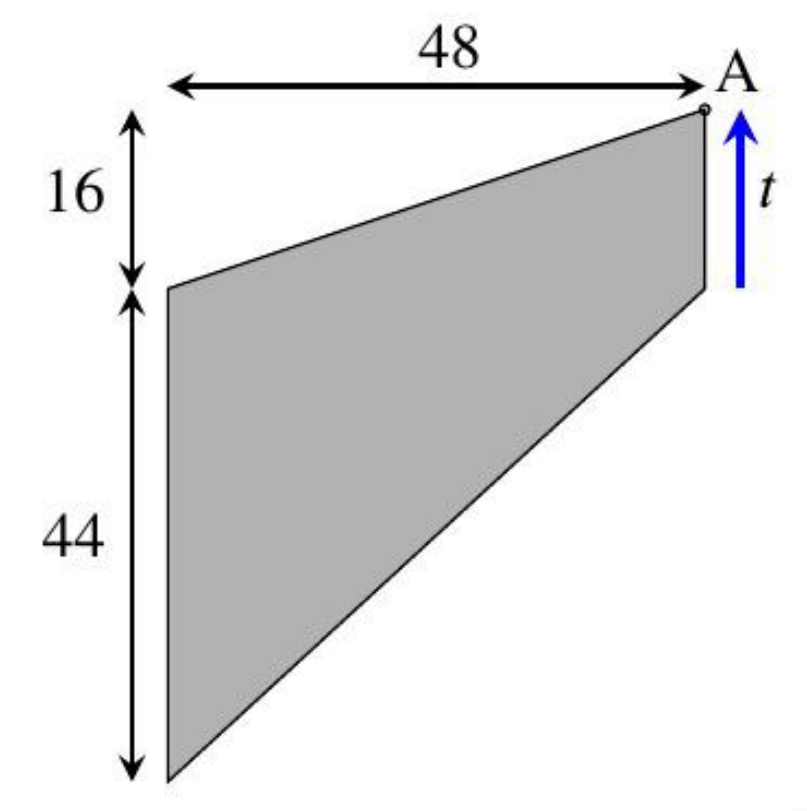

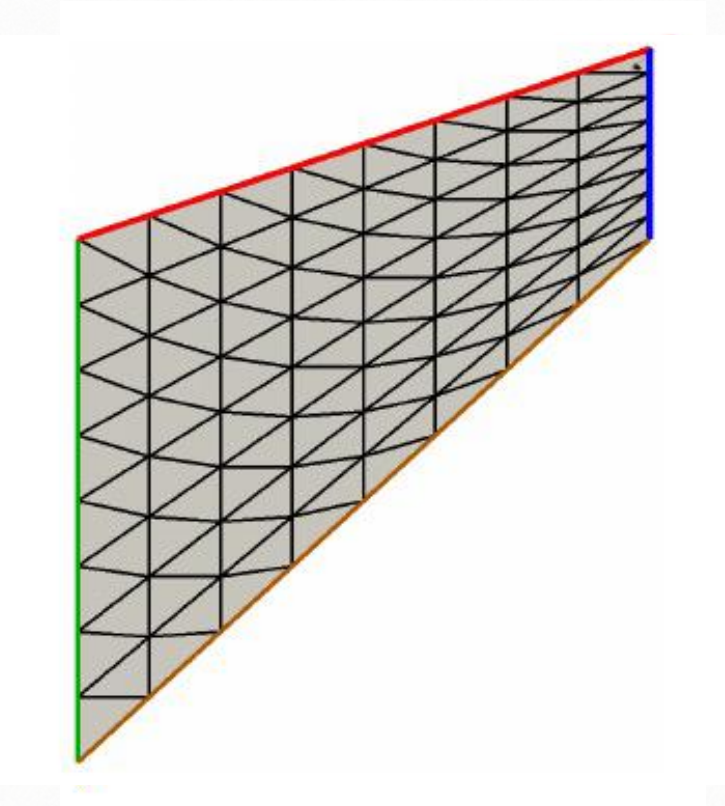

Young's modulus $\mathrm{E} = 200 \cdot 10^9$ Pa and Poisson's ratio $\nu = 0.3$.

Duke UNIVERSITY

Cook's Membrane (Compressible Elasticity)

Tip displacement convergence

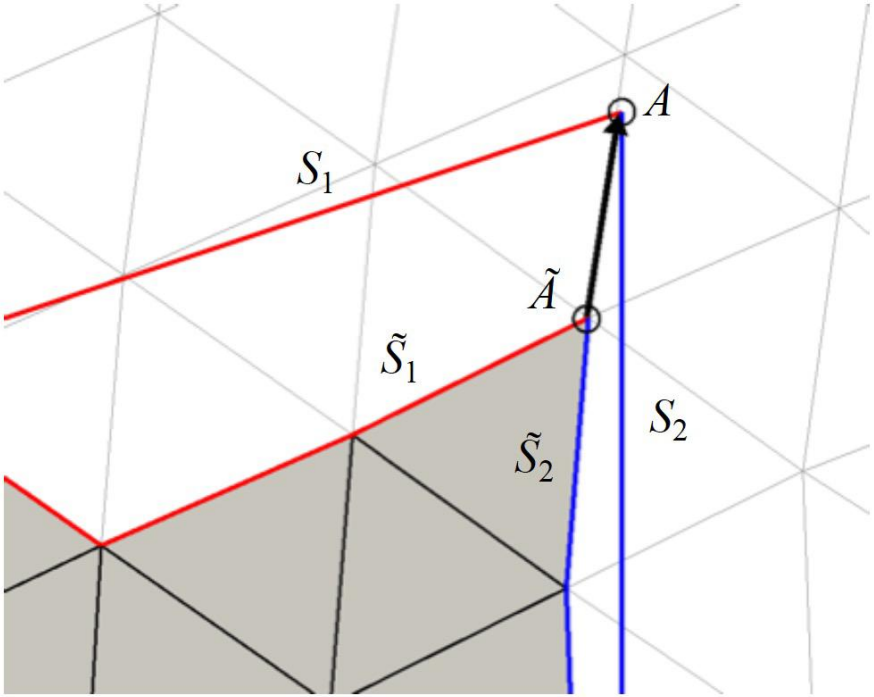

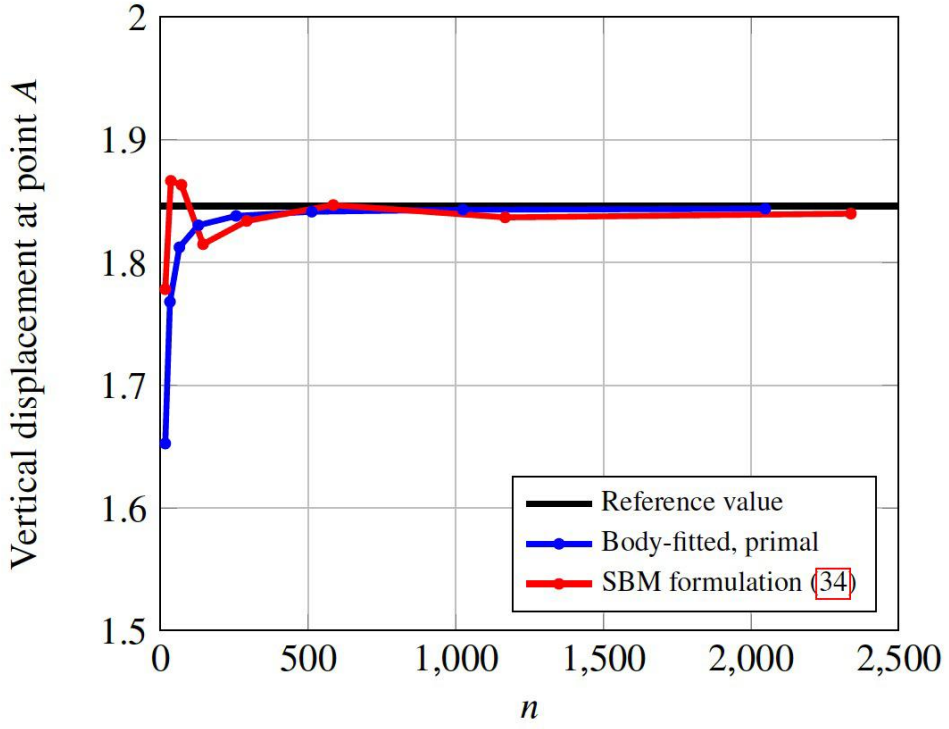

$$u_y|_A = \frac{1}{n_A} \sum_{i=1}^{n_A} (u_y^{(i)} + \nabla u_y^{(i)} \boldsymbol{d})|_{\tilde{A}}$$

(b) Vertical displacement at point A, where n is the total number of edges along $S_1 \cup S_2$, for the primal body-fitted formulation, or the total number of edges along $\tilde{S}_1 \cup \tilde{S}_2$

Duke UNIVERSITY

Three-Dimensional Performance Assessment

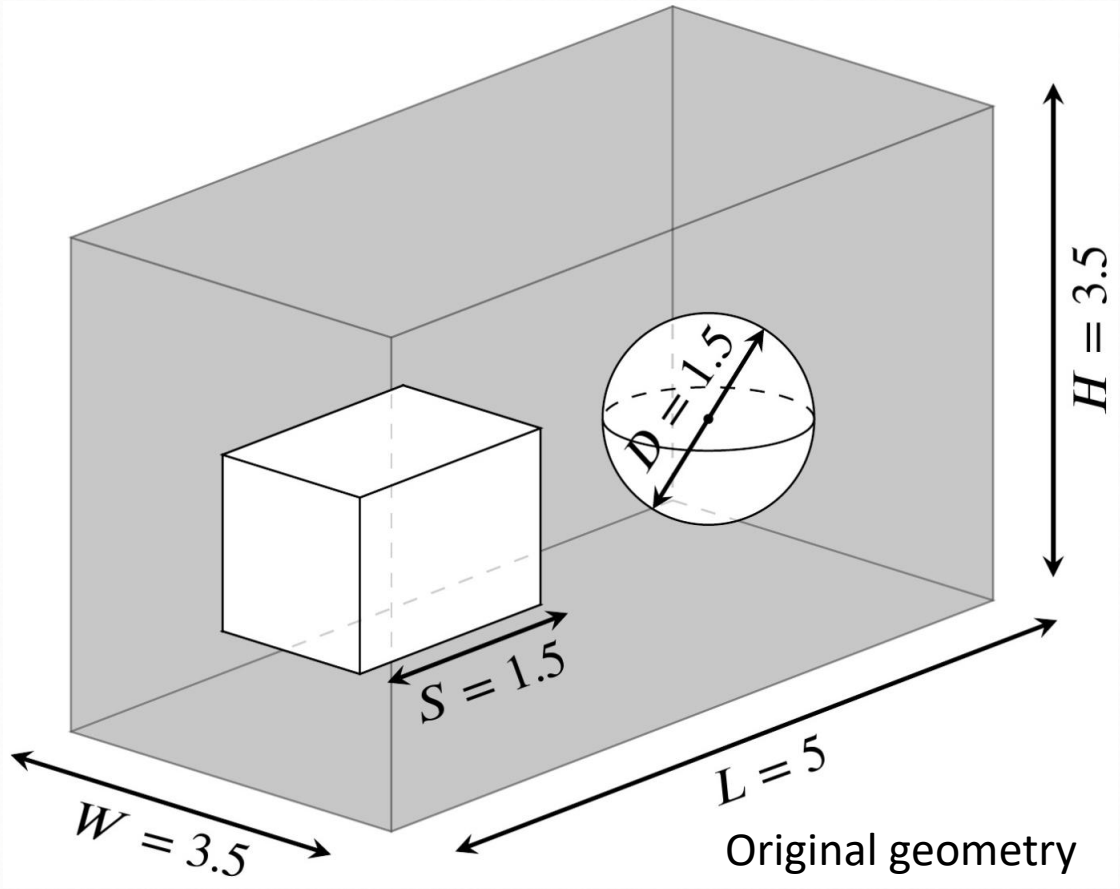

Original geometry

Young's modulus= 200.10^6 MPa

Poisson ratio = 0.3

Boundary conditions

- **Strong enforcement of Dirichlet conditions on outer boundary**
- **Traction conditions on inner boundaries**

$$\boldsymbol{u} = \begin{Bmatrix} u_x \\ u_y \\ u_z \end{Bmatrix} = \frac{1}{10} \begin{Bmatrix} -\cos(\pi x)\sin(\pi y)\cos(\pi z) \\ \sin(\pi x/7)\sin(\pi y/3)\cos(\pi z/5) \\ \sin(\pi xyz/2) \end{Bmatrix}$$

Three-Dimensional Performance Assessment

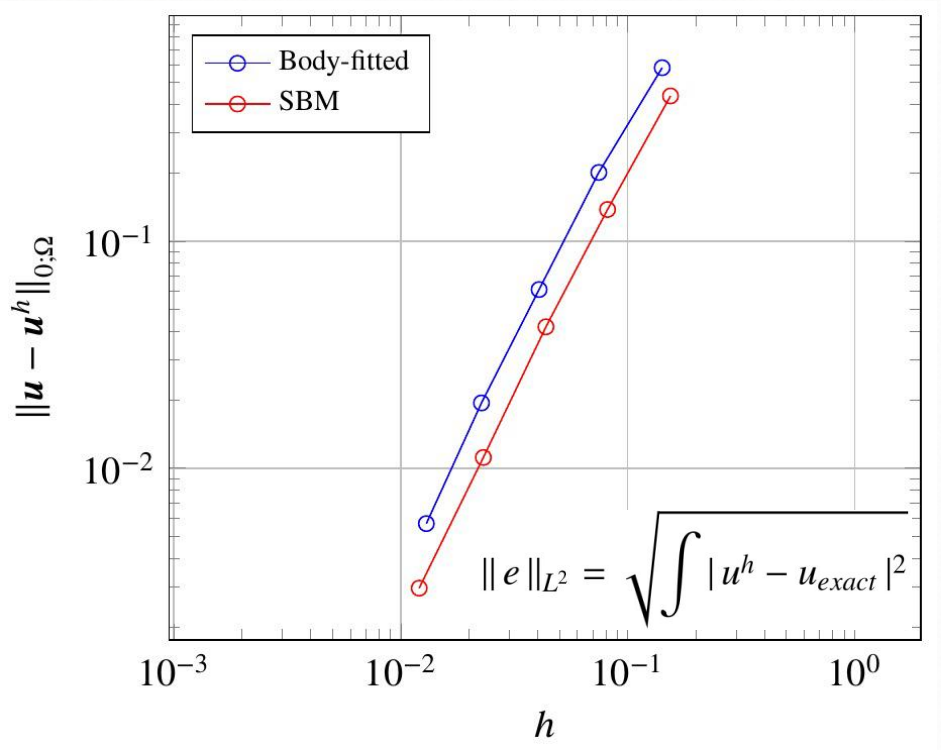

L^2-error vs mesh size

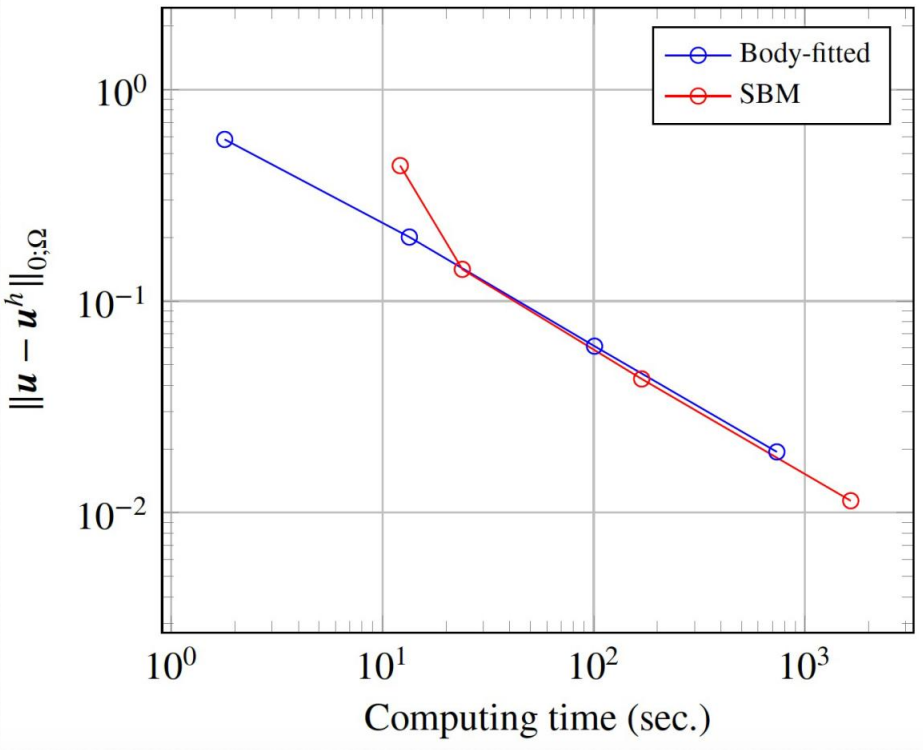

L^2-error vs computing time

SBM costs you like a standard body-fitted FEM, but... no meshing overhead

Duke UNIVERSITY

Pulling/Twisting of Three-Dimensional Stent

No body force

Boundary conditions

- ***u*** = 0 (left),
- ***u*** = {2.5 y, -2.5 x, -0.5}(right)
- Traction free BC at all other boundaries

Poisson ratio = 0.452

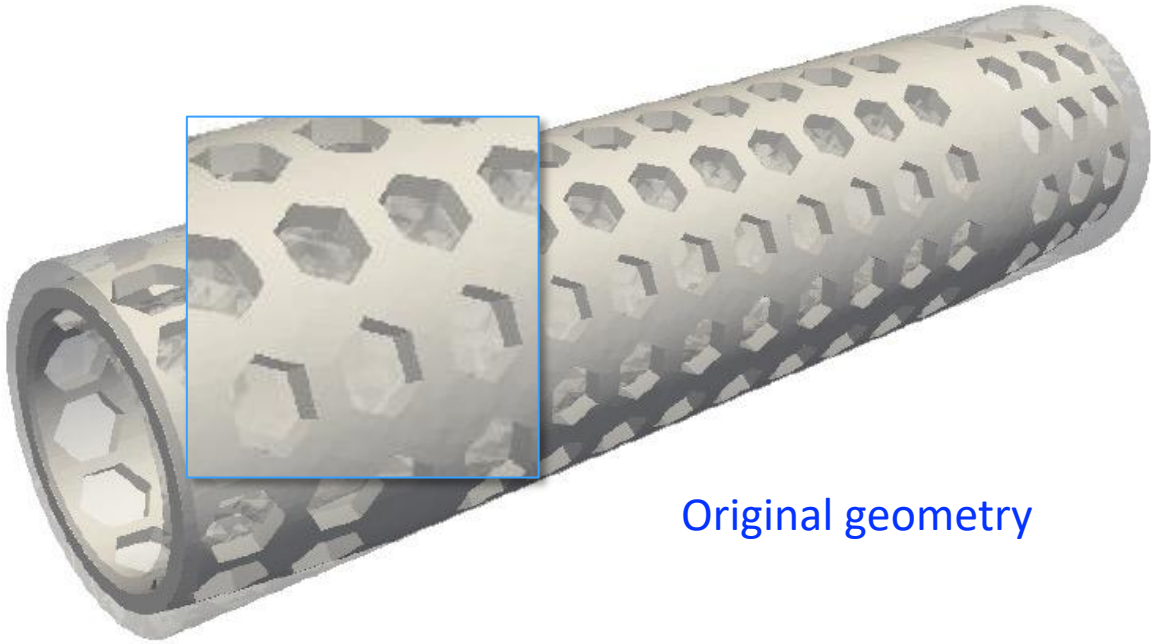

Original geometry

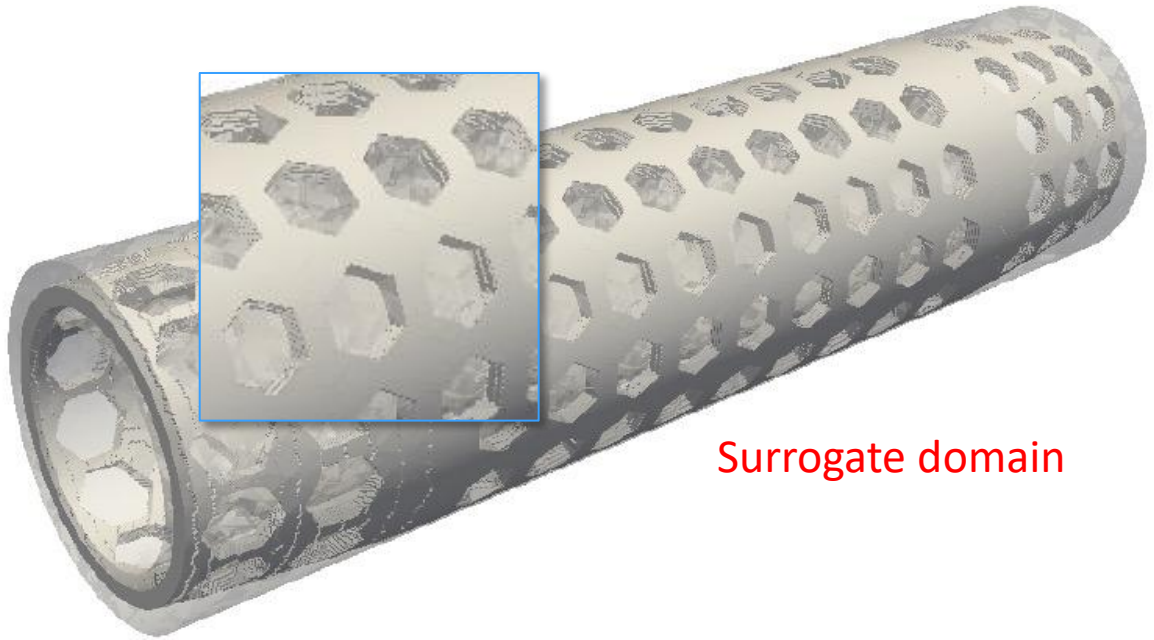

Surrogate domain

Duke UNIVERSITY

Pulling/Twisting of Three-Dimensional Stent

Solution (displacement)

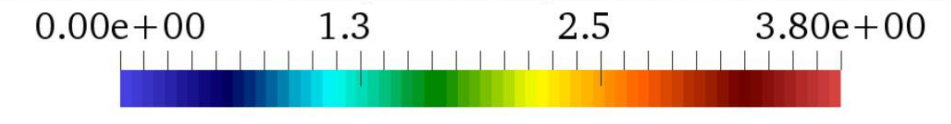

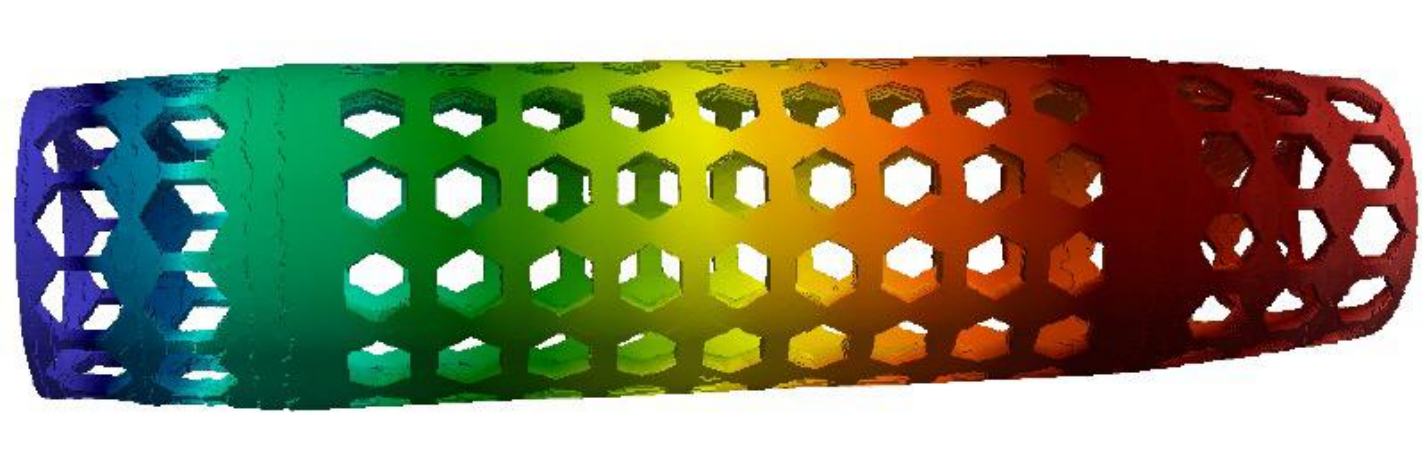

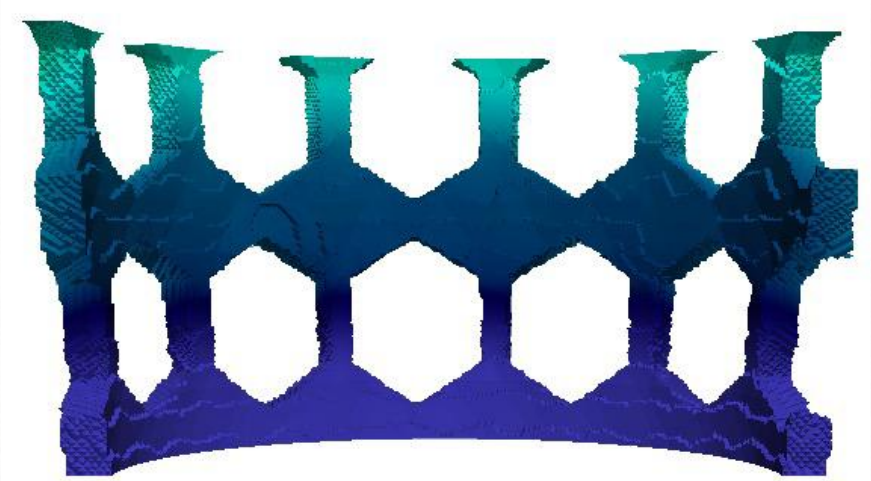

Duke UNIVERSITY

Compression of 3D Porous Rock Specimen

Rock REV: L = 0.505, W =0.3, D = 0.27

No body force

Boundary conditions

- ***u*** = 0 (bottom),
- ***u*** = -5E-04 (top)
- Traction free BC at all other boundaries

Poisson ratio = 0.452

Total elements = 5.2 million

Total active elements = 3.46 million

Total cores = 240

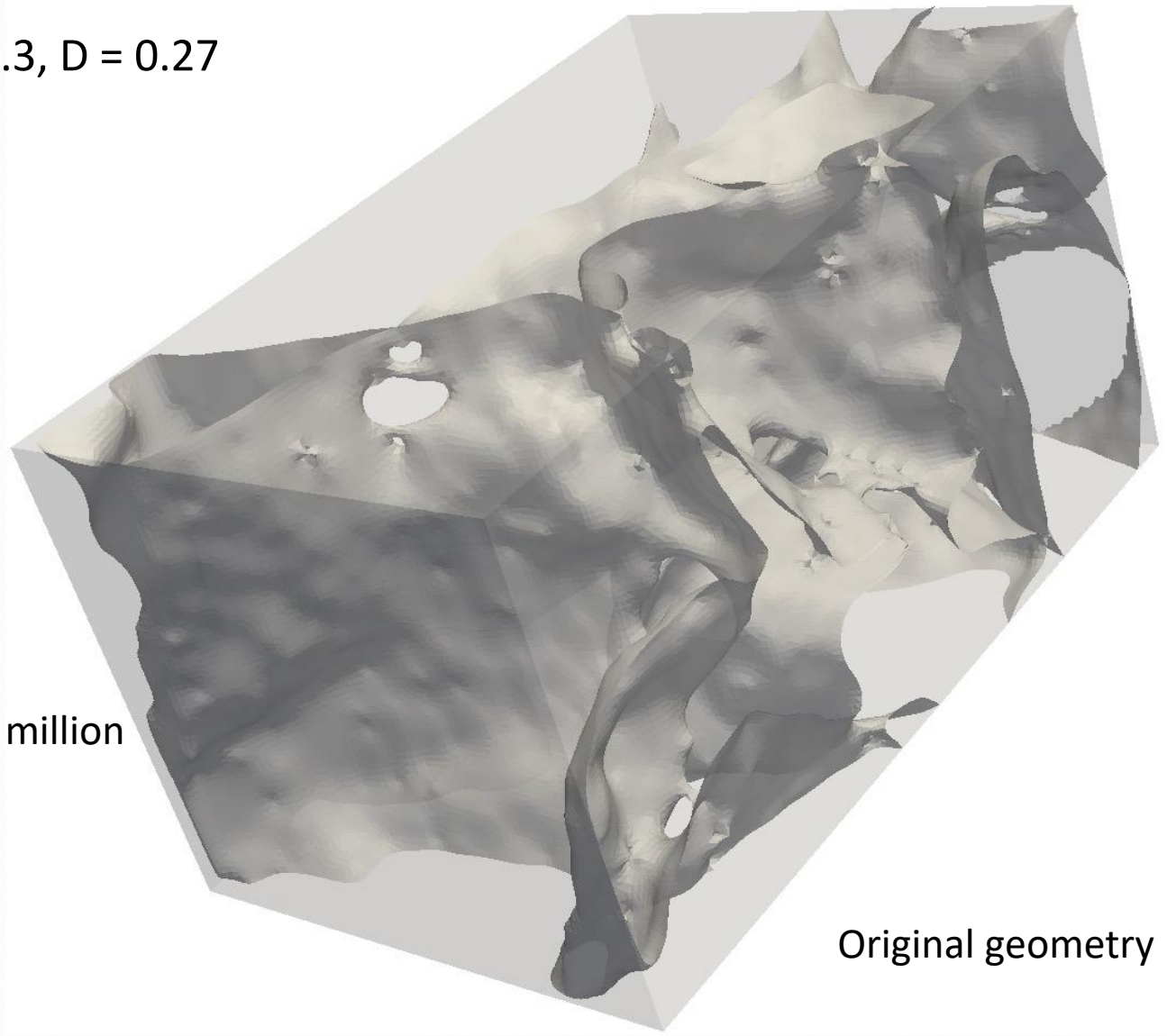

Original geometry

Compression of 3D Porous Rock Specimen

Rock REV: L = 0.505, W =0.3, D = 0.27

Setup time:

- Compute intersection between STL surface and background grid.
- Generate surrogate domain and boundaries.
- Calculate distance vector **d**.

Setup time = 220 seconds!

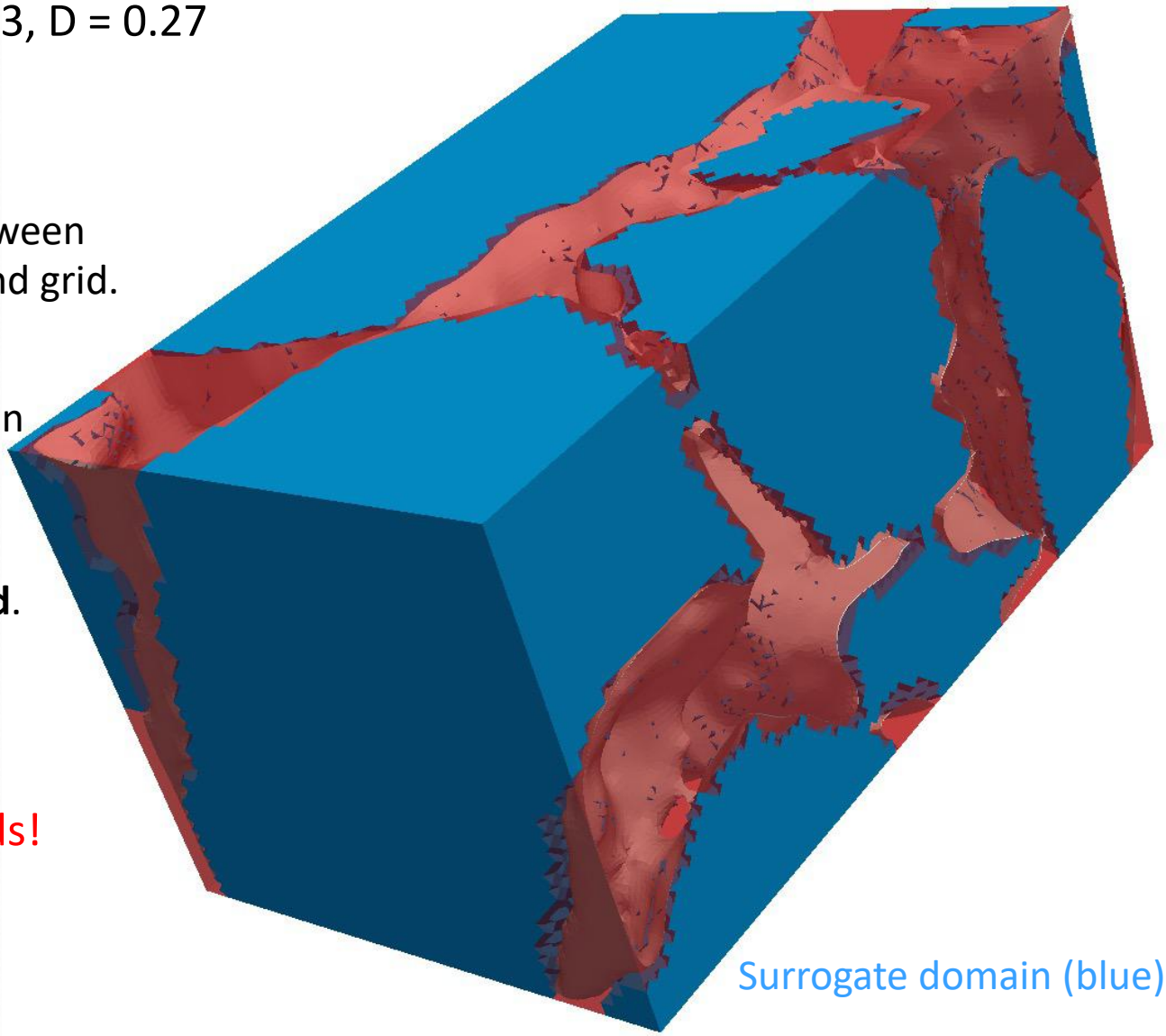

Surrogate domain (blue)

Compression of 3D Porous Rock Specimen

Rock REV: L = 0.505, W =0.3, D = 0.27

Setup time:

- Compute intersection between STL surface and background grid.
- Generate surrogate domain and boundaries.
- Calculate distance vector **d**.

Setup time = 220 seconds!

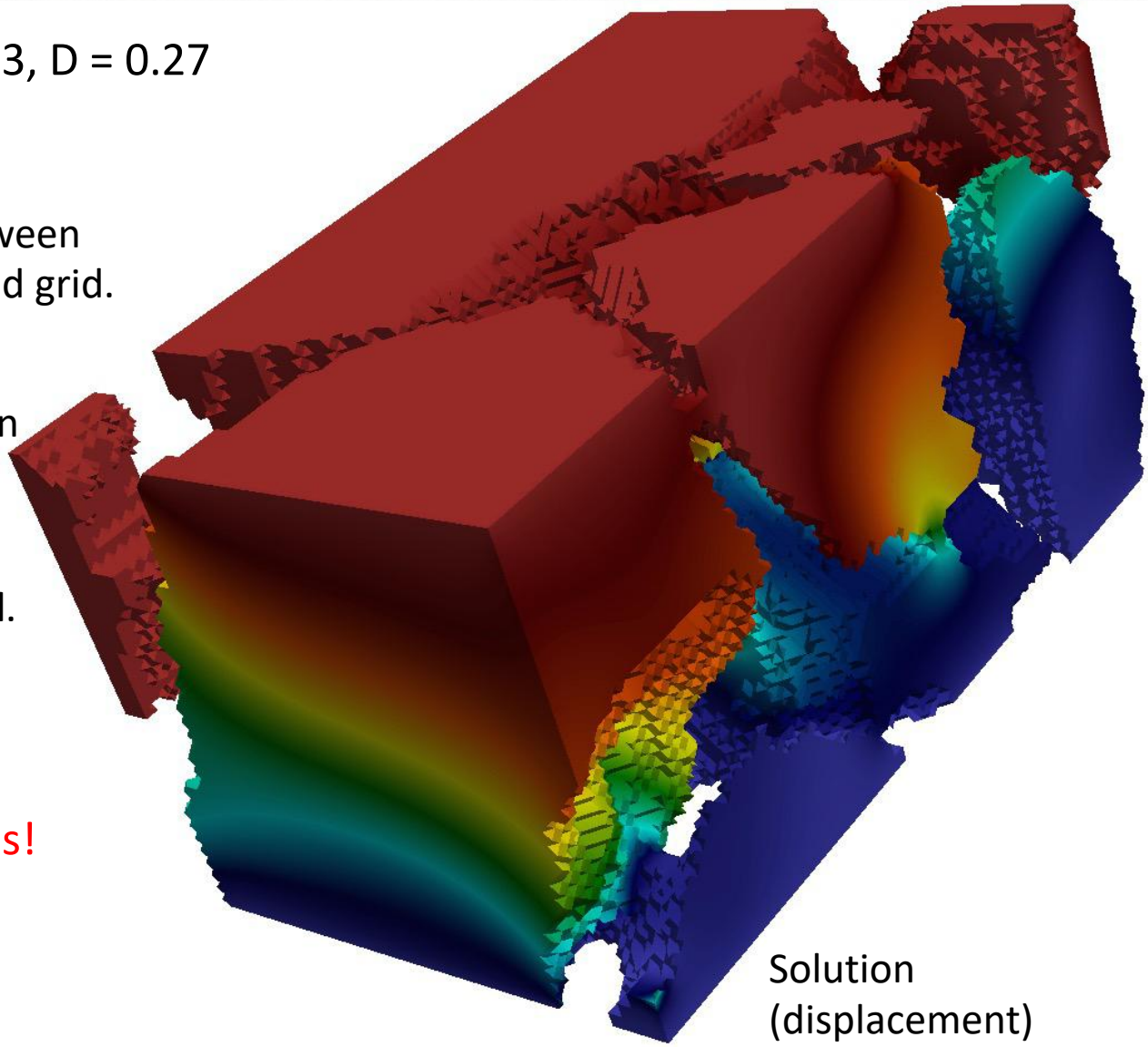

Solution (displacement)

Compression of 3D Porous Rock Specimen

Rock REV: L = 0.50

No body force

Boundary conditions

- $\boldsymbol{u} = 0$ (left),
- $\boldsymbol{u}$ = -5E-04 (right)
- Traction free BC at other boundaries

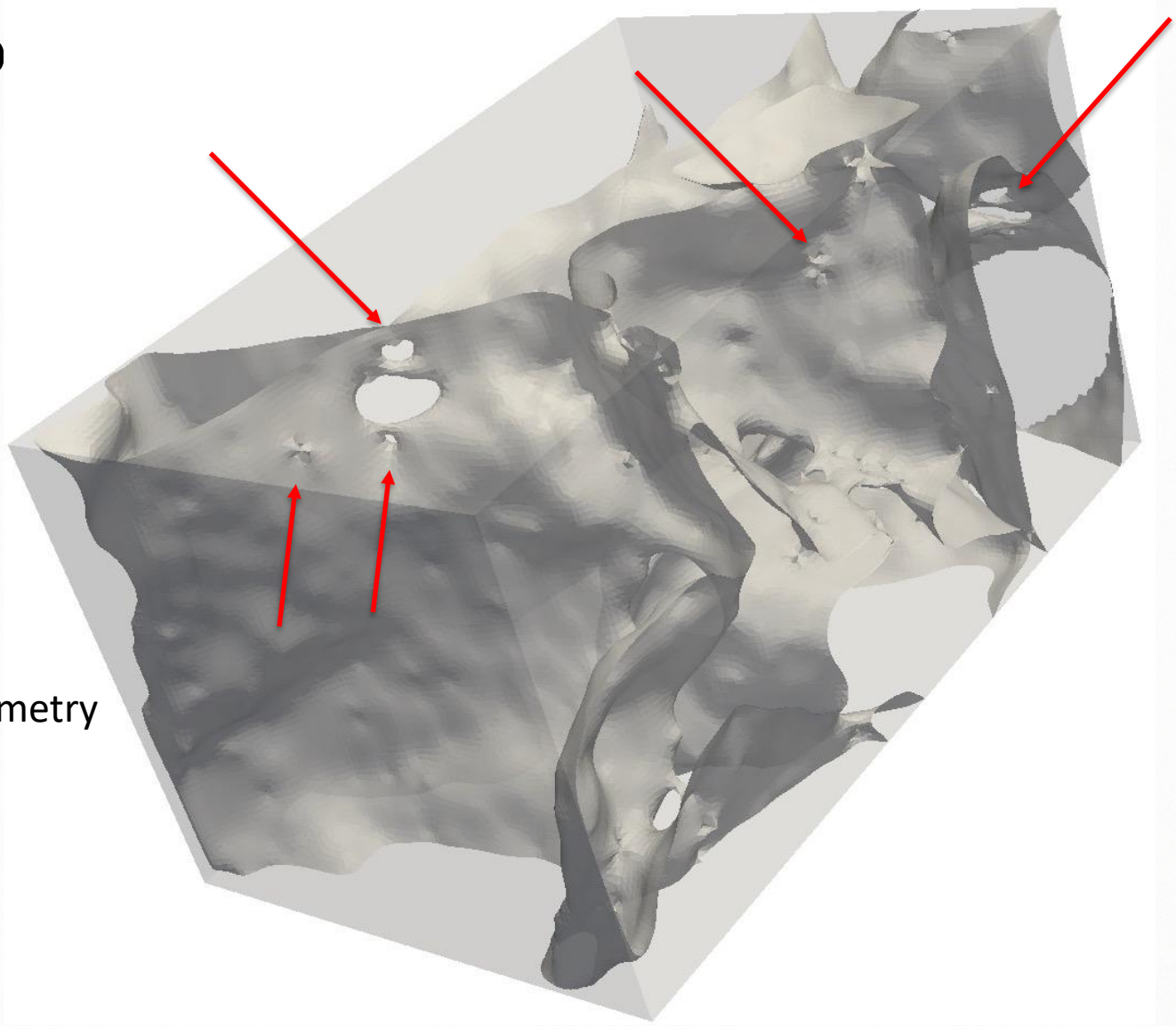

Original geometry

Compression of 3D Porous Rock Specimen

Rock REV: L = 0.505, W =0.3, D = 0.27

No body force

Boundary conditions

- $\boldsymbol{u} = 0$ (left),
- $\boldsymbol{u}$ = -5E-04 (right)
- Traction free BC at all other boundaries

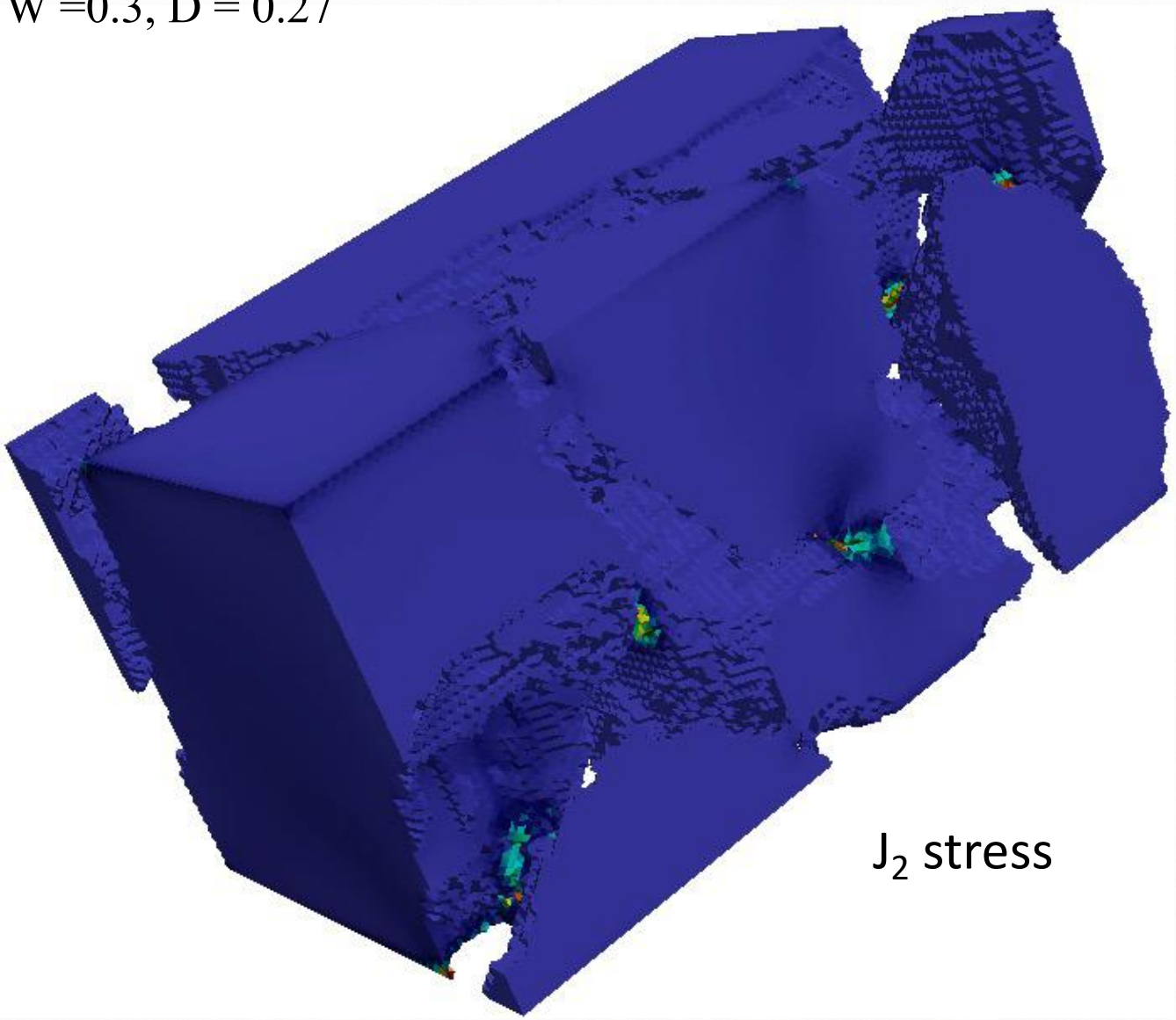

J_2 stress

Duke UNIVERSI

Compression of 3D Porous Rock Specimen

Rock REV: L = 0.505, W =0.3, D = 0.27

No body force

Boundary conditions

- $\boldsymbol{u} = 0$ (left),
- $\boldsymbol{u}$ = -5E-04 (right)
- Traction free BC at all other boundaries

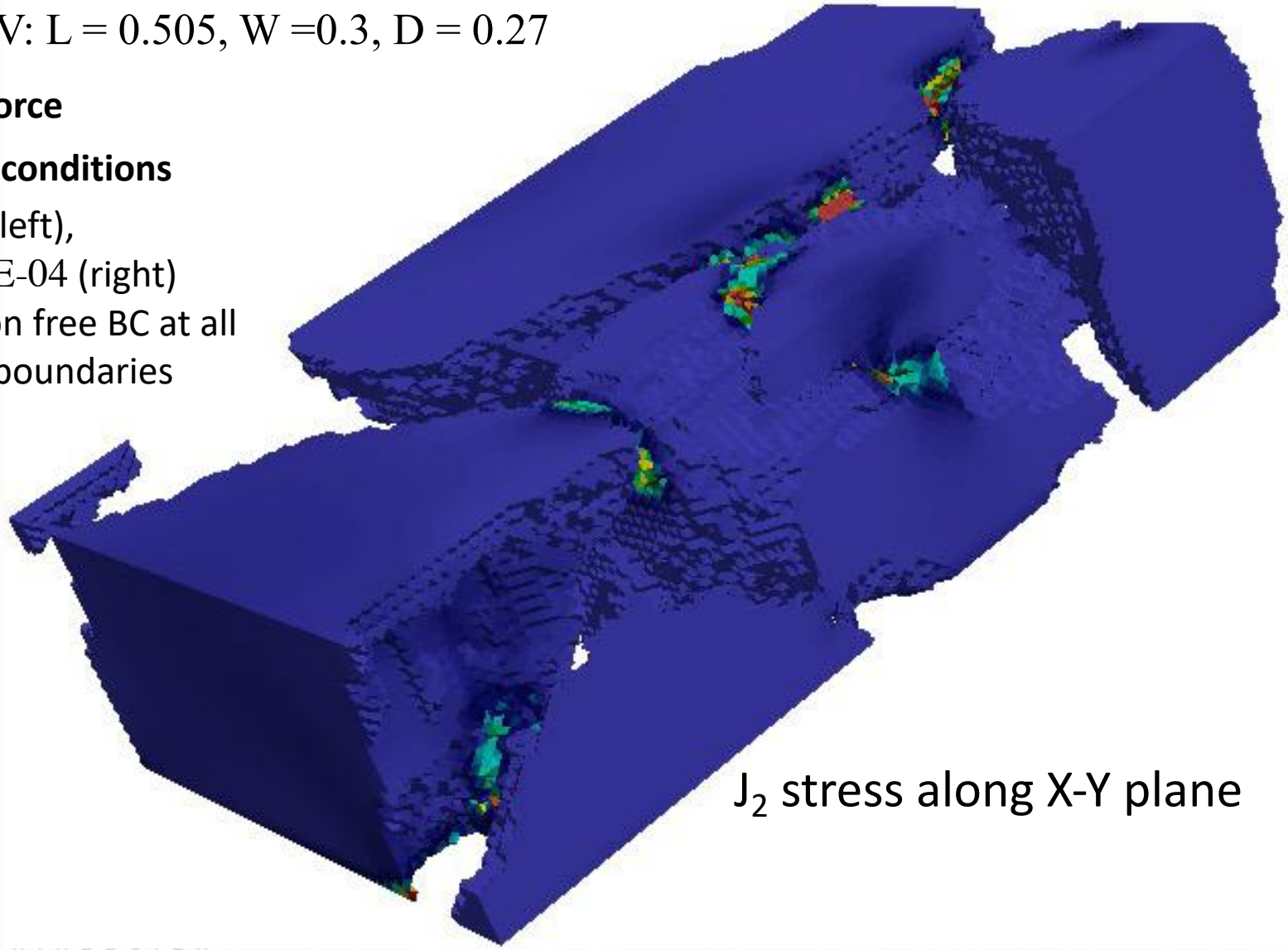

J_2 stress along X-Y plane

Compression of 3D Porous Rock Specimen

Rock REV: L = 0.505, W =0.3, D = 0.27

No body force

Boundary conditions

- $\boldsymbol{u} = 0$ (left),
- $\boldsymbol{u}$ = -5E-04 (right)
- Traction free BC at all other boundaries

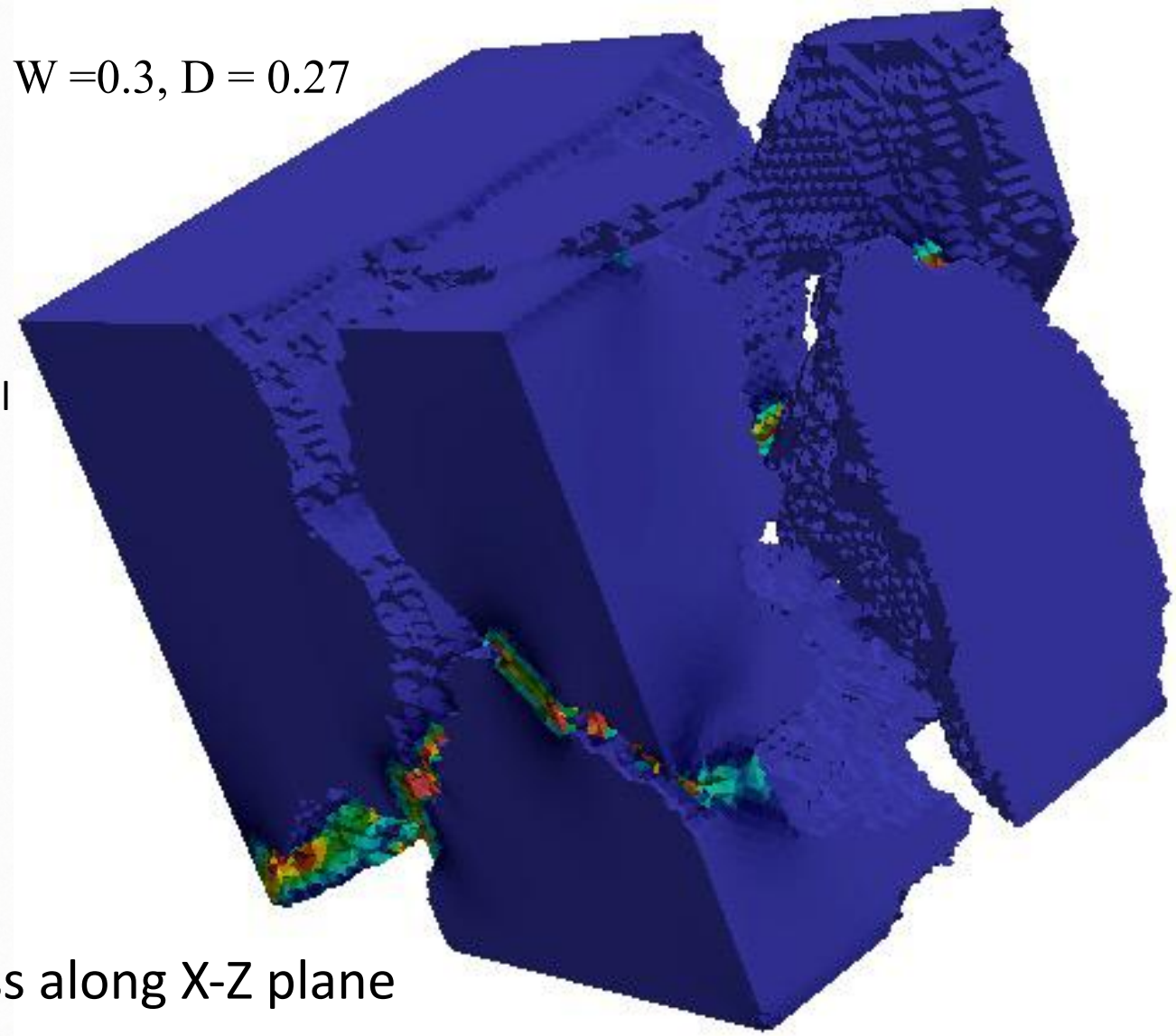

J_2 stress along X-Z plane

Compression of 3D Porous Rock Specimen

Rock REV: L = 0.505, W =0.3, D = 0.27

No body force

Boundary conditions

- $\boldsymbol{u} = 0$ (left),
- $\boldsymbol{u}$ = -5E-04 (right)
- Traction free BC at all other boundaries

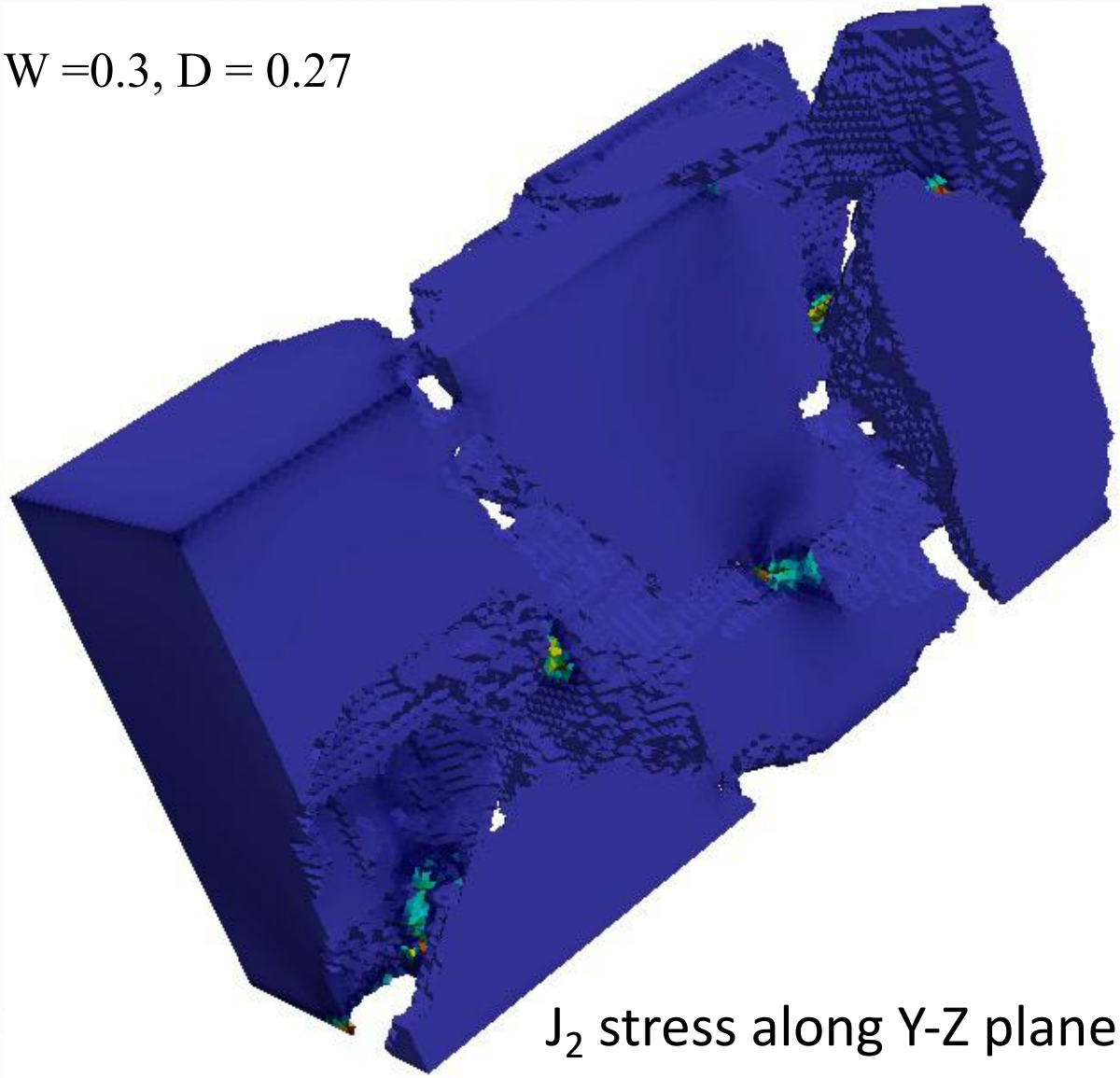

J_2 stress along Y-Z plane

SBM Simulations of Thermo-Mechanics

“Sponge-like” boundary test

Geometry

Surrogate boundary

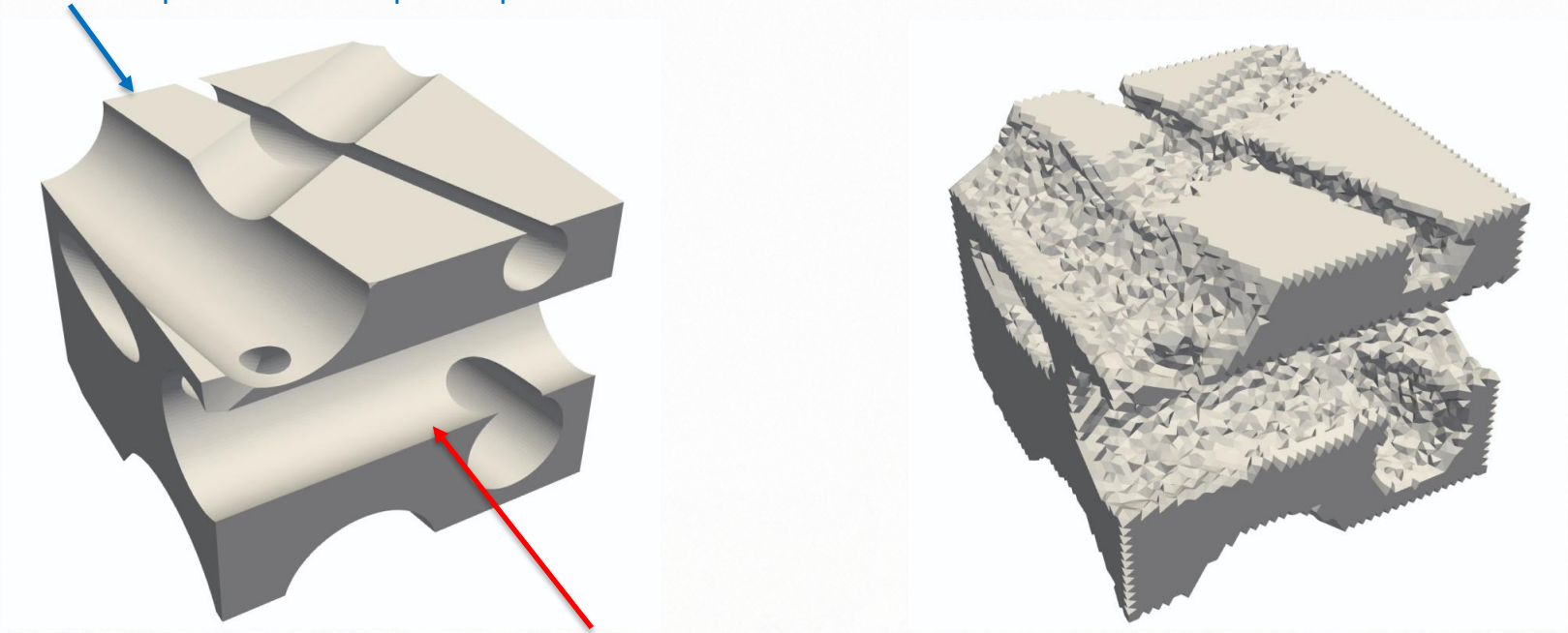

SBM Simulations of Thermo-Mechanics

“Sponge-like” boundary test

Temperature T, $t = 5.03$

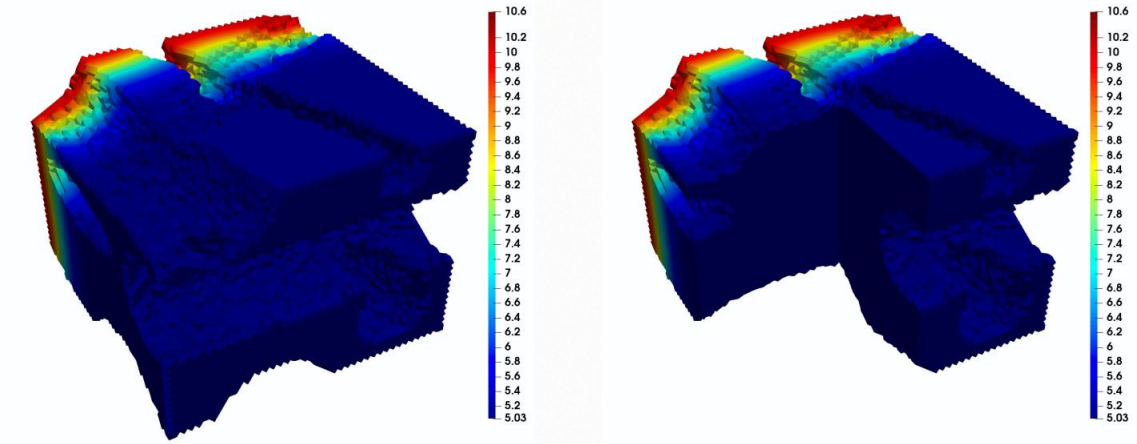

Temperature T, $t = 10$

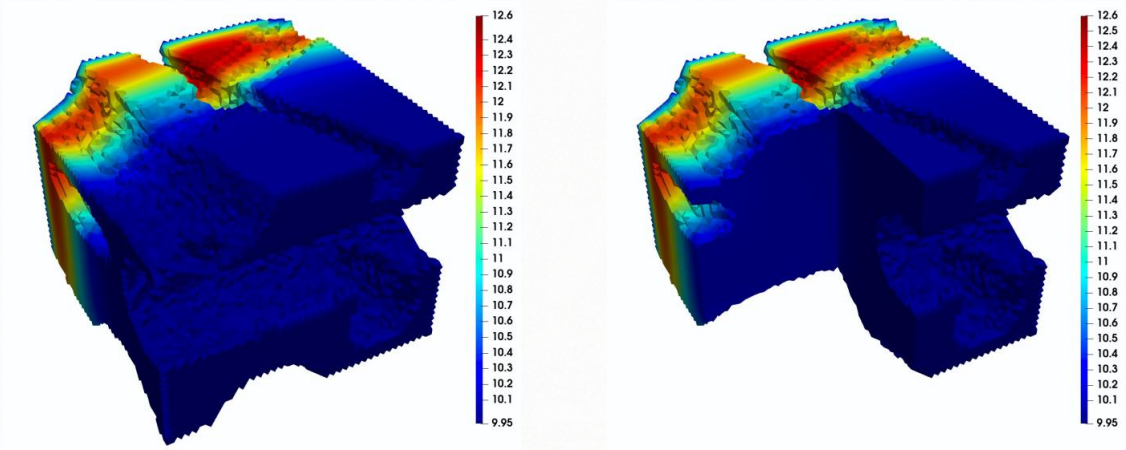

SBM Simulations of Thermo-Mechanics

“Sponge-like” boundary test

Displacement $\boldsymbol{u}$, $t = 5.03$

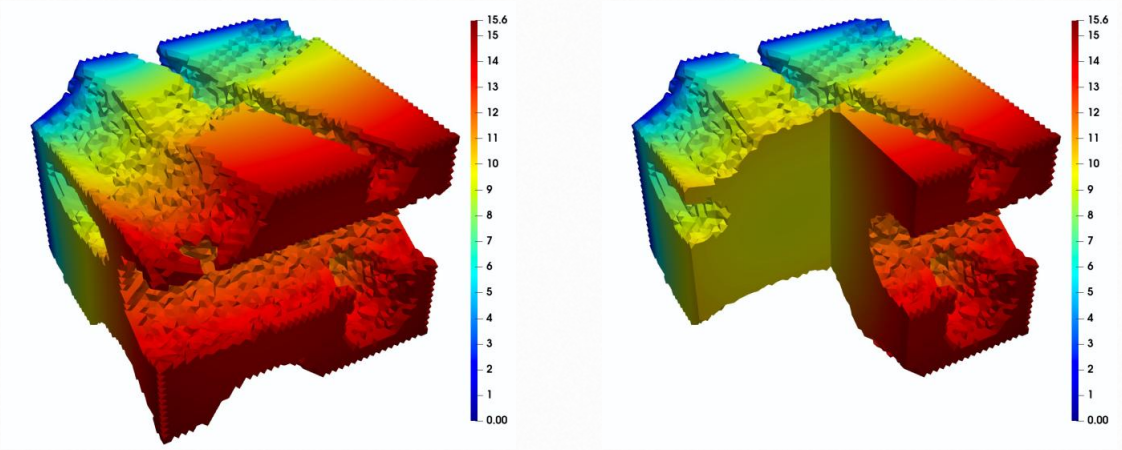

Displacement $\boldsymbol{u}$, $t = 10$

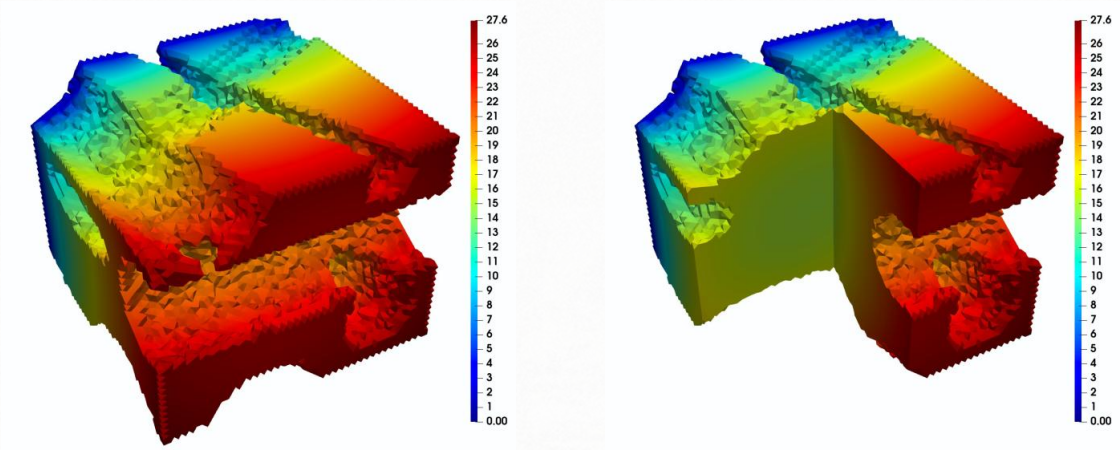

SBM Simulations of Thermo-Mechanics

Simulation on a complex structure (Naval Research Laboratory):

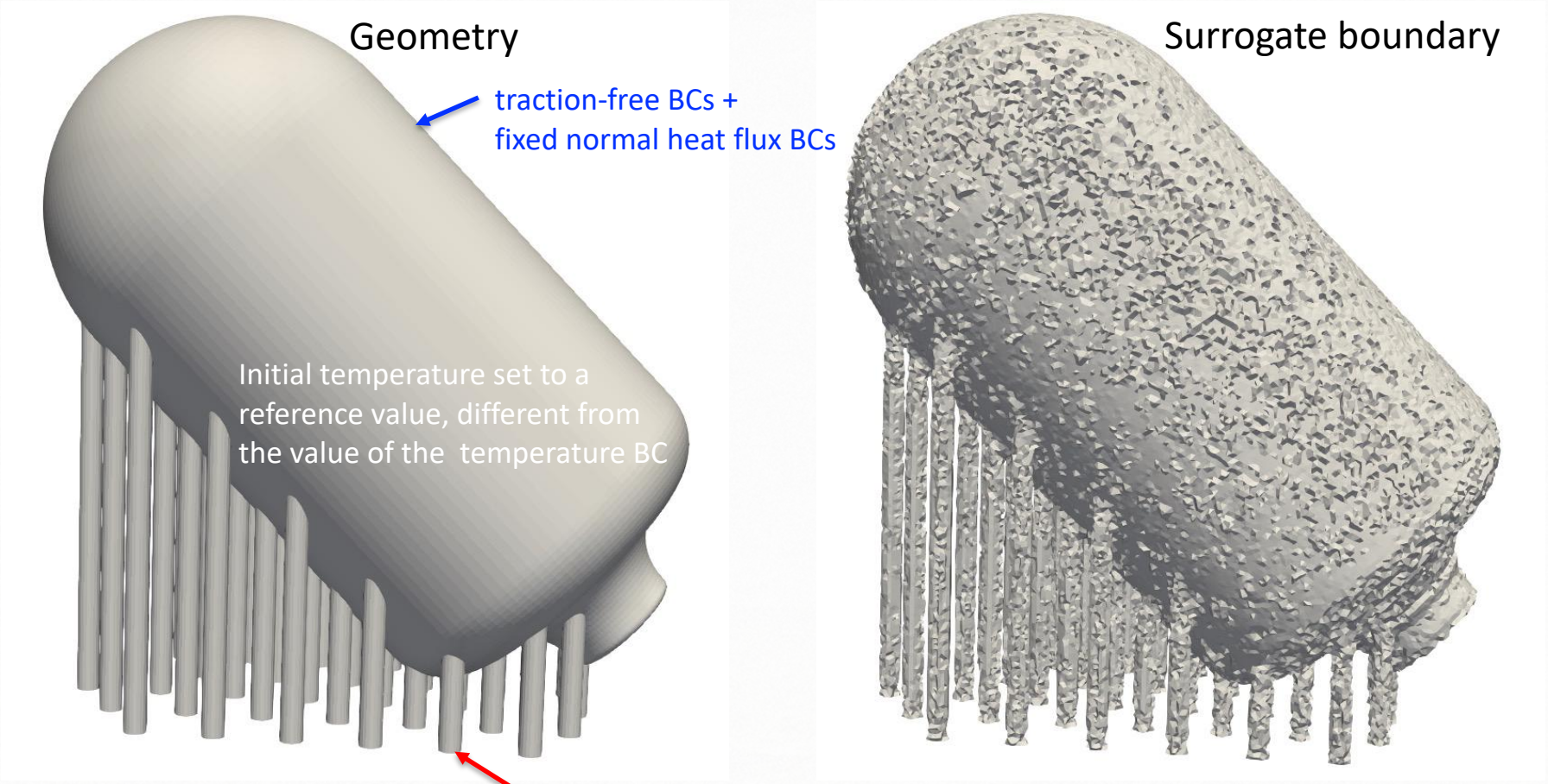

SBM Simulations of Thermo-Mechanics

Simulation on a complex structure (Naval Research Laboratory):

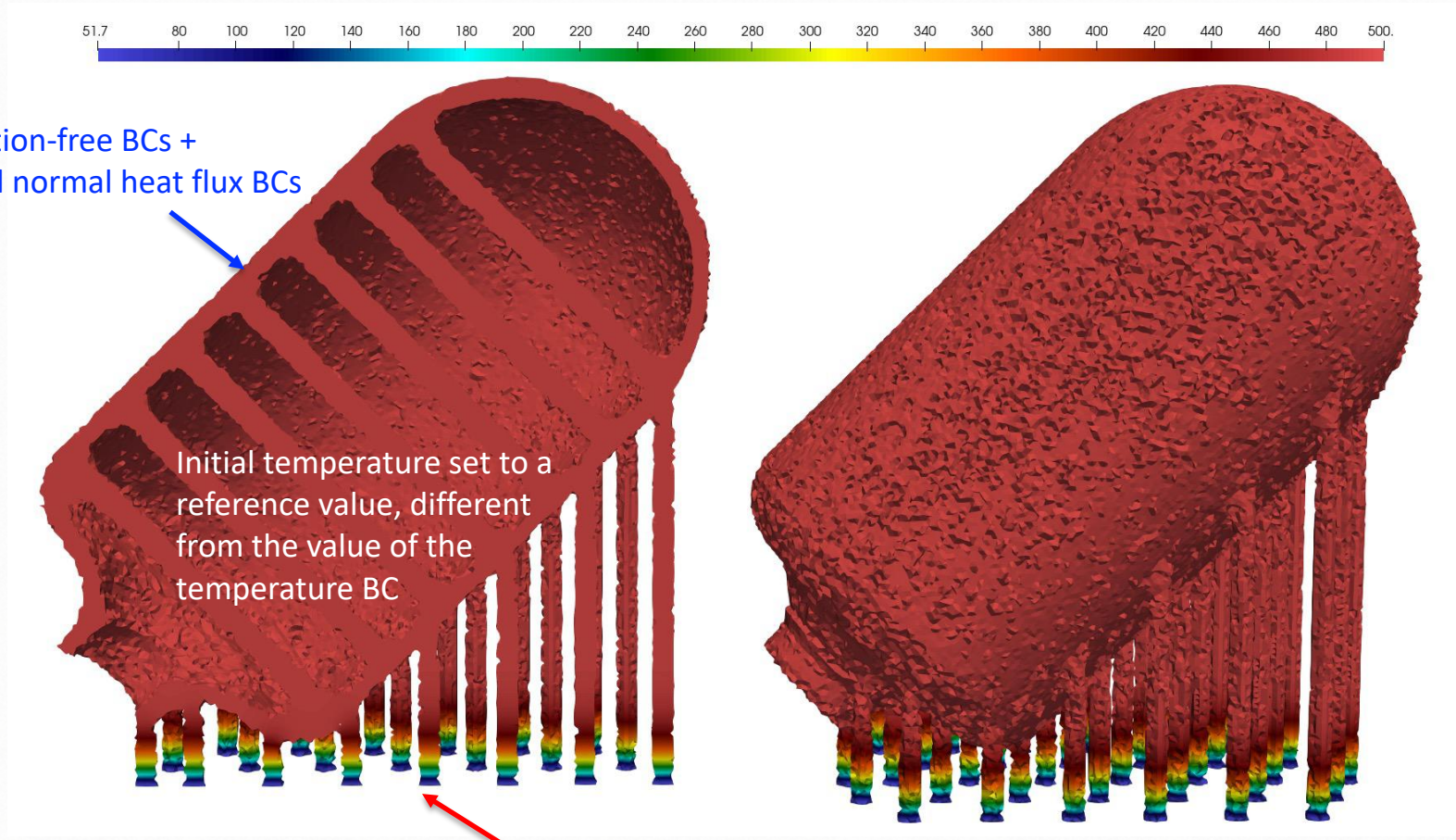

Duke UNIVERSITY

SBM Simulations of Thermo-Mechanics

Simulation on a complex structure (Naval Research Laboratory):

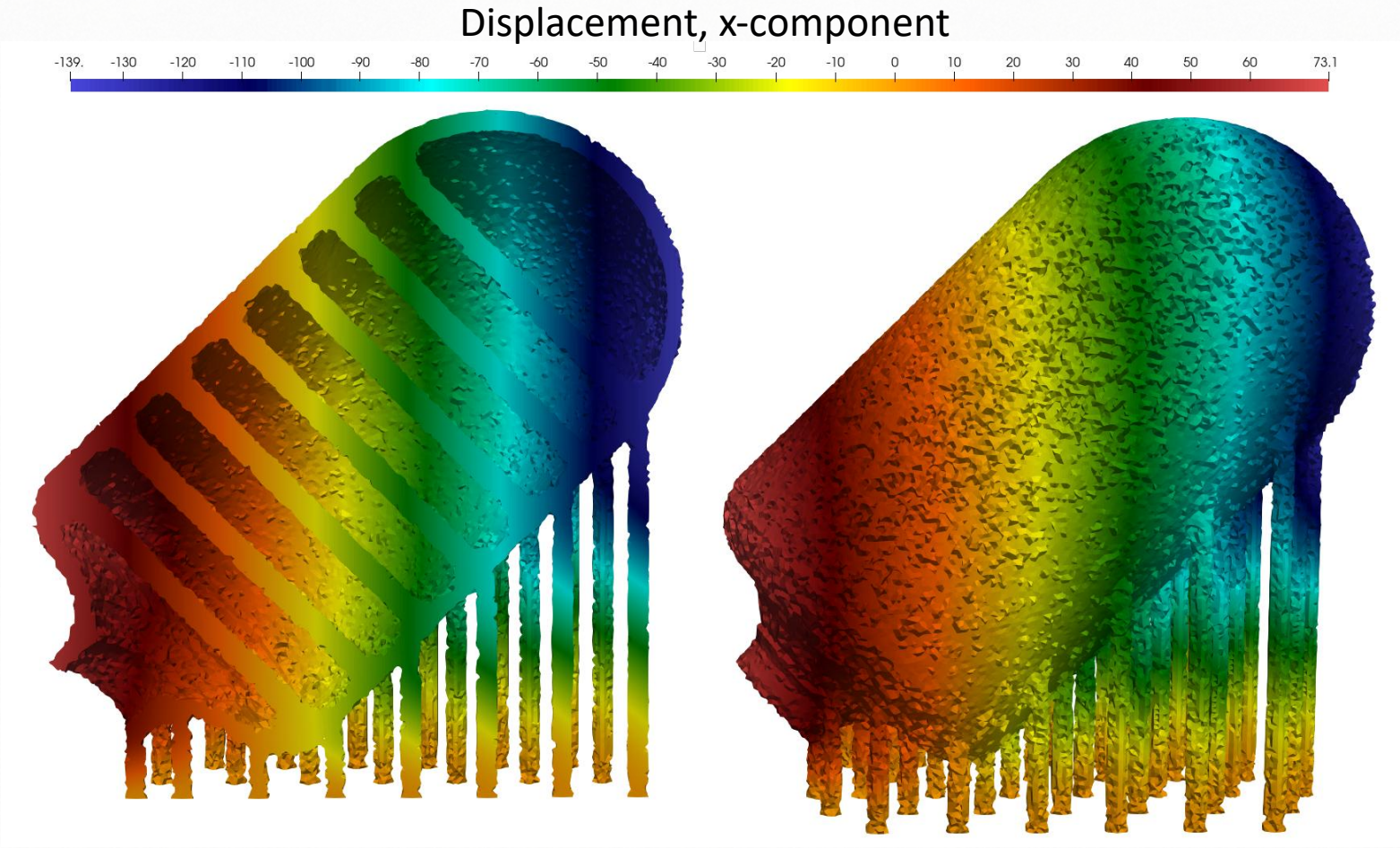

SBM Simulations of Thermo-Mechanics

Simulation on a complex structure (Naval Research Laboratory):

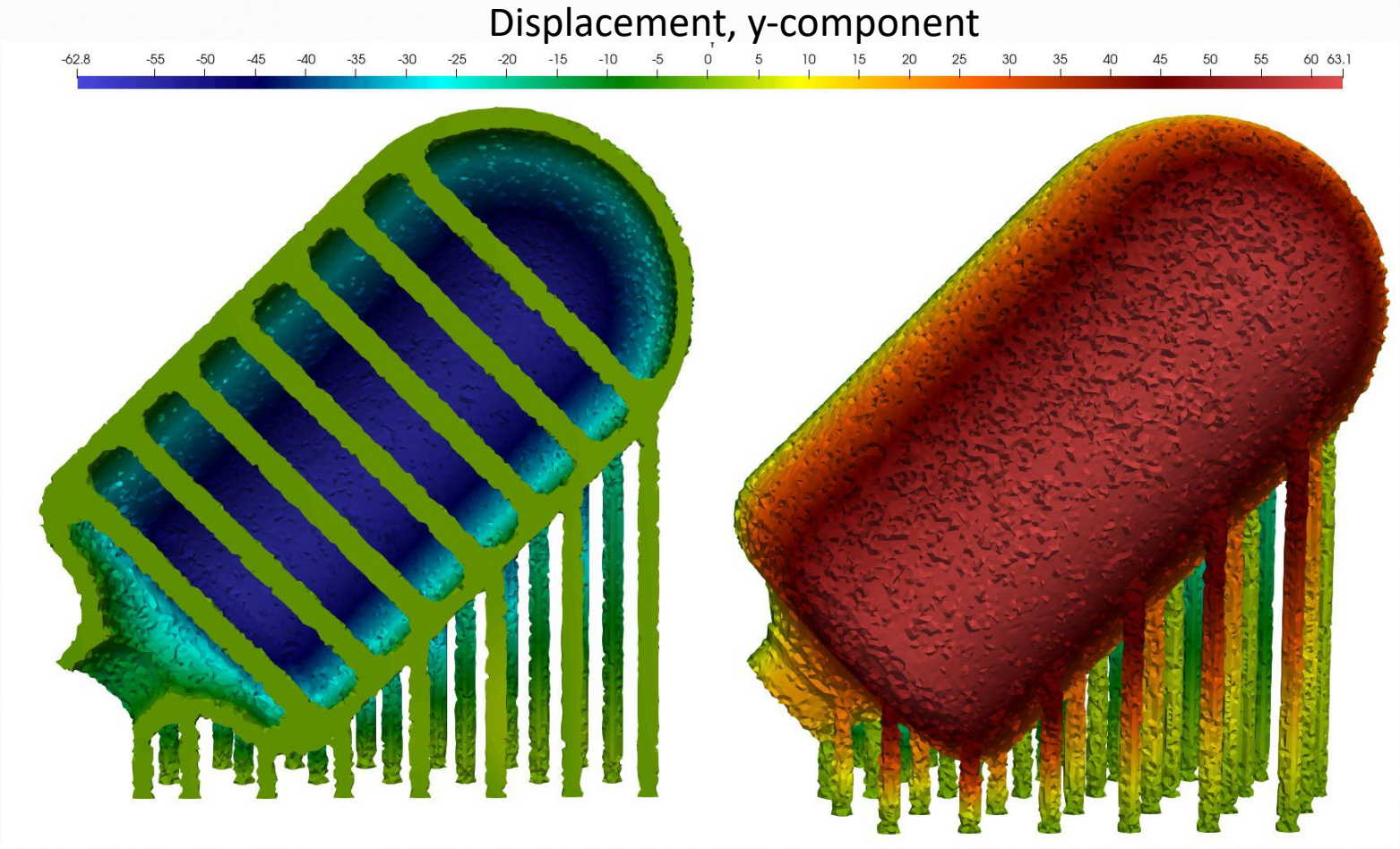

SBM Simulations of Thermo-Mechanics

Simulation on a complex structure (Naval Research Laboratory):

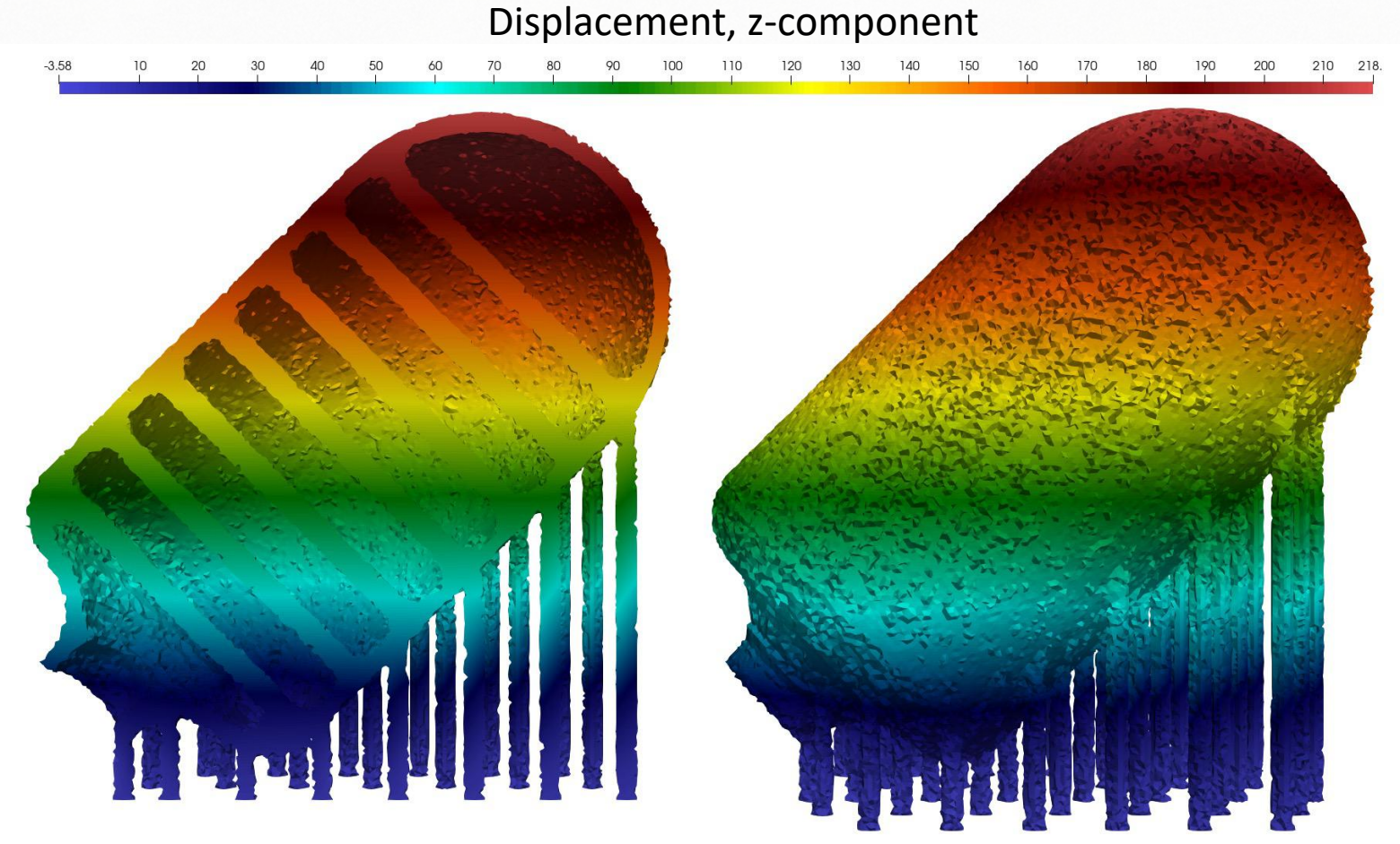

The Shifted Fracture Method

[Collaboration with Antonio Rodriguez-Ferran Universitat Politècnica de Catalunya]

The Shifted Fracture Method (SFM) in a nutshell:

- An attempt to overcome the challenges in the X-FEM/G-FEM/PU-FEM approach maintaining a comparable accuracy
- A *surrogate fracture* is introduced and constituted of edges/faces of the mesh that are in some sense close to the true fracture
- Fracture interface conditions are computed on the *surrogate fracture*
- The value of interface conditions is *shifted* (or perturbed) by means of Taylor expansions, to preserve accuracy and avoid mesh dependencies

Advantages of the Shifted Fracture Method:

- No cut cells: simplified data–structure and quadratures
- No small-cut cell problem affecting stability and matrix conditioning
- SFM solutions are mesh independent, unlike node-release techniques
- Continuous representation of the fracture surface in three dimensions

Credit for Shifted Fracture Method & Thermomechanics

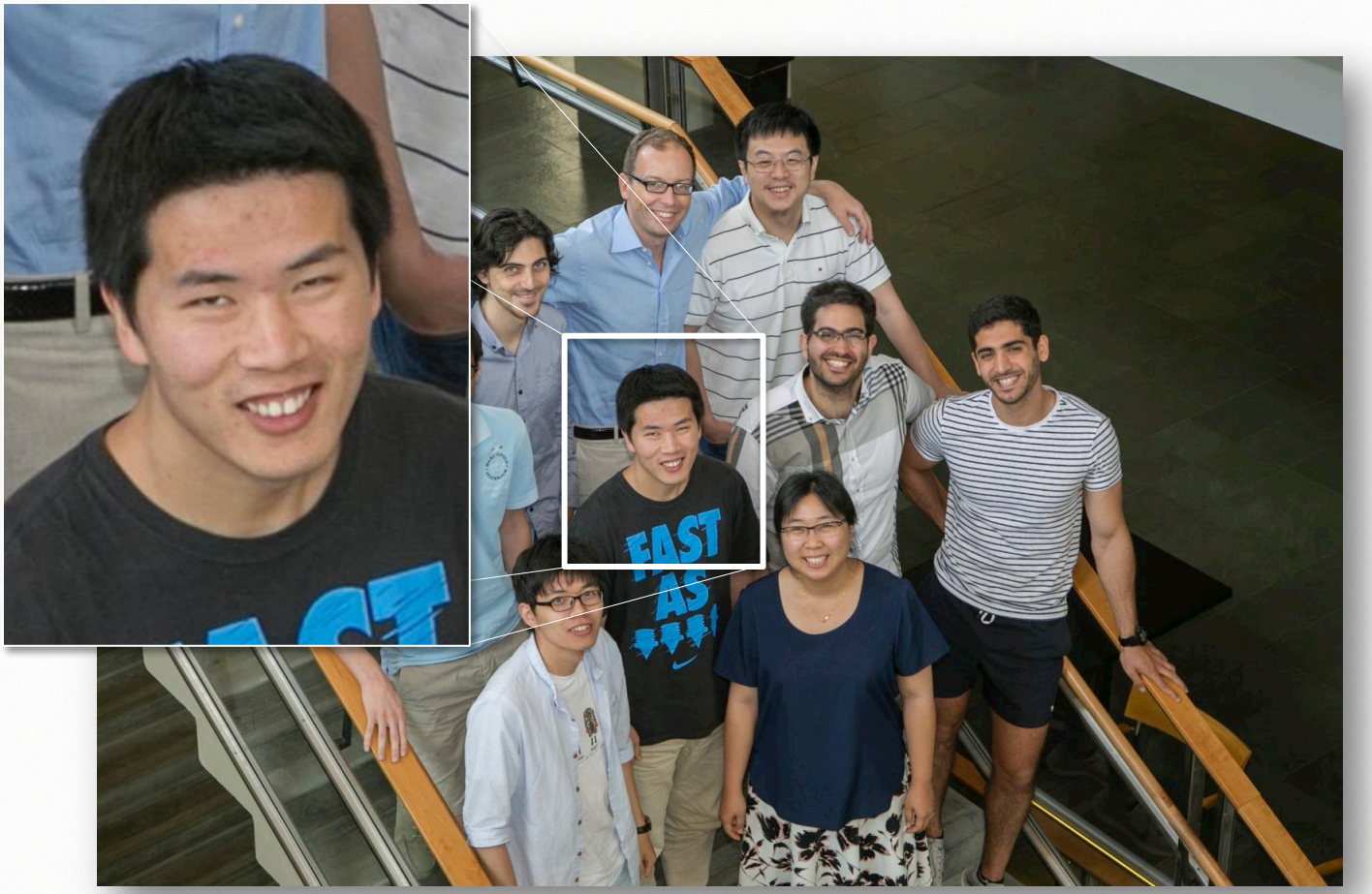

Ph.D. thesis of Kangan Li (… looking for jobs)

[in collaboration with Antonio Rodriguez-Ferran
Universitat Politècnica de Catalunya]

Duke UNIVERSITY

Overview: Cohesive Zone Models

$$[\![\chi]\!] = \chi^- - \chi^+ \qquad \{\!\{\chi\}\!\}_\lambda = \lambda\chi^+ + (1-\lambda)\chi^-$$

Governing equations

Linear elasticity in mixed form

$$0 = \boldsymbol{b} + \nabla \cdot \boldsymbol{\sigma}(\boldsymbol{\varepsilon}) \,,$$

$$\boldsymbol{\varepsilon} = \nabla^s \boldsymbol{u} \,.$$

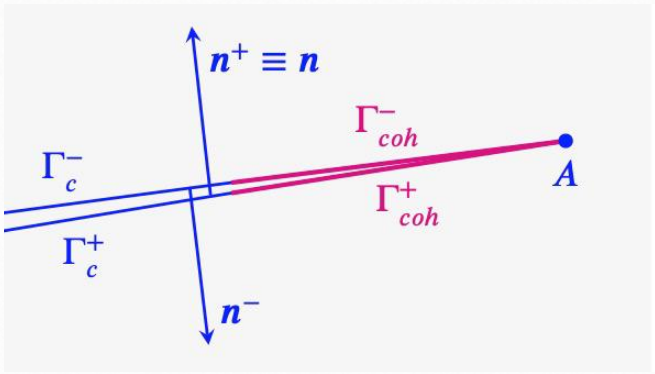

Cohesive zone model [*Pandolfi-Ortiz, IJNME* ***44*** *(1999)*]

CZMs were initially proposed by Dugdale, Barenblatt, Hillerborg, Bazant, *et al.*:

$$\boldsymbol{t} \equiv \boldsymbol{t}^+ = \boldsymbol{\sigma}(\boldsymbol{\varepsilon})^+ \cdot \boldsymbol{n}^+ = -\boldsymbol{\sigma}(\boldsymbol{\varepsilon})^- \cdot \boldsymbol{n}^- = -\boldsymbol{t}^- \quad \text{on } \Gamma_c$$

$$\boldsymbol{t} = \boldsymbol{t}_{coh}(\boldsymbol{w}) \quad \text{on } \Gamma_c$$

$$\boldsymbol{w}(\boldsymbol{u}) = \boldsymbol{u}^- - \boldsymbol{u}^+ = [\![\boldsymbol{u}]\!]$$

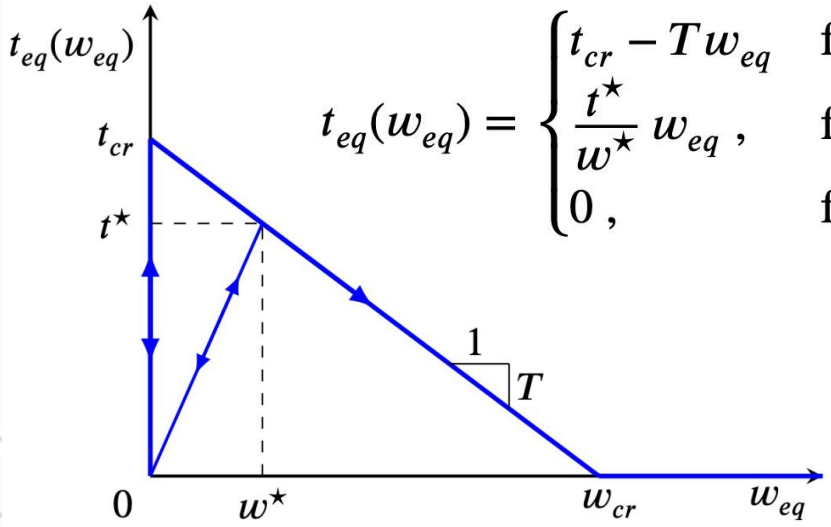

$$t_{eq}(w_{eq}) = \begin{cases} t_{cr} - T w_{eq} & \text{for } 0 < w_{eq} = w^\star < w_{cr} \,,\ \dot{w}^\star > 0 \,, \\ \dfrac{t^\star}{w^\star} w_{eq} \,, & \text{for } 0 \le w_{eq} < w^\star < w_{cr} \,,\ \dot{w}^\star = 0 \,, \\ 0 \,, & \text{for } w_{eq} \ge w_{cr} \,, \end{cases}$$

$$\boldsymbol{w}(\boldsymbol{u}) = w_n \boldsymbol{n} + w_s \boldsymbol{\tau}$$

$$w_{eq} = \sqrt{w_n^2 + \beta^2 w_s^2}$$

$$\boldsymbol{t}_{coh} = t_n \boldsymbol{n} + t_s \boldsymbol{\tau}$$

$$t_n = t_{eq}(w_{eq}) \frac{w_n}{w_{eq}} \,,$$

$$t_s = \beta^2 t_{eq}(w_{eq}) \frac{w_s}{w_{eq}} \,,$$

Overview: Cohesive Zone Models

X-FEM/PU-FEM variational formulation [Moës-Belytschko or Wells-Sluys]

Variational equations

$$(\nabla\boldsymbol{\phi}, \boldsymbol{\sigma}(\boldsymbol{\varepsilon}))_{\Omega\setminus\Gamma_c} + (\boldsymbol{\psi}, \boldsymbol{\varepsilon} - \nabla^s\boldsymbol{u})_{\Omega\setminus\Gamma_c} + \langle[\![\boldsymbol{\phi}]\!], \boldsymbol{t}_{coh}\rangle_{\Gamma_c} - (\boldsymbol{\phi}, \boldsymbol{b})_{\Omega\setminus\Gamma_c} - \langle\boldsymbol{\phi}, \boldsymbol{t}_N\rangle_{\Gamma_N} = 0$$

Euler-Lagrange equations on the fracture surface

$$\{\!\{\boldsymbol{\sigma}\}\!\}_\lambda \boldsymbol{n} - \boldsymbol{t}_{coh} = \boldsymbol{0}\,, \qquad \text{on } \Gamma_c$$

Cohesive traction

$$[\![\boldsymbol{\sigma}]\!]\,\boldsymbol{n} = \boldsymbol{0}\,, \qquad \text{on } \Gamma_c$$

Normal stress continuity/balance

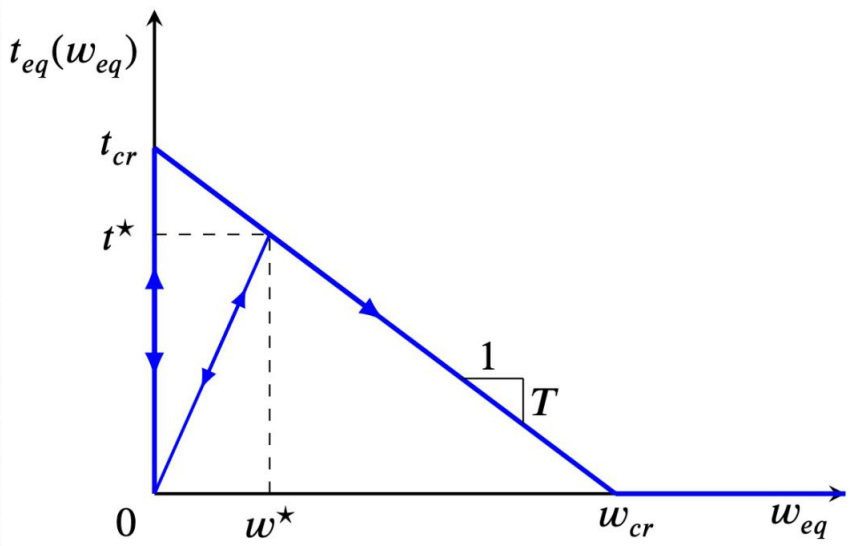

$$[\![\chi]\!] = \chi^- - \chi^+ \qquad \{\!\{\chi\}\!\}_\lambda = \lambda\chi^+ + (1-\lambda)\chi^-$$

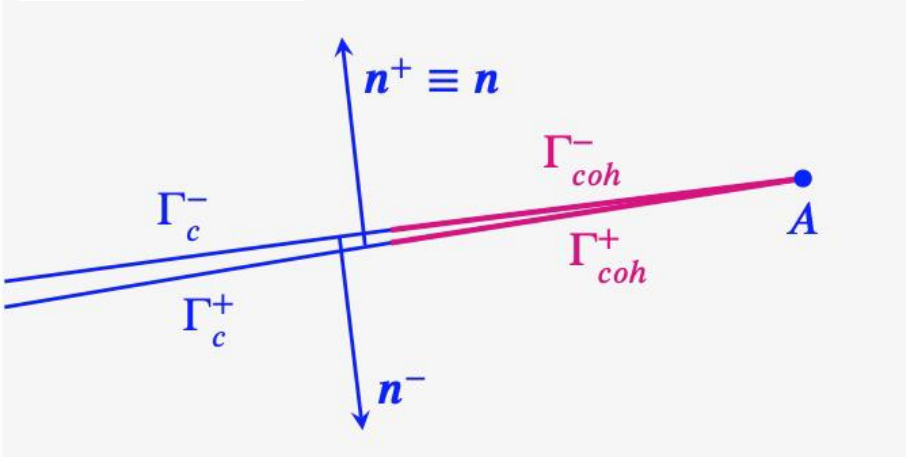

Duke UNIVERSITY

The Cohesive Shifted Fracture Approach

Geometric setting of the Shifted Fracture Approach

Surrogate fracture: the set of edges/faces closest to the true crack (in red)

***d*:** the distance vector of the surrogate crack from the true crack

$\tilde{A}$: the surrogate crack tip, corresponding to A

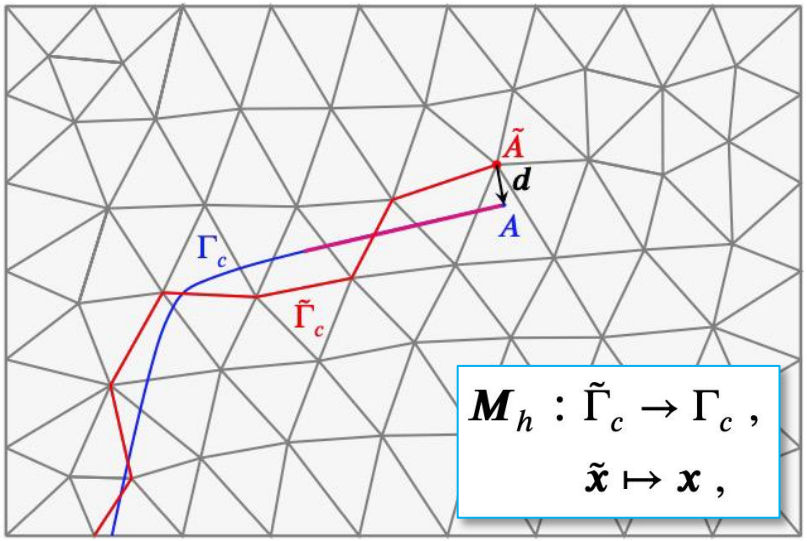

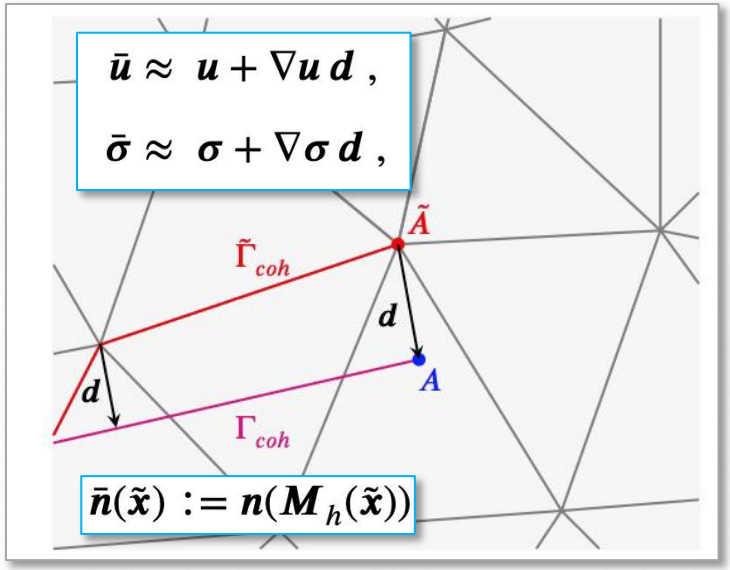

Idea of the Shifted Fracture Method: use Taylor expansions to evaluate *approximate* fracture conditions on the surrogate fracture

$$\bar{t} = t_{coh}(w(\bar{u})) = \bar{\sigma}\bar{n} \approx (\sigma + \nabla\sigma\, d)\,\bar{n} \approx t_{coh}(w(u + \nabla u\, d)) \quad \text{on } \tilde{\Gamma}_{coh} .$$

Duke UNIVERSITY

The Cohesive Shifted Fracture Approach

Derivation of the variational equations

Function spaces (piecewise linear FEMs, discontinuous across the ***surrogate*** crack)

$$\mathscr{S}_{\boldsymbol{u}}^{h}(\Omega \setminus \tilde{\Gamma}_c) = \{\boldsymbol{v} \in (C^0(\Omega \setminus \tilde{\Gamma}_c))^d \ : \ \boldsymbol{v}_{|\Gamma_D} = \boldsymbol{u}_D \,,\ \boldsymbol{v}\,|_T \in (\mathscr{P}^1(T))^d \,,\ \forall T \in \mathscr{T}_h\} \,,$$
$$\mathscr{S}_{\boldsymbol{\varepsilon}}^{h}(\Omega \setminus \tilde{\Gamma}_c) = \{\boldsymbol{\omega} \in (C^0(\Omega \setminus \tilde{\Gamma}_c))^{d\times d} \ : \ \boldsymbol{\omega}\,|_T \in (\mathscr{P}^1(T))^{d\times d} \,, \boldsymbol{\omega} = \boldsymbol{\omega}^t,\ \forall T \in \mathscr{T}_h\} \,,$$

$$\mathscr{V}_{\boldsymbol{u}}^{h}(\Omega \setminus \tilde{\Gamma}_c) = \{\boldsymbol{v} \in (C^0(\Omega \setminus \tilde{\Gamma}_c))^d \ : \ \boldsymbol{v}_{|\Gamma_D} = \boldsymbol{0} \,,\ \boldsymbol{v}\,|_T \in (\mathscr{P}^1(T))^d \,,\ \forall T \in \mathscr{T}_h\} \,,$$
$$\mathscr{V}_{\boldsymbol{\varepsilon}}^{h}(\Omega \setminus \tilde{\Gamma}_c) = \mathscr{S}_{\boldsymbol{\varepsilon}}^{h}(\Omega \setminus \tilde{\Gamma}_c) \,.$$

Galerkin projection:

$$-(\boldsymbol{\phi}, \nabla \cdot \boldsymbol{\sigma}(\boldsymbol{\varepsilon}))_{\Omega\setminus\tilde{\Gamma}_c} = (\boldsymbol{\phi}, \boldsymbol{b})_{\Omega\setminus\tilde{\Gamma}_c} \,,$$
$$(\boldsymbol{\psi}, \boldsymbol{\varepsilon})_{\Omega\setminus\tilde{\Gamma}_c} = (\boldsymbol{\psi}, \nabla^s \boldsymbol{u})_{\Omega\setminus\tilde{\Gamma}_c} \,,$$

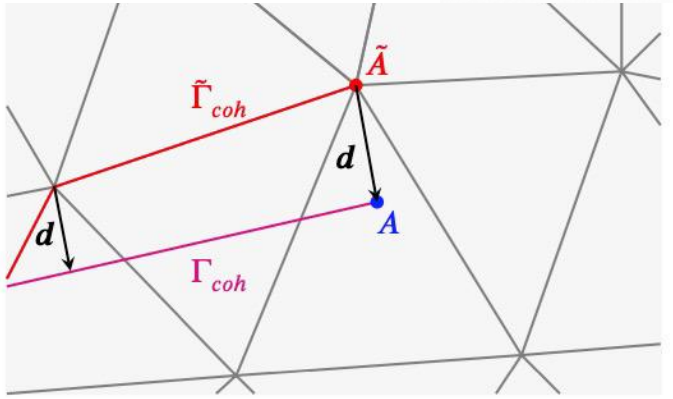

Integrating by parts …

$$(\nabla\boldsymbol{\phi}, \boldsymbol{\sigma}(\boldsymbol{\varepsilon}))_{\Omega\setminus\tilde{\Gamma}_c} + \langle [\![\boldsymbol{\phi}]\!], \{\!\{\boldsymbol{\sigma}(\boldsymbol{\varepsilon})\}\!\}_{\lambda}\tilde{\boldsymbol{n}}\rangle_{\tilde{\Gamma}_c}$$
$$+ \langle \{\!\{\boldsymbol{\phi}\}\!\}_{1-\lambda}, [\![\boldsymbol{\sigma}(\boldsymbol{\varepsilon})]\!]\tilde{\boldsymbol{n}}\rangle_{\tilde{\Gamma}_c} = (\boldsymbol{\phi}, \boldsymbol{b})_{\Omega\setminus\tilde{\Gamma}_c} + \langle \boldsymbol{\phi}, \boldsymbol{t}_N\rangle_{\Gamma_N} \,,$$

Duke UNIVERSITY

The Cohesive Shifted Fracture Approach

Shifted interface conditions

$$(\nabla\boldsymbol{\phi},\boldsymbol{\sigma}(\boldsymbol{\varepsilon}))_{\Omega\setminus\tilde{\Gamma}_c}+\langle[\![\boldsymbol{\phi}]\!],\{\!\{\boldsymbol{\sigma}(\boldsymbol{\varepsilon})\}\!\}_{\lambda}\tilde{\boldsymbol{n}}\rangle_{\tilde{\Gamma}_c}+\langle\{\!\{\boldsymbol{\phi}\}\!\}_{1-\lambda},[\![\boldsymbol{\sigma}(\boldsymbol{\varepsilon})]\!]\tilde{\boldsymbol{n}}\rangle_{\tilde{\Gamma}_c}=(\boldsymbol{\phi},\boldsymbol{b})_{\Omega\setminus\tilde{\Gamma}_c}+\langle\boldsymbol{\phi},\boldsymbol{t}_N\rangle_{\Gamma_N}$$

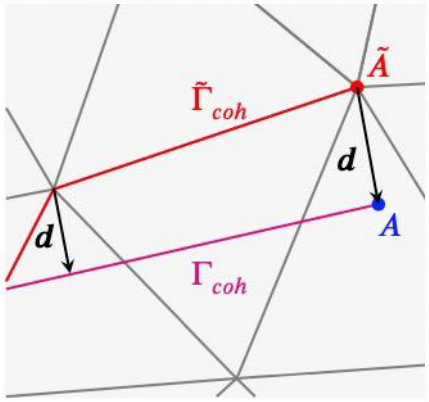

Duke UNIVERSITY

The Cohesive Shifted Fracture Approach

Shifted interface conditions

$$(\nabla\boldsymbol{\phi},\boldsymbol{\sigma}(\boldsymbol{\varepsilon}))_{\Omega\setminus\tilde{\Gamma}_c}+\langle[\![\boldsymbol{\phi}]\!],\{\!\{\boldsymbol{\sigma}(\boldsymbol{\varepsilon})\}\!\}_\lambda\tilde{\boldsymbol{n}}\rangle_{\tilde{\Gamma}_c}+\langle\{\!\{\boldsymbol{\phi}\}\!\}_{1-\lambda},[\![\boldsymbol{\sigma}(\boldsymbol{\varepsilon})]\!]\tilde{\boldsymbol{n}}\rangle_{\tilde{\Gamma}_c}=(\boldsymbol{\phi},\boldsymbol{b})_{\Omega\setminus\tilde{\Gamma}_c}+\langle\boldsymbol{\phi},\boldsymbol{t}_N\rangle_{\Gamma_N}$$

$$\begin{aligned}\{\!\{\boldsymbol{\sigma}(\boldsymbol{\varepsilon})\}\!\}_\lambda\tilde{\boldsymbol{n}}&=\{\!\{\boldsymbol{\sigma}(\boldsymbol{\varepsilon})\}\!\}_\lambda((\tilde{\boldsymbol{n}}\cdot\boldsymbol{n})\boldsymbol{n}+(\tilde{\boldsymbol{n}}\cdot\boldsymbol{\tau})\boldsymbol{\tau})\\&=(\tilde{\boldsymbol{n}}(\tilde{\boldsymbol{x}})\cdot\bar{\boldsymbol{n}}(\tilde{\boldsymbol{x}}))\,\{\!\{\boldsymbol{\sigma}(\boldsymbol{\varepsilon}(\tilde{\boldsymbol{x}}))\}\!\}_\lambda\,\bar{\boldsymbol{n}}(\tilde{\boldsymbol{x}})+(\tilde{\boldsymbol{n}}(\tilde{\boldsymbol{x}})\cdot\bar{\boldsymbol{\tau}}(\tilde{\boldsymbol{x}}))\,\{\!\{\boldsymbol{\sigma}(\boldsymbol{\varepsilon}(\tilde{\boldsymbol{x}}))\}\!\}_\lambda\,\bar{\boldsymbol{\tau}}(\tilde{\boldsymbol{x}})\end{aligned}$$

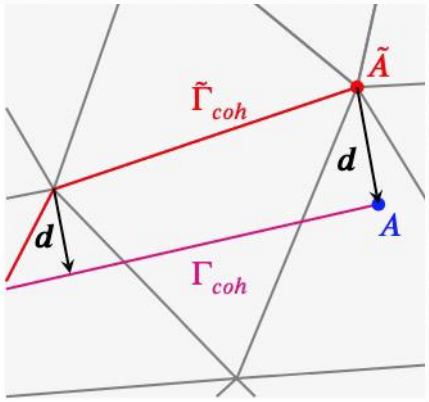

Duke UNIVERSITY

The Cohesive Shifted Fracture Approach

Shifted interface conditions

$$(\nabla\boldsymbol{\phi}, \boldsymbol{\sigma}(\boldsymbol{\varepsilon}))_{\Omega\setminus\tilde{\Gamma}_c} + \langle [\![\boldsymbol{\phi}]\!], \{\!\{\boldsymbol{\sigma}(\boldsymbol{\varepsilon})\}\!\}_\lambda \tilde{\boldsymbol{n}}\rangle_{\tilde{\Gamma}_c} + \langle \{\!\{\boldsymbol{\phi}\}\!\}_{1-\lambda}, [\![\boldsymbol{\sigma}(\boldsymbol{\varepsilon})]\!]\tilde{\boldsymbol{n}}\rangle_{\tilde{\Gamma}_c} = (\boldsymbol{\phi}, \boldsymbol{b})_{\Omega\setminus\tilde{\Gamma}_c} + \langle \boldsymbol{\phi}, \boldsymbol{t}_N\rangle_{\Gamma_N}$$

$$\begin{aligned}\{\!\{\boldsymbol{\sigma}(\boldsymbol{\varepsilon})\}\!\}_\lambda \tilde{\boldsymbol{n}} &= \{\!\{\boldsymbol{\sigma}(\boldsymbol{\varepsilon})\}\!\}_\lambda((\tilde{\boldsymbol{n}}\cdot\boldsymbol{n})\boldsymbol{n} + (\tilde{\boldsymbol{n}}\cdot\boldsymbol{\tau})\boldsymbol{\tau}) \\ &= (\tilde{\boldsymbol{n}}(\tilde{\boldsymbol{x}})\cdot\bar{\boldsymbol{n}}(\tilde{\boldsymbol{x}}))\,\{\!\{\boldsymbol{\sigma}(\boldsymbol{\varepsilon}(\tilde{\boldsymbol{x}}))\}\!\}_\lambda\,\bar{\boldsymbol{n}}(\tilde{\boldsymbol{x}}) + (\tilde{\boldsymbol{n}}(\tilde{\boldsymbol{x}})\cdot\bar{\boldsymbol{\tau}}(\tilde{\boldsymbol{x}}))\,\{\!\{\boldsymbol{\sigma}(\boldsymbol{\varepsilon}(\tilde{\boldsymbol{x}}))\}\!\}_\lambda\,\bar{\boldsymbol{\tau}}(\tilde{\boldsymbol{x}})\end{aligned}$$

$$\begin{aligned}\{\!\{\boldsymbol{\sigma}(\boldsymbol{\varepsilon}(\tilde{\boldsymbol{x}}))\}\!\}_\lambda\,\bar{\boldsymbol{n}}(\tilde{\boldsymbol{x}}) &= \{\!\{\boldsymbol{\sigma}\,\bar{\boldsymbol{n}}\}\!\}_\lambda = \{\!\{(\bar{\boldsymbol{\sigma}} - \nabla\boldsymbol{\sigma}\,\boldsymbol{d})\,\bar{\boldsymbol{n}}\}\!\}_\lambda \\ &= \{\!\{\bar{\boldsymbol{t}} - (\nabla\boldsymbol{\sigma}\,\boldsymbol{d})\,\bar{\boldsymbol{n}}\}\!\}_\lambda = \bar{\boldsymbol{t}} - \{\!\{(\nabla\boldsymbol{\sigma}\,\boldsymbol{d})\}\!\}_\lambda\,\bar{\boldsymbol{n}},\end{aligned}$$

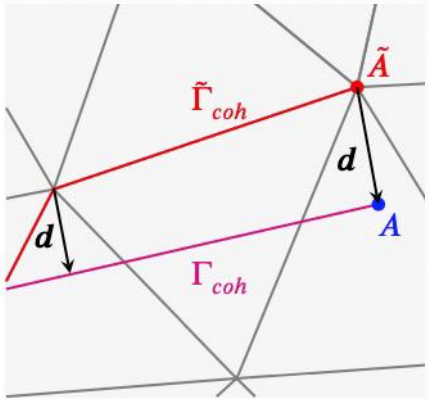

$$\bar{\boldsymbol{u}} \approx \boldsymbol{u} + \nabla\boldsymbol{u}\,\boldsymbol{d}\,,$$

$$\bar{\boldsymbol{\sigma}} \approx \boldsymbol{\sigma} + \nabla\boldsymbol{\sigma}\,\boldsymbol{d}\,,$$

Duke UNIVERSITY

The Cohesive Shifted Fracture Approach

Shifted interface conditions

$$(\nabla\boldsymbol{\phi},\boldsymbol{\sigma}(\boldsymbol{\varepsilon}))_{\Omega\setminus\tilde{\Gamma}_c} + \langle[\![\boldsymbol{\phi}]\!],\{\!\{\boldsymbol{\sigma}(\boldsymbol{\varepsilon})\}\!\}_\lambda\tilde{\boldsymbol{n}}\rangle_{\tilde{\Gamma}_c} + \langle\{\!\{\boldsymbol{\phi}\}\!\}_{1-\lambda},[\![\boldsymbol{\sigma}(\boldsymbol{\varepsilon})]\!]\tilde{\boldsymbol{n}}\rangle_{\tilde{\Gamma}_c} = (\boldsymbol{\phi},\boldsymbol{b})_{\Omega\setminus\tilde{\Gamma}_c} + \langle\boldsymbol{\phi},\boldsymbol{t}_N\rangle_{\Gamma_N}$$

$$\begin{aligned}\{\!\{\boldsymbol{\sigma}(\boldsymbol{\varepsilon})\}\!\}_\lambda\tilde{\boldsymbol{n}} &= \{\!\{\boldsymbol{\sigma}(\boldsymbol{\varepsilon})\}\!\}_\lambda((\tilde{\boldsymbol{n}}\cdot\boldsymbol{n})\boldsymbol{n}+(\tilde{\boldsymbol{n}}\cdot\boldsymbol{\tau})\boldsymbol{\tau})\\ &= (\tilde{\boldsymbol{n}}(\tilde{\boldsymbol{x}})\cdot\bar{\boldsymbol{n}}(\tilde{\boldsymbol{x}}))\,\{\!\{\boldsymbol{\sigma}(\boldsymbol{\varepsilon}(\tilde{\boldsymbol{x}}))\}\!\}_\lambda\,\bar{\boldsymbol{n}}(\tilde{\boldsymbol{x}}) + (\tilde{\boldsymbol{n}}(\tilde{\boldsymbol{x}})\cdot\bar{\boldsymbol{\tau}}(\tilde{\boldsymbol{x}}))\,\{\!\{\boldsymbol{\sigma}(\boldsymbol{\varepsilon}(\tilde{\boldsymbol{x}}))\}\!\}_\lambda\,\bar{\boldsymbol{\tau}}(\tilde{\boldsymbol{x}})\end{aligned}$$

$$\begin{aligned}\{\!\{\boldsymbol{\sigma}(\boldsymbol{\varepsilon}(\tilde{\boldsymbol{x}}))\}\!\}_\lambda\,\bar{\boldsymbol{n}}(\tilde{\boldsymbol{x}}) &= \{\!\{\boldsymbol{\sigma}\,\bar{\boldsymbol{n}}\}\!\}_\lambda = \{\!\{(\bar{\boldsymbol{\sigma}}-\nabla\boldsymbol{\sigma}\,\boldsymbol{d})\,\bar{\boldsymbol{n}}\}\!\}_\lambda\\ &= \{\!\{\bar{\boldsymbol{t}}-(\nabla\boldsymbol{\sigma}\,\boldsymbol{d})\,\bar{\boldsymbol{n}}\}\!\}_\lambda = \bar{\boldsymbol{t}} - \{\!\{(\nabla\boldsymbol{\sigma}\,\boldsymbol{d})\}\!\}_\lambda\,\bar{\boldsymbol{n}},\end{aligned}$$

$$\bar{\boldsymbol{t}} = \boldsymbol{t}_{coh}(\boldsymbol{w}(\bar{\boldsymbol{u}})) \approx \boldsymbol{t}_{coh}(\boldsymbol{w}(\boldsymbol{u}+\nabla\boldsymbol{u}\,\boldsymbol{d})), \quad \text{on } \tilde{\Gamma}_{coh}$$

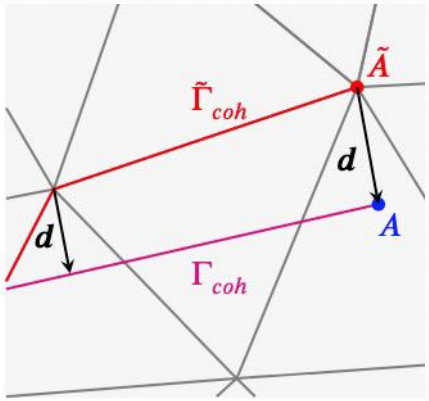

$$\bar{\boldsymbol{u}} \approx \boldsymbol{u}+\nabla\boldsymbol{u}\,\boldsymbol{d}\,,$$

$$\bar{\boldsymbol{\sigma}} \approx \boldsymbol{\sigma}+\nabla\boldsymbol{\sigma}\,\boldsymbol{d}\,,$$

Duke UNIVERSITY

The Cohesive Shifted Fracture Approach

Shifted interface conditions

$$(\nabla\boldsymbol{\phi},\boldsymbol{\sigma}(\boldsymbol{\varepsilon}))_{\Omega\setminus\tilde{\Gamma}_c} + \langle[\![\boldsymbol{\phi}]\!],\{\!\{\boldsymbol{\sigma}(\boldsymbol{\varepsilon})\}\!\}_\lambda\tilde{\boldsymbol{n}}\rangle_{\tilde{\Gamma}_c} + \langle\{\!\{\boldsymbol{\phi}\}\!\}_{1-\lambda},[\![\boldsymbol{\sigma}(\boldsymbol{\varepsilon})]\!]\tilde{\boldsymbol{n}}\rangle_{\tilde{\Gamma}_c} = (\boldsymbol{\phi},\boldsymbol{b})_{\Omega\setminus\tilde{\Gamma}_c} + \langle\boldsymbol{\phi},\boldsymbol{t}_N\rangle_{\Gamma_N}$$

$$\begin{aligned}\{\!\{\boldsymbol{\sigma}(\boldsymbol{\varepsilon})\}\!\}_\lambda\tilde{\boldsymbol{n}} &= \{\!\{\boldsymbol{\sigma}(\boldsymbol{\varepsilon})\}\!\}_\lambda((\tilde{\boldsymbol{n}}\cdot\boldsymbol{n})\boldsymbol{n}+(\tilde{\boldsymbol{n}}\cdot\boldsymbol{\tau})\boldsymbol{\tau})\\ &= (\tilde{\boldsymbol{n}}(\tilde{\boldsymbol{x}})\cdot\bar{\boldsymbol{n}}(\tilde{\boldsymbol{x}}))\,\{\!\{\boldsymbol{\sigma}(\boldsymbol{\varepsilon}(\tilde{\boldsymbol{x}}))\}\!\}_\lambda\,\bar{\boldsymbol{n}}(\tilde{\boldsymbol{x}}) + (\tilde{\boldsymbol{n}}(\tilde{\boldsymbol{x}})\cdot\bar{\boldsymbol{\tau}}(\tilde{\boldsymbol{x}}))\,\{\!\{\boldsymbol{\sigma}(\boldsymbol{\varepsilon}(\tilde{\boldsymbol{x}}))\}\!\}_\lambda\,\bar{\boldsymbol{\tau}}(\tilde{\boldsymbol{x}})\end{aligned}$$

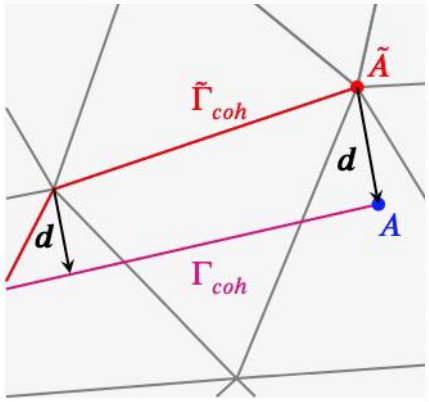

$$\begin{aligned}\{\!\{\boldsymbol{\sigma}(\boldsymbol{\varepsilon}(\tilde{\boldsymbol{x}}))\}\!\}_\lambda\,\bar{\boldsymbol{n}}(\tilde{\boldsymbol{x}}) &= \{\!\{\boldsymbol{\sigma}\,\bar{\boldsymbol{n}}\}\!\}_\lambda = \{\!\{(\bar{\boldsymbol{\sigma}}-\nabla\boldsymbol{\sigma}\,\boldsymbol{d})\,\bar{\boldsymbol{n}}\}\!\}_\lambda\\ &= \{\!\{\bar{\boldsymbol{t}}-(\nabla\boldsymbol{\sigma}\,\boldsymbol{d})\,\bar{\boldsymbol{n}}\}\!\}_\lambda = \bar{\boldsymbol{t}} - \{\!\{(\nabla\boldsymbol{\sigma}\,\boldsymbol{d})\}\!\}_\lambda\,\bar{\boldsymbol{n}},\end{aligned}$$

$$\bar{\boldsymbol{t}} = \boldsymbol{t}_{coh}(\boldsymbol{w}(\bar{\boldsymbol{u}})) \approx \boldsymbol{t}_{coh}(\boldsymbol{w}(\boldsymbol{u}+\nabla\boldsymbol{u}\,\boldsymbol{d})), \quad \text{on } \tilde{\Gamma}_{coh}$$

$$\bar{\boldsymbol{u}} \approx \boldsymbol{u}+\nabla\boldsymbol{u}\,\boldsymbol{d},$$

$$\bar{\boldsymbol{\sigma}} \approx \boldsymbol{\sigma}+\nabla\boldsymbol{\sigma}\,\boldsymbol{d},$$

$$\begin{aligned}\langle[\![\boldsymbol{\phi}]\!],\{\!\{\boldsymbol{\sigma}(\boldsymbol{\varepsilon})\}\!\}_\lambda\tilde{\boldsymbol{n}}\rangle_{\tilde{\Gamma}_c} &= \langle[\![\boldsymbol{\phi}]\!],(\tilde{\boldsymbol{n}}\cdot\bar{\boldsymbol{n}})\,(\bar{\boldsymbol{t}}-\{\!\{(\nabla\boldsymbol{\sigma}(\boldsymbol{\varepsilon})\,\boldsymbol{d})\}\!\}_\lambda\,\bar{\boldsymbol{n}})+(\tilde{\boldsymbol{n}}\cdot\bar{\boldsymbol{\tau}})\,\{\!\{\boldsymbol{\sigma}(\boldsymbol{\varepsilon})\}\!\}_\lambda\,\bar{\boldsymbol{\tau}}\rangle_{\tilde{\Gamma}_c}\\ &= \langle[\![\boldsymbol{\phi}]\!],(\tilde{\boldsymbol{n}}\cdot\bar{\boldsymbol{n}})\,\boldsymbol{t}_{coh}(\boldsymbol{w}(\boldsymbol{u}+\nabla\boldsymbol{u}\,\boldsymbol{d}))\rangle_{\tilde{\Gamma}_{coh}} - \langle[\![\boldsymbol{\phi}]\!],(\tilde{\boldsymbol{n}}\cdot\bar{\boldsymbol{n}})\,(\{\!\{(\nabla\boldsymbol{\sigma}(\boldsymbol{\varepsilon})\,\boldsymbol{d})\}\!\}_\lambda\,\bar{\boldsymbol{n}})-(\tilde{\boldsymbol{n}}\cdot\bar{\boldsymbol{\tau}})\,\{\!\{\boldsymbol{\sigma}(\boldsymbol{\varepsilon})\}\!\}_\lambda\,\bar{\boldsymbol{\tau}}\rangle_{\tilde{\Gamma}_c}\end{aligned}$$

Duke UNIVERSITY

The Cohesive Shifted Fracture Approach

Shifted interface conditions

$$(\nabla\boldsymbol{\phi},\boldsymbol{\sigma}(\boldsymbol{\varepsilon}))_{\Omega\setminus\tilde{\Gamma}_c} + \langle[\![\boldsymbol{\phi}]\!],\{\!\{\boldsymbol{\sigma}(\boldsymbol{\varepsilon})\}\!\}_\lambda\tilde{\boldsymbol{n}}\rangle_{\tilde{\Gamma}_c} + \langle\{\!\{\boldsymbol{\phi}\}\!\}_{1-\lambda},[\![\boldsymbol{\sigma}(\boldsymbol{\varepsilon})]\!]\tilde{\boldsymbol{n}}\rangle_{\tilde{\Gamma}_c} = (\boldsymbol{\phi},\boldsymbol{b})_{\Omega\setminus\tilde{\Gamma}_c} + \langle\boldsymbol{\phi},\boldsymbol{t}_N\rangle_{\Gamma_N}$$

$$\begin{aligned}\{\!\{\boldsymbol{\sigma}(\boldsymbol{\varepsilon})\}\!\}_\lambda\tilde{\boldsymbol{n}} &= \{\!\{\boldsymbol{\sigma}(\boldsymbol{\varepsilon})\}\!\}_\lambda((\tilde{\boldsymbol{n}}\cdot\boldsymbol{n})\boldsymbol{n}+(\tilde{\boldsymbol{n}}\cdot\boldsymbol{\tau})\boldsymbol{\tau})\\ &= (\tilde{\boldsymbol{n}}(\tilde{\boldsymbol{x}})\cdot\bar{\boldsymbol{n}}(\tilde{\boldsymbol{x}}))\,\{\!\{\boldsymbol{\sigma}(\boldsymbol{\varepsilon}(\tilde{\boldsymbol{x}}))\}\!\}_\lambda\,\bar{\boldsymbol{n}}(\tilde{\boldsymbol{x}}) + (\tilde{\boldsymbol{n}}(\tilde{\boldsymbol{x}})\cdot\bar{\boldsymbol{\tau}}(\tilde{\boldsymbol{x}}))\,\{\!\{\boldsymbol{\sigma}(\boldsymbol{\varepsilon}(\tilde{\boldsymbol{x}}))\}\!\}_\lambda\,\bar{\boldsymbol{\tau}}(\tilde{\boldsymbol{x}})\end{aligned}$$

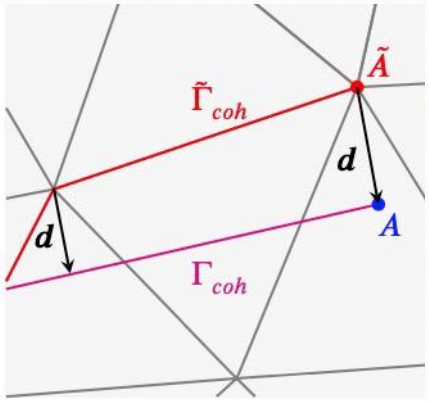

$$\begin{aligned}\{\!\{\boldsymbol{\sigma}(\boldsymbol{\varepsilon}(\tilde{\boldsymbol{x}}))\}\!\}_\lambda\,\bar{\boldsymbol{n}}(\tilde{\boldsymbol{x}}) &= \{\!\{\boldsymbol{\sigma}\,\bar{\boldsymbol{n}}\}\!\}_\lambda = \{\!\{(\bar{\boldsymbol{\sigma}}-\nabla\boldsymbol{\sigma}\,\boldsymbol{d})\,\bar{\boldsymbol{n}}\}\!\}_\lambda\\ &= \{\!\{\bar{\boldsymbol{t}}-(\nabla\boldsymbol{\sigma}\,\boldsymbol{d})\,\bar{\boldsymbol{n}}\}\!\}_\lambda = \bar{\boldsymbol{t}} - \{\!\{(\nabla\boldsymbol{\sigma}\,\boldsymbol{d})\}\!\}_\lambda\,\bar{\boldsymbol{n}},\end{aligned}$$

$$\bar{\boldsymbol{t}} = \boldsymbol{t}_{coh}(\boldsymbol{w}(\bar{\boldsymbol{u}})) \approx \boldsymbol{t}_{coh}(\boldsymbol{w}(\boldsymbol{u}+\nabla\boldsymbol{u}\,\boldsymbol{d})), \quad \text{on } \tilde{\Gamma}_{coh}$$

$$\bar{\boldsymbol{u}} \approx \boldsymbol{u}+\nabla\boldsymbol{u}\,\boldsymbol{d},$$

$$\bar{\boldsymbol{\sigma}} \approx \boldsymbol{\sigma}+\nabla\boldsymbol{\sigma}\,\boldsymbol{d},$$

$$\begin{aligned}\langle[\![\boldsymbol{\phi}]\!],\{\!\{\boldsymbol{\sigma}(\boldsymbol{\varepsilon})\}\!\}_\lambda\tilde{\boldsymbol{n}}\rangle_{\tilde{\Gamma}_c} &= \langle[\![\boldsymbol{\phi}]\!],(\tilde{\boldsymbol{n}}\cdot\bar{\boldsymbol{n}})\,(\bar{\boldsymbol{t}}-\{\!\{(\nabla\boldsymbol{\sigma}(\boldsymbol{\varepsilon})\,\boldsymbol{d})\}\!\}_\lambda\,\bar{\boldsymbol{n}})+(\tilde{\boldsymbol{n}}\cdot\bar{\boldsymbol{\tau}})\,\{\!\{\boldsymbol{\sigma}(\boldsymbol{\varepsilon})\}\!\}_\lambda\,\bar{\boldsymbol{\tau}}\rangle_{\tilde{\Gamma}_c}\\ &= \langle[\![\boldsymbol{\phi}]\!],(\tilde{\boldsymbol{n}}\cdot\bar{\boldsymbol{n}})\,\boldsymbol{t}_{coh}(\boldsymbol{w}(\boldsymbol{u}+\nabla\boldsymbol{u}\,\boldsymbol{d}))\rangle_{\tilde{\Gamma}_{coh}} - \langle[\![\boldsymbol{\phi}]\!],(\tilde{\boldsymbol{n}}\cdot\bar{\boldsymbol{n}})\,(\{\!\{(\nabla\boldsymbol{\sigma}(\boldsymbol{\varepsilon})\,\boldsymbol{d})\}\!\}_\lambda\,\bar{\boldsymbol{n}})-(\tilde{\boldsymbol{n}}\cdot\bar{\boldsymbol{\tau}})\,\{\!\{\boldsymbol{\sigma}(\boldsymbol{\varepsilon})\}\!\}_\lambda\,\bar{\boldsymbol{\tau}}\rangle_{\tilde{\Gamma}_c}\end{aligned}$$

$$\begin{aligned}\langle\{\!\{\boldsymbol{\phi}\}\!\}_{1-\lambda},[\![\boldsymbol{\sigma}(\boldsymbol{\varepsilon})]\!]\tilde{\boldsymbol{n}}\rangle_{\tilde{\Gamma}_c} &= \langle\{\!\{\boldsymbol{\phi}\}\!\}_{1-\lambda},(\tilde{\boldsymbol{n}}\cdot\bar{\boldsymbol{n}})\,[\![\bar{\boldsymbol{\sigma}}(\boldsymbol{\varepsilon})-\nabla\boldsymbol{\sigma}(\boldsymbol{\varepsilon})\boldsymbol{d}]\!]\,\bar{\boldsymbol{n}}+(\tilde{\boldsymbol{n}}\cdot\bar{\boldsymbol{\tau}})\,[\![\boldsymbol{\sigma}(\boldsymbol{\varepsilon})]\!]\,\bar{\boldsymbol{\tau}}\rangle_{\tilde{\Gamma}_c}\\ &= \langle\{\!\{\boldsymbol{\phi}\}\!\}_{1-\lambda},-(\tilde{\boldsymbol{n}}\cdot\bar{\boldsymbol{n}})\,[\![\nabla\boldsymbol{\sigma}(\boldsymbol{\varepsilon})\boldsymbol{d}]\!]\,\bar{\boldsymbol{n}}+(\tilde{\boldsymbol{n}}\cdot\bar{\boldsymbol{\tau}})\,[\![\boldsymbol{\sigma}(\boldsymbol{\varepsilon})]\!]\,\bar{\boldsymbol{\tau}}\rangle_{\tilde{\Gamma}_c}\\ &= \langle\{\!\{\boldsymbol{\phi}\}\!\}_{1-\lambda},[\![\boldsymbol{\sigma}(\boldsymbol{\varepsilon})]\!]\tilde{\boldsymbol{n}}-(\tilde{\boldsymbol{n}}\cdot\bar{\boldsymbol{n}})\,[\![\boldsymbol{\sigma}(\boldsymbol{\varepsilon})+\nabla\boldsymbol{\sigma}(\boldsymbol{\varepsilon})\boldsymbol{d}]\!]\,\bar{\boldsymbol{n}}\rangle_{\tilde{\Gamma}_c}\ .\end{aligned}$$

Duke UNIVERSITY

The Cohesive Shifted Fracture Approach

Shifted interface conditions

$$(\nabla\boldsymbol{\phi},\boldsymbol{\sigma}(\boldsymbol{\varepsilon}))_{\Omega\setminus\tilde{\Gamma}_c} + \langle[\![\boldsymbol{\phi}]\!],\{\!\{\boldsymbol{\sigma}(\boldsymbol{\varepsilon})\}\!\}_\lambda\tilde{\boldsymbol{n}}\rangle_{\tilde{\Gamma}_c} + \langle\{\!\{\boldsymbol{\phi}\}\!\}_{1-\lambda},[\![\boldsymbol{\sigma}(\boldsymbol{\varepsilon})]\!]\tilde{\boldsymbol{n}}\rangle_{\tilde{\Gamma}_c} = (\boldsymbol{\phi},\boldsymbol{b})_{\Omega\setminus\tilde{\Gamma}_c} + \langle\boldsymbol{\phi},\boldsymbol{t}_N\rangle_{\Gamma_N}$$

$$\begin{aligned}\{\!\{\boldsymbol{\sigma}(\boldsymbol{\varepsilon})\}\!\}_\lambda\tilde{\boldsymbol{n}} &= \{\!\{\boldsymbol{\sigma}(\boldsymbol{\varepsilon})\}\!\}_\lambda((\tilde{\boldsymbol{n}}\cdot\boldsymbol{n})\boldsymbol{n}+(\tilde{\boldsymbol{n}}\cdot\boldsymbol{\tau})\boldsymbol{\tau})\\ &= (\tilde{\boldsymbol{n}}(\tilde{\boldsymbol{x}})\cdot\bar{\boldsymbol{n}}(\tilde{\boldsymbol{x}}))\,\{\!\{\boldsymbol{\sigma}(\boldsymbol{\varepsilon}(\tilde{\boldsymbol{x}}))\}\!\}_\lambda\,\bar{\boldsymbol{n}}(\tilde{\boldsymbol{x}}) + (\tilde{\boldsymbol{n}}(\tilde{\boldsymbol{x}})\cdot\bar{\boldsymbol{\tau}}(\tilde{\boldsymbol{x}}))\,\{\!\{\boldsymbol{\sigma}(\boldsymbol{\varepsilon}(\tilde{\boldsymbol{x}}))\}\!\}_\lambda\,\bar{\boldsymbol{\tau}}(\tilde{\boldsymbol{x}})\end{aligned}$$

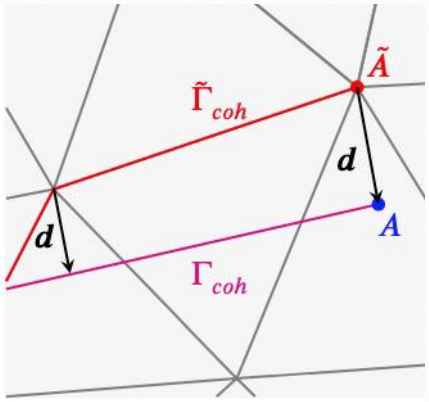

$$\begin{aligned}\{\!\{\boldsymbol{\sigma}(\boldsymbol{\varepsilon}(\tilde{\boldsymbol{x}}))\}\!\}_\lambda\,\bar{\boldsymbol{n}}(\tilde{\boldsymbol{x}}) &= \{\!\{\boldsymbol{\sigma}\,\bar{\boldsymbol{n}}\}\!\}_\lambda = \{\!\{(\bar{\boldsymbol{\sigma}}-\nabla\boldsymbol{\sigma}\,\boldsymbol{d})\,\bar{\boldsymbol{n}}\}\!\}_\lambda\\ &= \{\!\{\bar{\boldsymbol{t}}-(\nabla\boldsymbol{\sigma}\,\boldsymbol{d})\,\bar{\boldsymbol{n}}\}\!\}_\lambda = \bar{\boldsymbol{t}} - \{\!\{(\nabla\boldsymbol{\sigma}\,\boldsymbol{d})\}\!\}_\lambda\,\bar{\boldsymbol{n}},\end{aligned}$$

$$\bar{\boldsymbol{t}} = \boldsymbol{t}_{coh}(\boldsymbol{w}(\bar{\boldsymbol{u}})) \approx \boldsymbol{t}_{coh}(\boldsymbol{w}(\boldsymbol{u}+\nabla\boldsymbol{u}\,\boldsymbol{d})), \quad \text{on } \tilde{\Gamma}_{coh}$$

$$\bar{\boldsymbol{u}} \approx \boldsymbol{u}+\nabla\boldsymbol{u}\,\boldsymbol{d},$$

$$\bar{\boldsymbol{\sigma}} \approx \boldsymbol{\sigma}+\nabla\boldsymbol{\sigma}\,\boldsymbol{d},$$

$$\begin{aligned}\langle[\![\boldsymbol{\phi}]\!],\{\!\{\boldsymbol{\sigma}(\boldsymbol{\varepsilon})\}\!\}_\lambda\tilde{\boldsymbol{n}}\rangle_{\tilde{\Gamma}_c} &= \langle[\![\boldsymbol{\phi}]\!],(\tilde{\boldsymbol{n}}\cdot\bar{\boldsymbol{n}})\,(\bar{\boldsymbol{t}}-\{\!\{(\nabla\boldsymbol{\sigma}(\boldsymbol{\varepsilon})\,\boldsymbol{d})\}\!\}_\lambda\,\bar{\boldsymbol{n}})+(\tilde{\boldsymbol{n}}\cdot\bar{\boldsymbol{\tau}})\,\{\!\{\boldsymbol{\sigma}(\boldsymbol{\varepsilon})\}\!\}_\lambda\,\bar{\boldsymbol{\tau}}\rangle_{\tilde{\Gamma}_c}\\ &= \langle[\![\boldsymbol{\phi}]\!],(\tilde{\boldsymbol{n}}\cdot\bar{\boldsymbol{n}})\,\boldsymbol{t}_{coh}(\boldsymbol{w}(\boldsymbol{u}+\nabla\boldsymbol{u}\,\boldsymbol{d}))\rangle_{\tilde{\Gamma}_{coh}} - \langle[\![\boldsymbol{\phi}]\!],(\tilde{\boldsymbol{n}}\cdot\bar{\boldsymbol{n}})\,(\{\!\{(\nabla\boldsymbol{\sigma}(\boldsymbol{\varepsilon})\,\boldsymbol{d})\}\!\}_\lambda\,\bar{\boldsymbol{n}})-(\tilde{\boldsymbol{n}}\cdot\bar{\boldsymbol{\tau}})\,\{\!\{\boldsymbol{\sigma}(\boldsymbol{\varepsilon})\}\!\}_\lambda\,\bar{\boldsymbol{\tau}}\rangle_{\tilde{\Gamma}_c}\end{aligned}$$

$$\begin{aligned}\langle\{\!\{\boldsymbol{\phi}\}\!\}_{1-\lambda},[\![\boldsymbol{\sigma}(\boldsymbol{\varepsilon})]\!]\tilde{\boldsymbol{n}}\rangle_{\tilde{\Gamma}_c} &= \langle\{\!\{\boldsymbol{\phi}\}\!\}_{1-\lambda},(\tilde{\boldsymbol{n}}\cdot\bar{\boldsymbol{n}})\,[\![\bar{\boldsymbol{\sigma}}(\boldsymbol{\varepsilon})-\nabla\boldsymbol{\sigma}(\boldsymbol{\varepsilon})\boldsymbol{d}]\!]\,\bar{\boldsymbol{n}}+(\tilde{\boldsymbol{n}}\cdot\bar{\boldsymbol{\tau}})\,[\![\boldsymbol{\sigma}(\boldsymbol{\varepsilon})]\!]\,\bar{\boldsymbol{\tau}}\rangle_{\tilde{\Gamma}_c}\\ &= \langle\{\!\{\boldsymbol{\phi}\}\!\}_{1-\lambda},-(\tilde{\boldsymbol{n}}\cdot\bar{\boldsymbol{n}})\,[\![\nabla\boldsymbol{\sigma}(\boldsymbol{\varepsilon})\boldsymbol{d}]\!]\,\bar{\boldsymbol{n}}+(\tilde{\boldsymbol{n}}\cdot\bar{\boldsymbol{\tau}})\,[\![\boldsymbol{\sigma}(\boldsymbol{\varepsilon})]\!]\,\bar{\boldsymbol{\tau}}\rangle_{\tilde{\Gamma}_c}\\ &= \langle\{\!\{\boldsymbol{\phi}\}\!\}_{1-\lambda},[\![\boldsymbol{\sigma}(\boldsymbol{\varepsilon})]\!]\tilde{\boldsymbol{n}}-(\tilde{\boldsymbol{n}}\cdot\bar{\boldsymbol{n}})\,[\![\boldsymbol{\sigma}(\boldsymbol{\varepsilon})+\nabla\boldsymbol{\sigma}(\boldsymbol{\varepsilon})\boldsymbol{d}]\!]\,\bar{\boldsymbol{n}}\rangle_{\tilde{\Gamma}_c}\ .\end{aligned}$$

$$[\![\bar{\boldsymbol{\sigma}}(\boldsymbol{\varepsilon})]\!]\,\bar{\boldsymbol{n}} = \boldsymbol{0}$$

Duke UNIVERSITY

The Cohesive Shifted Fracture Approach

X-FEM/PU-FEM vs shifted variational formulations

X-FEM/PU-FEM Euler-Lagrange equations:

$$\{\!\{\boldsymbol{\sigma}\}\!\}_\lambda \boldsymbol{n} - \boldsymbol{t}_{coh} = \boldsymbol{0}\,, \qquad \text{on } \Gamma_c$$

$$[\![\boldsymbol{\sigma}]\!]\,\boldsymbol{n} = \boldsymbol{0}\,, \qquad \text{on } \Gamma_c$$

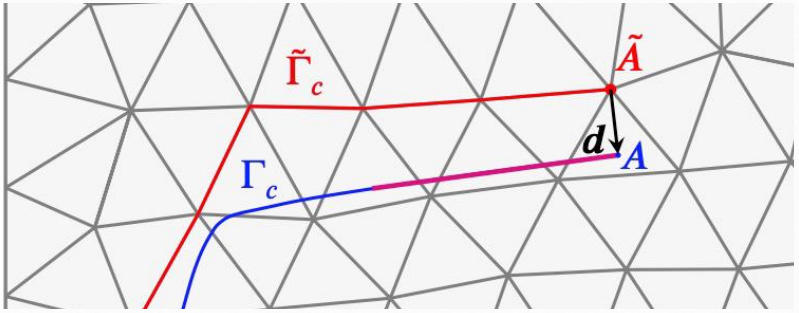

Shifted Fracture Method Euler-Lagrange equations:

$$(\tilde{\boldsymbol{n}} \cdot \boldsymbol{n})\left(\{\!\{\boldsymbol{S}(\boldsymbol{\sigma}(\boldsymbol{\varepsilon}))\}\!\}_\lambda \boldsymbol{n} - \boldsymbol{t}_{coh}(\boldsymbol{w}(\boldsymbol{S}(\boldsymbol{u}))\right) = \boldsymbol{0}\,, \qquad \text{on } \tilde{\Gamma}_c$$

$$(\tilde{\boldsymbol{n}} \cdot \boldsymbol{n})[\![\boldsymbol{S}(\boldsymbol{\sigma}(\boldsymbol{\varepsilon}))]\!]\,\boldsymbol{n} = \boldsymbol{0}\,, \qquad \text{on } \tilde{\Gamma}_c$$

Cohesive traction definition

Traction equilibrium

Fracture area correction (ensures grid independence of fracture energy)

X-FEM/PU-FEM *weak form:*

$$(\nabla\boldsymbol{\phi}, \boldsymbol{\sigma}(\boldsymbol{\varepsilon}))_{\Omega\setminus\Gamma_c} + (\boldsymbol{\psi}, \boldsymbol{\varepsilon} - \nabla^s\boldsymbol{u})_{\Omega\setminus\Gamma_c} + \langle[\![\boldsymbol{\phi}]\!], \boldsymbol{t}_{coh}\rangle_{\Gamma_c} - (\boldsymbol{\phi}, \boldsymbol{b})_{\Omega\setminus\Gamma_c} - \langle\boldsymbol{\phi}, \boldsymbol{t}_N\rangle_{\Gamma_N} = 0$$

Shifted Fracture Method weak form (VMS stabilization terms omitted):

$$\begin{aligned}
&(\nabla\boldsymbol{\phi}, \boldsymbol{\sigma}(\boldsymbol{\varepsilon}))_{\Omega\setminus\tilde{\Gamma}} + (\boldsymbol{\psi}, \boldsymbol{\varepsilon} - \nabla^s\boldsymbol{u})_{\Omega\setminus\tilde{\Gamma}} + \langle[\![\boldsymbol{\phi}]\!], (\tilde{\boldsymbol{n}} \cdot \boldsymbol{n})\,\boldsymbol{t}_{coh}(\boldsymbol{w}(\boldsymbol{u} + \nabla\boldsymbol{u}\,\boldsymbol{d}))\rangle_{\tilde{\Gamma}_c} \\
&+ \langle[\![\boldsymbol{\phi}]\!], \{\!\{\boldsymbol{\sigma}(\boldsymbol{\varepsilon})\}\!\}_\lambda \tilde{\boldsymbol{n}} - \{\!\{\boldsymbol{\sigma}(\boldsymbol{\varepsilon}) + \nabla\boldsymbol{\sigma}(\boldsymbol{\varepsilon})\boldsymbol{d}\}\!\}_\lambda (\tilde{\boldsymbol{n}} \cdot \boldsymbol{n})\boldsymbol{n}\rangle_{\tilde{\Gamma}_c} \\
&+ \langle\{\!\{\boldsymbol{\phi}\}\!\}_{1-\lambda}, [\![\boldsymbol{\sigma}(\boldsymbol{\varepsilon})]\!]\tilde{\boldsymbol{n}} - (\tilde{\boldsymbol{n}} \cdot \boldsymbol{n})\,[\![\boldsymbol{\sigma}(\boldsymbol{\varepsilon}) + \nabla\boldsymbol{\sigma}(\boldsymbol{\varepsilon})\boldsymbol{d}]\!]\,\boldsymbol{n}\rangle_{\tilde{\Gamma}_c} - (\boldsymbol{\phi}, \boldsymbol{b})_{\Omega\setminus\tilde{\Gamma}_c} - \langle\boldsymbol{\phi}, \boldsymbol{t}_N\rangle_{\Gamma_N} = 0
\end{aligned}$$

Duke UNIVERSITY

The Cohesive Shifted Fracture Approach

An efficient implementation

$$\textit{Find } [\boldsymbol{u}, \boldsymbol{\varepsilon}] \in V_{u,h}(\Omega) \times V_{\varepsilon,h}(\tilde{\Omega}_\ell) \textit{ such that, } \forall [\boldsymbol{\phi}, \boldsymbol{\psi}] \in V_{u,h}(\Omega) \times V_{\varepsilon,h}(\tilde{\Omega}_\ell) \,,$$

$$\mathscr{B}_{\text{SFM}}([\boldsymbol{u}, \boldsymbol{\varepsilon}]; [\boldsymbol{\phi}, \boldsymbol{\psi}]) = \mathscr{L}_{\text{SFM}}([\boldsymbol{\phi}, \boldsymbol{\psi}]) \,,$$

$$\mathscr{B}_{\text{SFM}}([\boldsymbol{u}, \boldsymbol{\varepsilon}]; [\boldsymbol{\phi}, \boldsymbol{\psi}]) = (\mathbf{C}\,\nabla^s \boldsymbol{u}, \nabla^s \boldsymbol{\phi})_{\Omega \setminus \tilde{\Omega}_\ell} + \mathscr{B}_{\text{SFM}}^{[\Omega_\ell \setminus \Gamma_c]}([\boldsymbol{u}, \boldsymbol{\varepsilon}]; [\boldsymbol{\phi}, \boldsymbol{\psi}]) \,,$$

$$\mathscr{L}_{\text{SFM}}([\boldsymbol{\phi}, \boldsymbol{\psi}]) = (\boldsymbol{\phi}, \boldsymbol{b})_{\Omega \setminus \tilde{\Omega}_\ell} + \langle \boldsymbol{\phi}, \boldsymbol{t}_N \rangle_{\Gamma_N} + \mathscr{L}_{\text{SFM}}^{[\tilde{\Omega}_\ell \setminus \tilde{\Gamma}_c]}([\boldsymbol{\phi}, \boldsymbol{\psi}]) \,.$$

Idea: The SFM mixed formulation is applied only on a layer of elements near the fracture, and a primal formulation is applied everywhere else

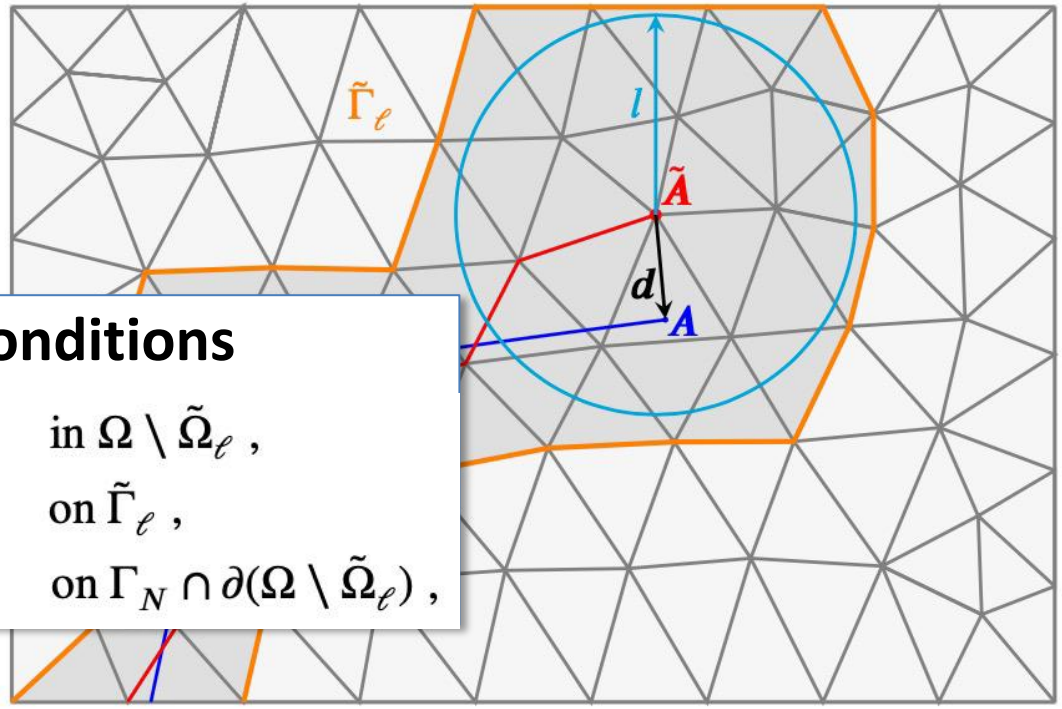

Euler-Lagrange coupling conditions

$$-\nabla \cdot \boldsymbol{\sigma}(\nabla^s \boldsymbol{u}) = \boldsymbol{b} \,, \qquad \text{in } \Omega \setminus \tilde{\Omega}_\ell \,,$$

$$\boldsymbol{\sigma}(\nabla^s \boldsymbol{u}^+)\,\boldsymbol{n}^+ + \boldsymbol{\sigma}(\boldsymbol{\varepsilon})^-\,\boldsymbol{n}^- = \mathbf{0} \,, \qquad \text{on } \tilde{\Gamma}_\ell \,,$$

$$(\mathbf{C}\,\nabla^s \boldsymbol{u})\,\boldsymbol{n} = \boldsymbol{t}_N \,, \qquad \text{on } \Gamma_N \cap \partial(\Omega \setminus \tilde{\Omega}_\ell) \,,$$

Duke UNIVERSITY

Numerical Examples

Three-point bending test: true and surrogate crack paths

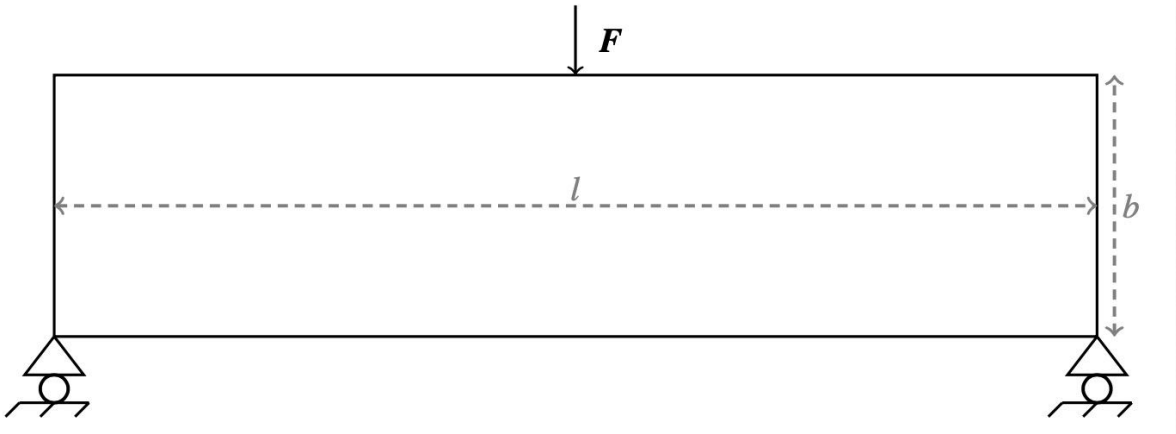

Note: The true crack path is directly estimated using the maximum principal stress criterion (i.e., it is not given *a priori*)

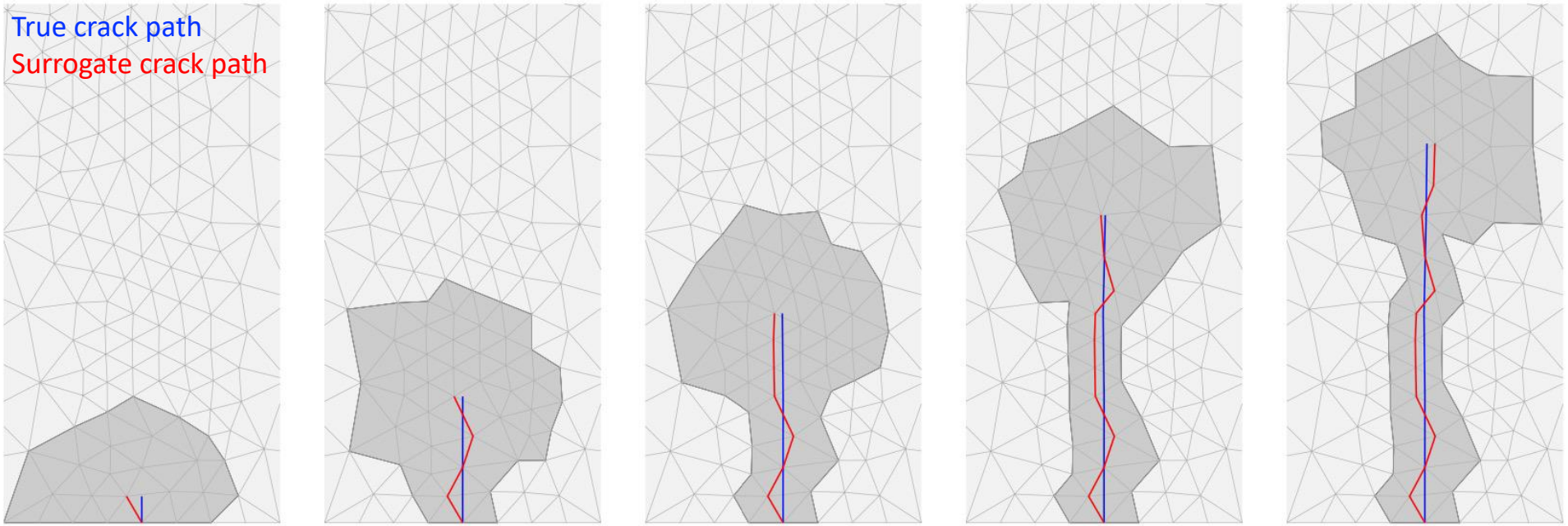

Numerical Examples

Three-point bending test: Mixed vs. efficient implementations

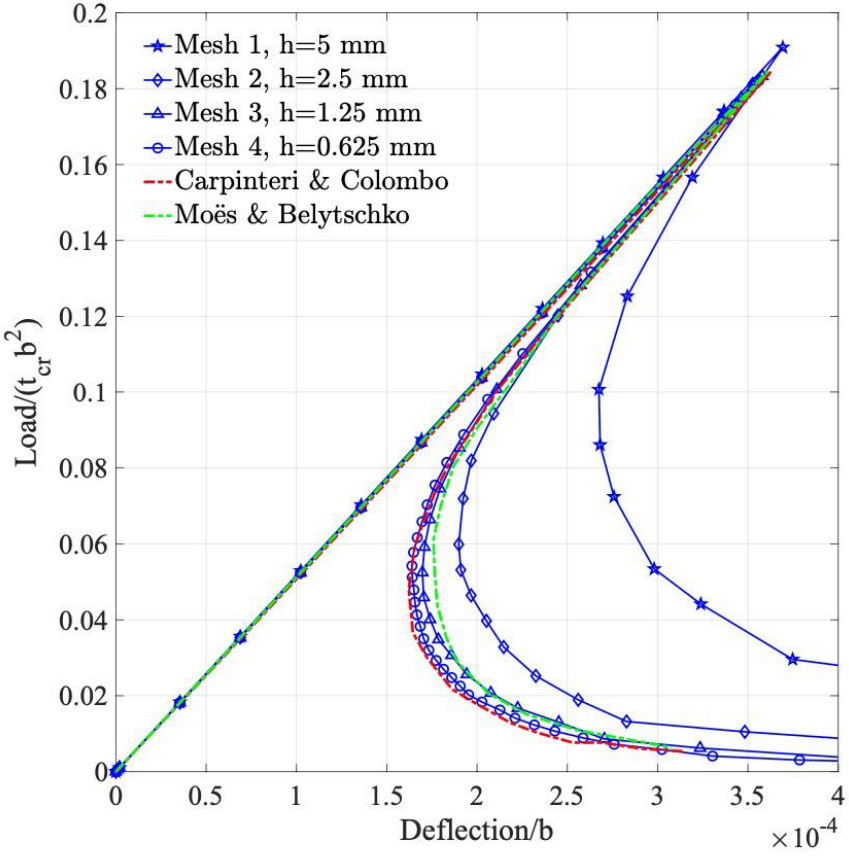

Meshes	Number of elements	Number of nodes	Average element size around crack path
Mesh 1	1,565	851	5 mm
Mesh 2	3,477	1,828	2.5 mm
Mesh 3	10,513	5,385	1.25 mm
Mesh 4	19,318	9,774	0.625 mm

Numerical Examples

Three-point bending test: SFM vs. node-release technique

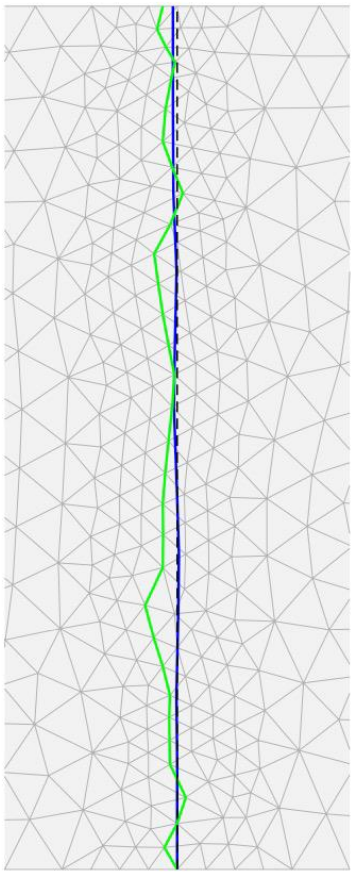

Mesh 1

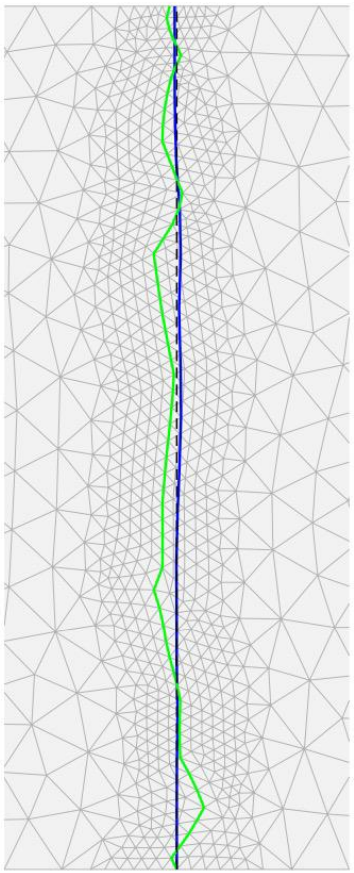

Mesh 2

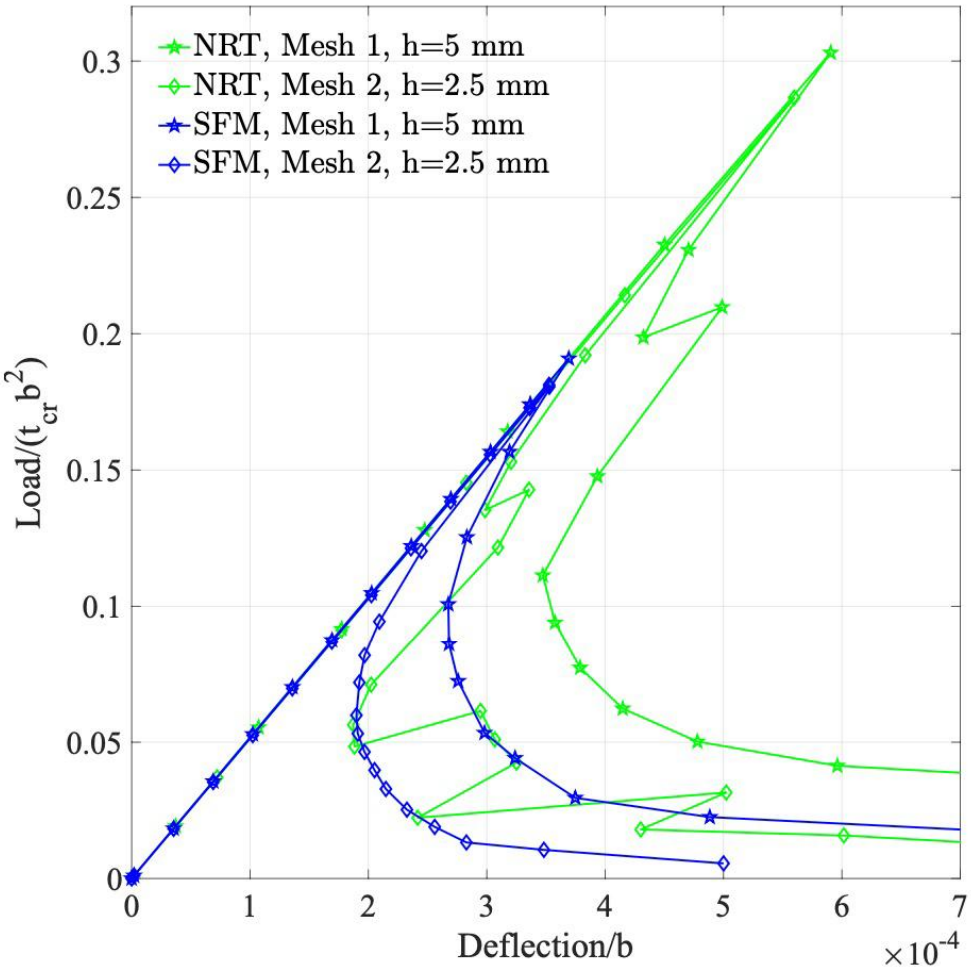

Duke UNIVERSITY

Numerical Examples

Three-point bending test: SFM vs. node-release technique

$$e_p = \int_{\Gamma_p} |x_e - x_p| \, |\boldsymbol{n}_p \cdot \boldsymbol{n}_e| \, \mathrm{d}\Gamma_p$$

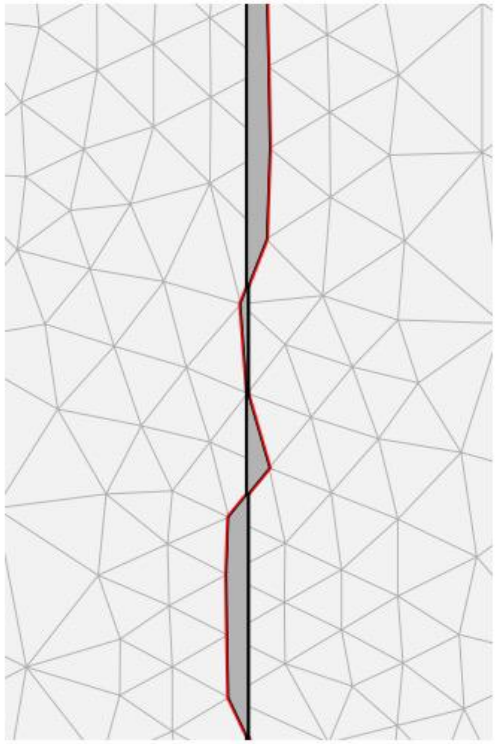

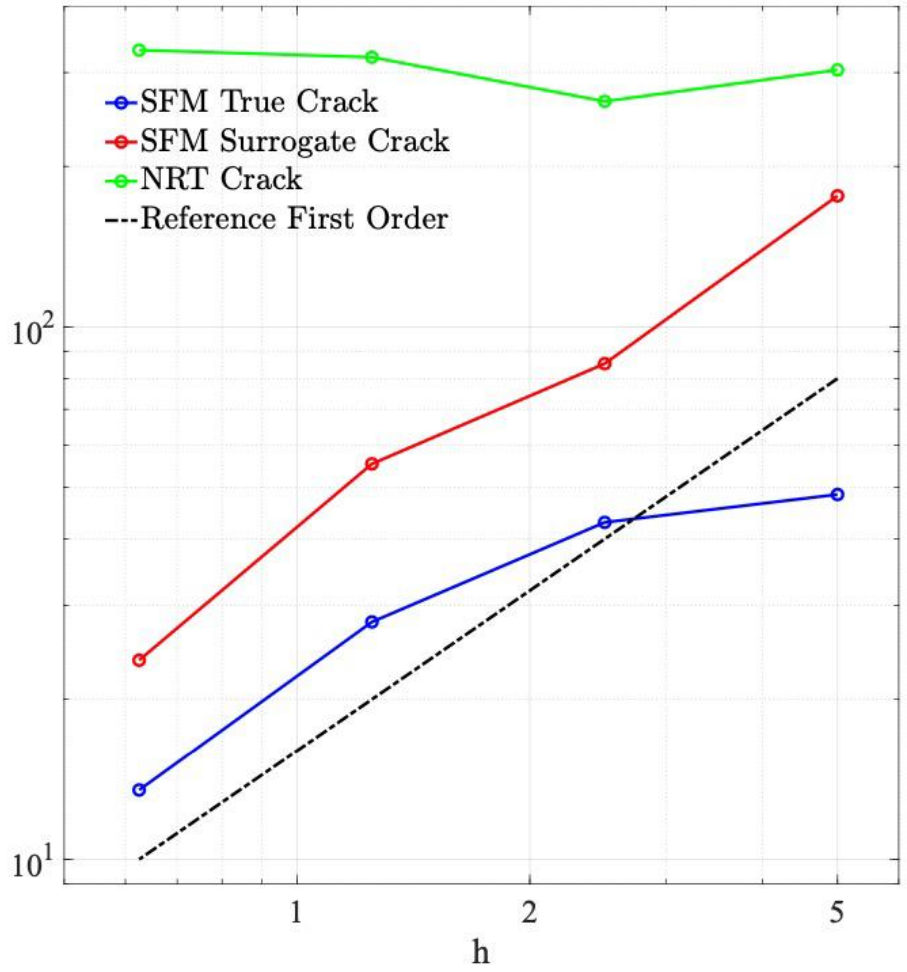

Numerical Examples

Three-point bending test: SFM vs. node-release technique

$$e_{\mathscr{W}} = |\mathscr{W}_{ed} - \mathscr{W}_{cd}|$$

$$\mathscr{W}_{ed} = \int_0^{u_f^*} \boldsymbol{f} \cdot d\boldsymbol{u} - \frac{1}{2}\boldsymbol{u}_f^* \cdot \boldsymbol{f}^* \rightarrow \int_0^{u_f} \boldsymbol{f} \cdot d\boldsymbol{u}$$

$$\mathscr{W}_{cd} = \int_{\Gamma_c} \left(\int_0^{w^*} t\, dw - \frac{1}{2} t^* w^* \right) d\Gamma_c \rightarrow \int_{\tilde{\Gamma}_c} G_F \, |\tilde{\boldsymbol{n}} \cdot \boldsymbol{n}| \, d\tilde{\Gamma}_c$$

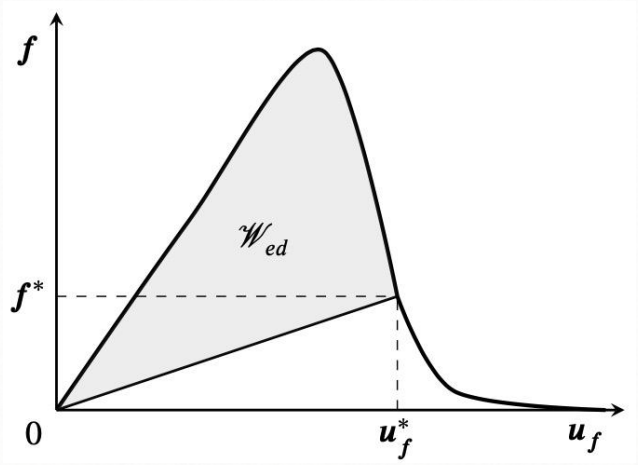

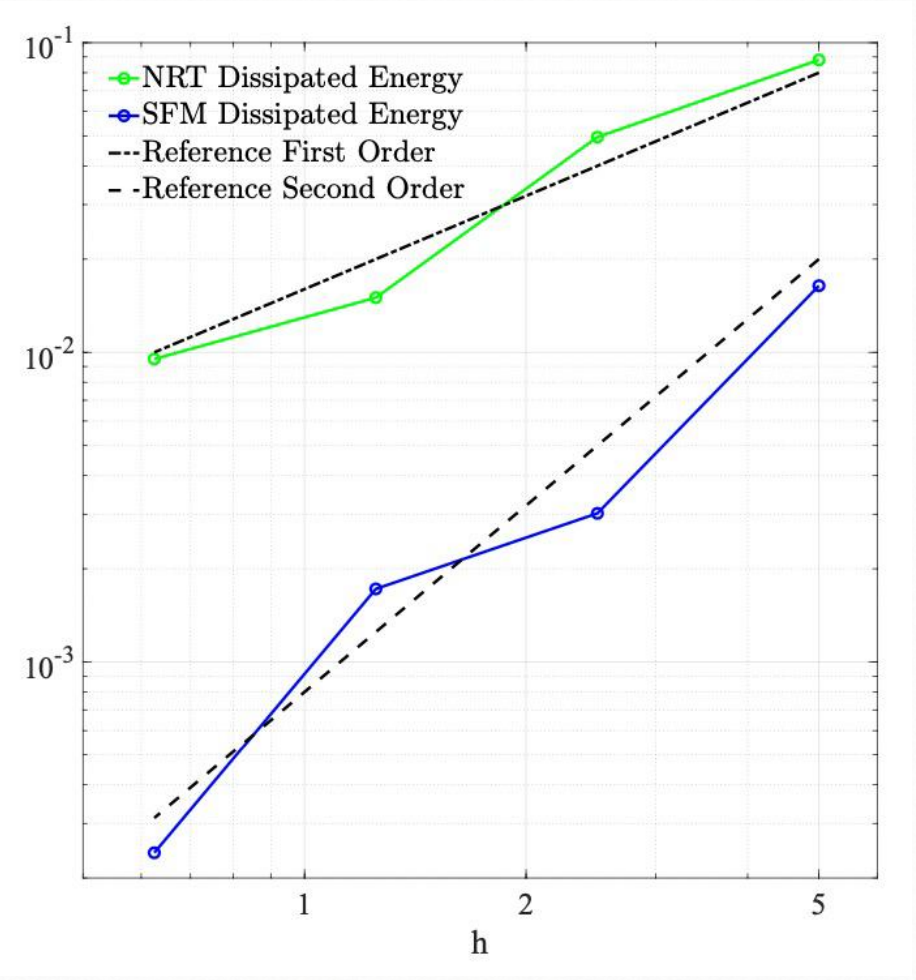

Duke UNIVERSITY

Numerical Examples

Three-point bending test for fracture toughness = 50 & 200 (ductile)

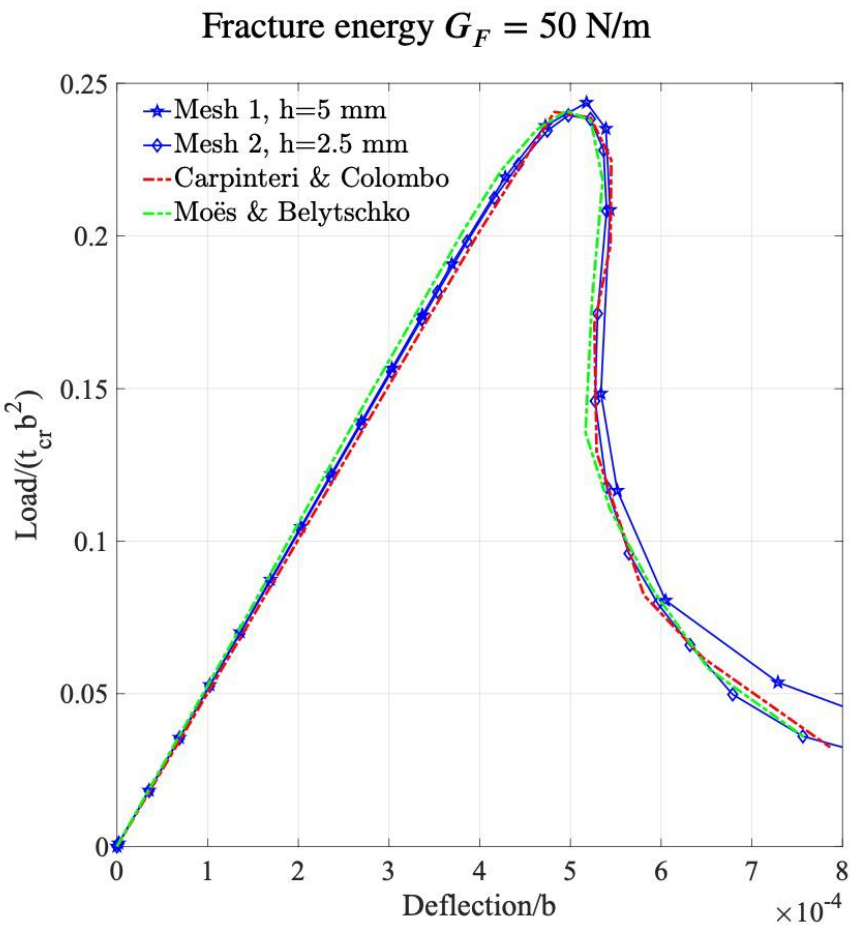

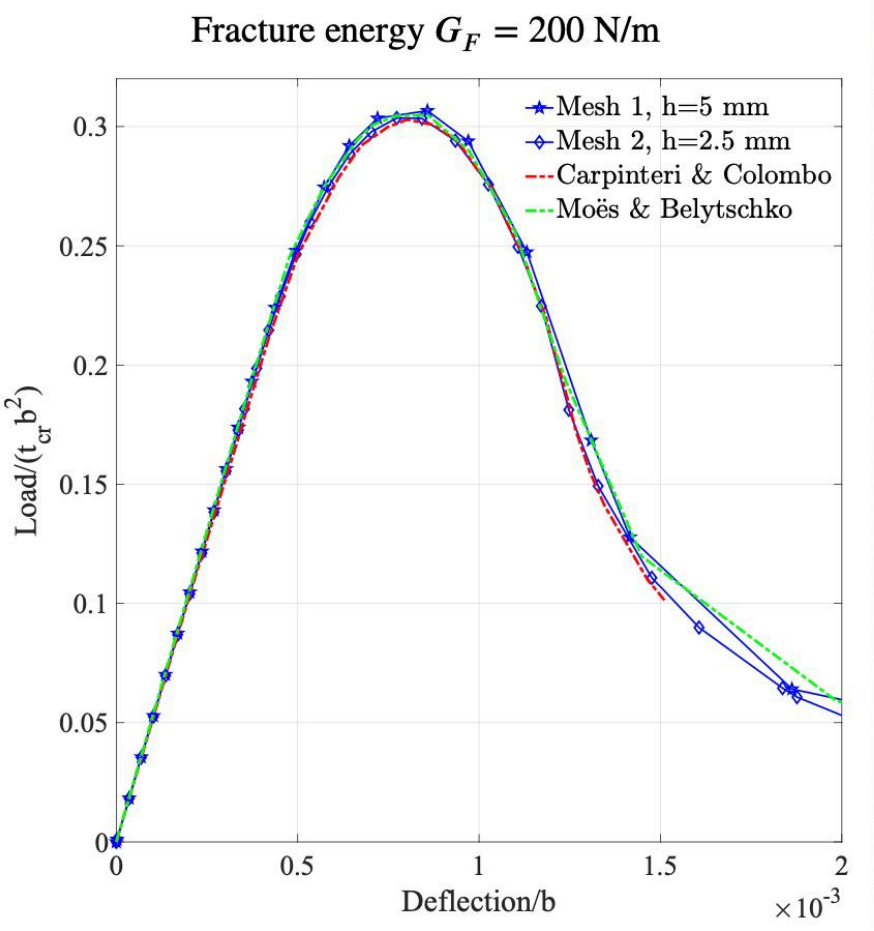

Duke UNIVERSITY

Numerical Examples

L-shaped panel:

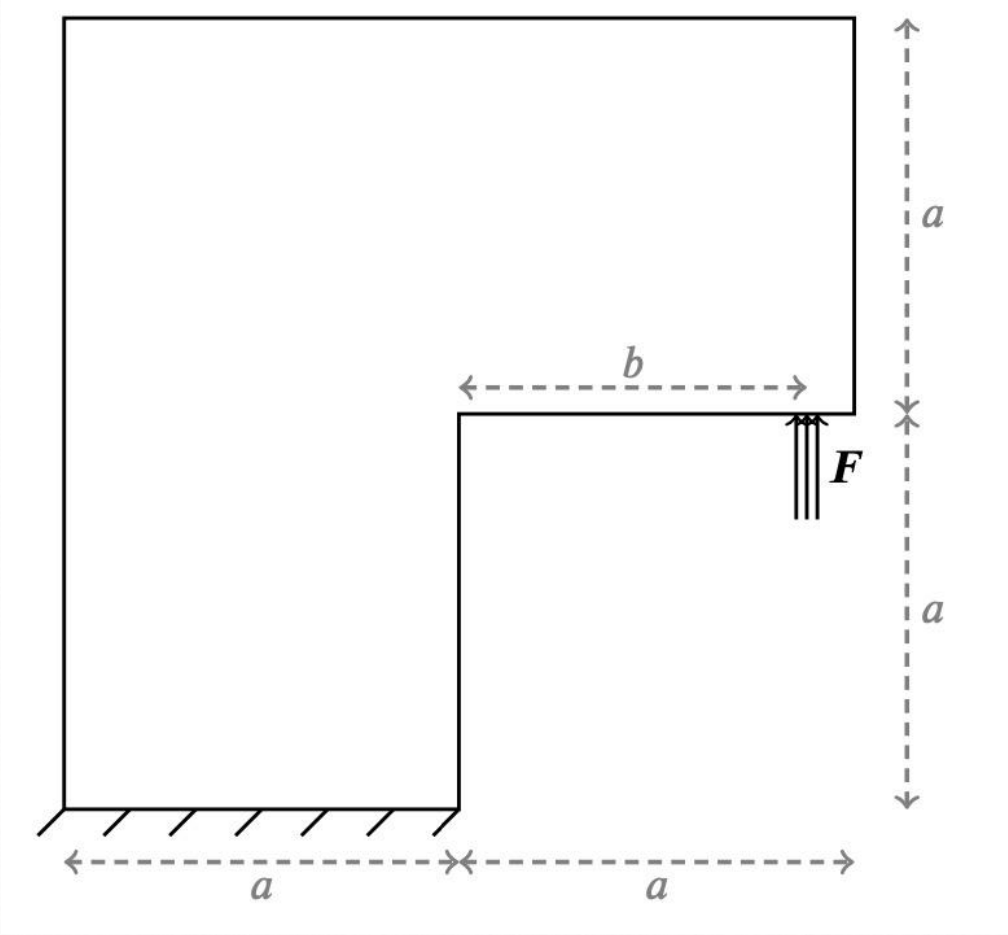

Duke UNIVERSITY

Numerical Examples

L-shaped panel:

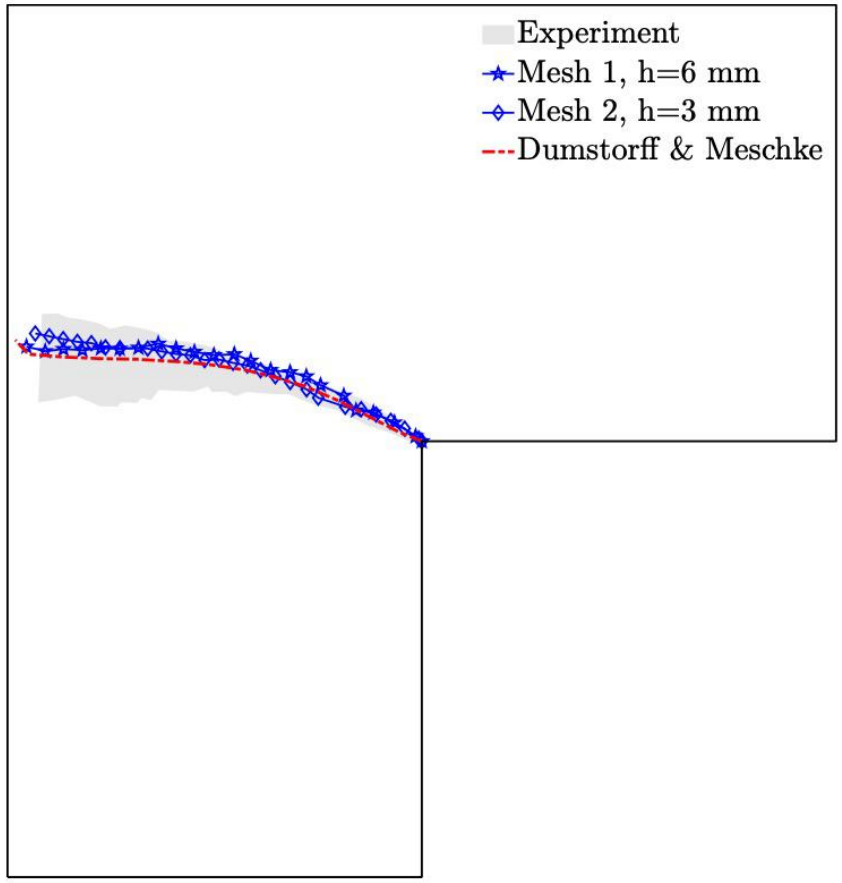

(a) SFM true crack path for the L-shape panel test with SIF.

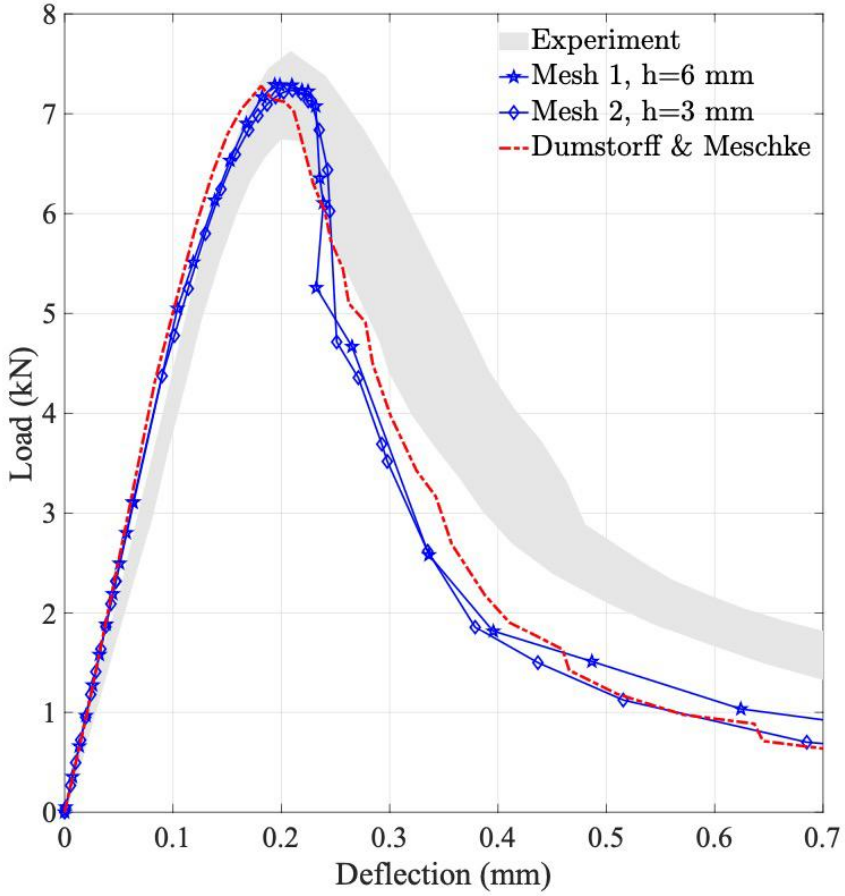

(b) Load-deflection curve for the L-shape panel test with SIF.

Duke UNIVERSITY

Numerical Examples

L-shaped panel:

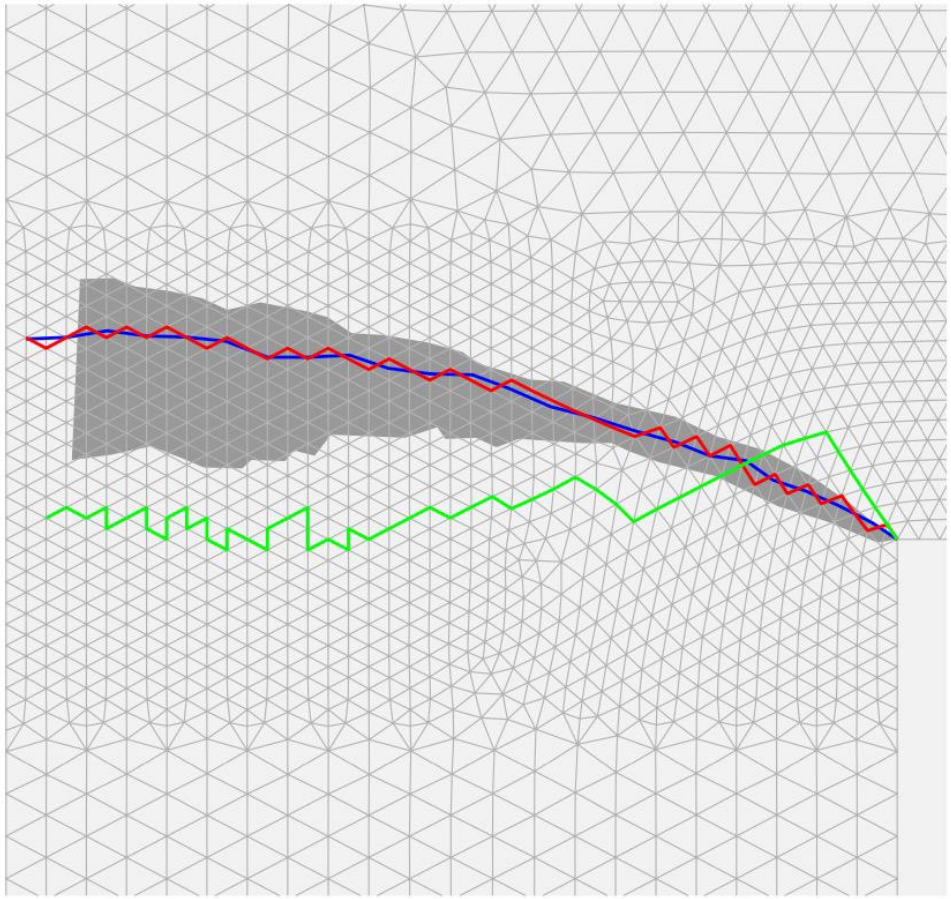

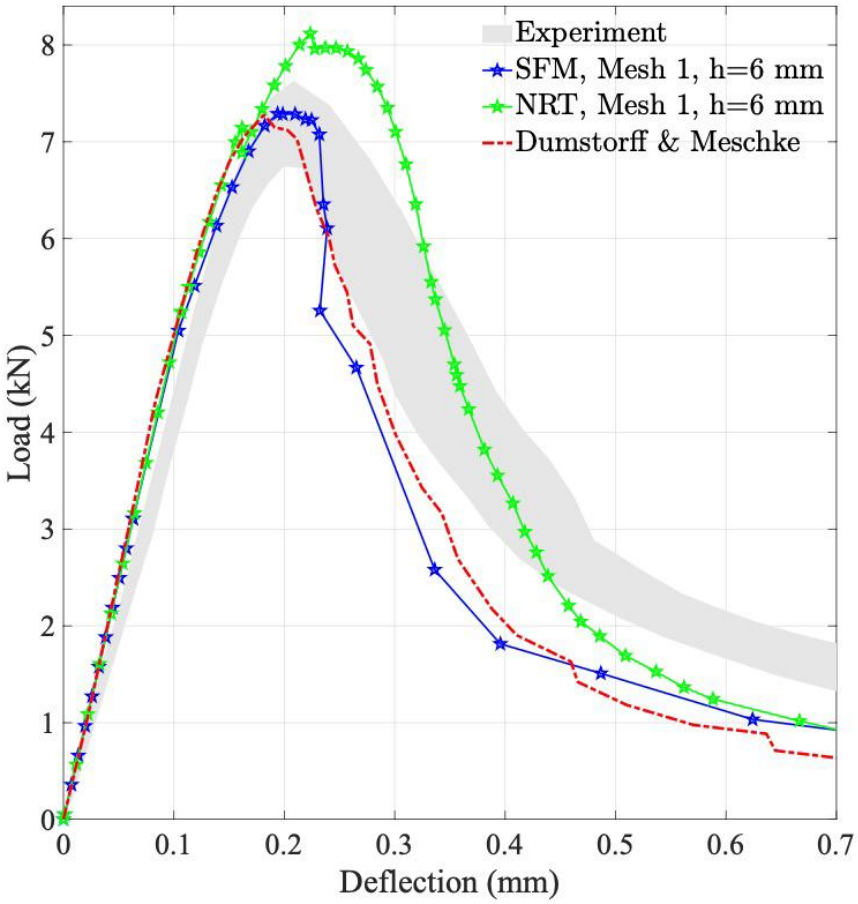

Duke UNIVERSITY

Numerical Examples

Four-point bending test:

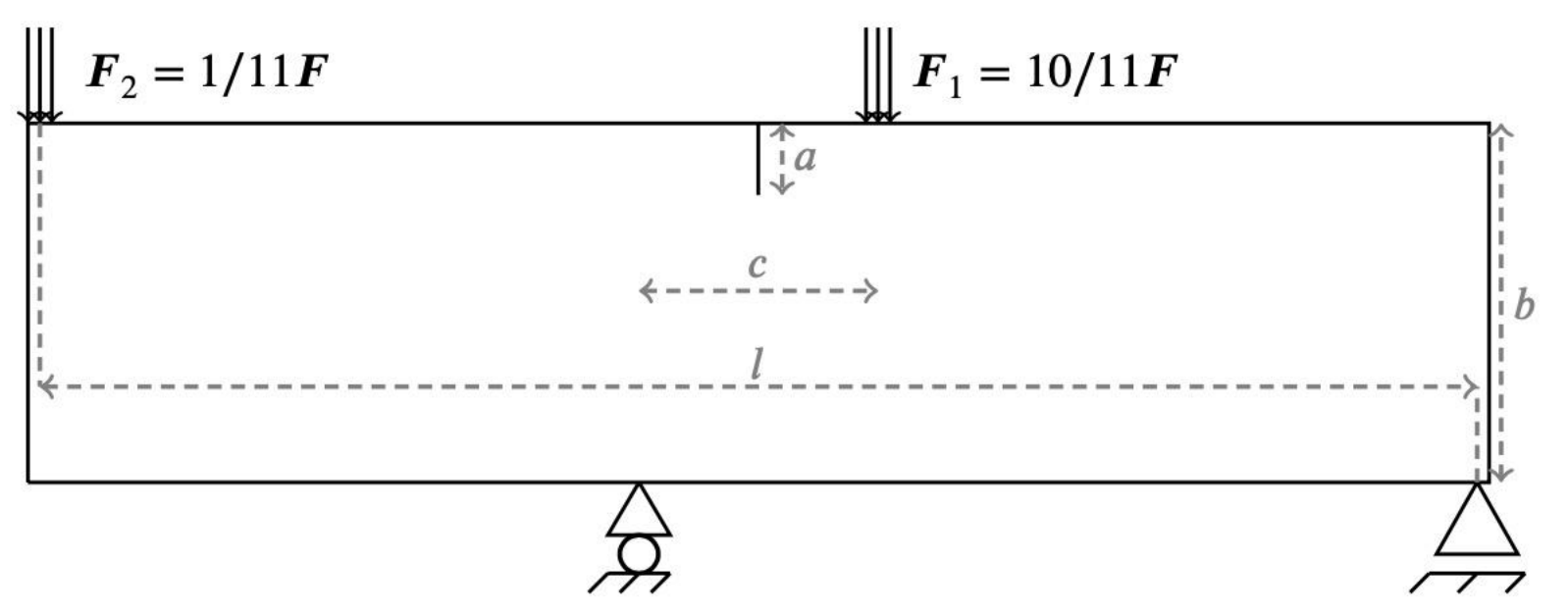

Duke UNIVERSITY

Numerical Examples

Four-point bending test:

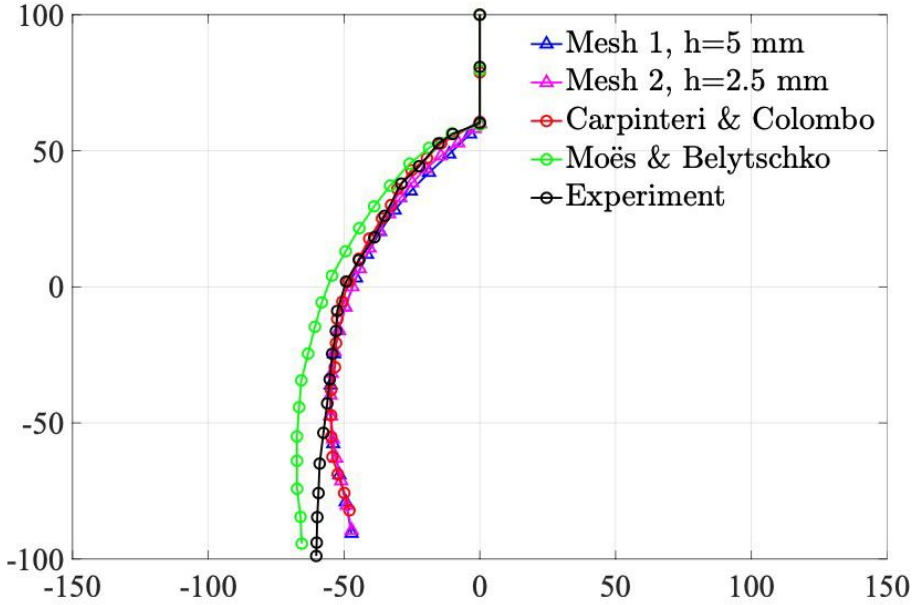

(a) SFM true crack path computed with the maximal tensile principal stress criterion.

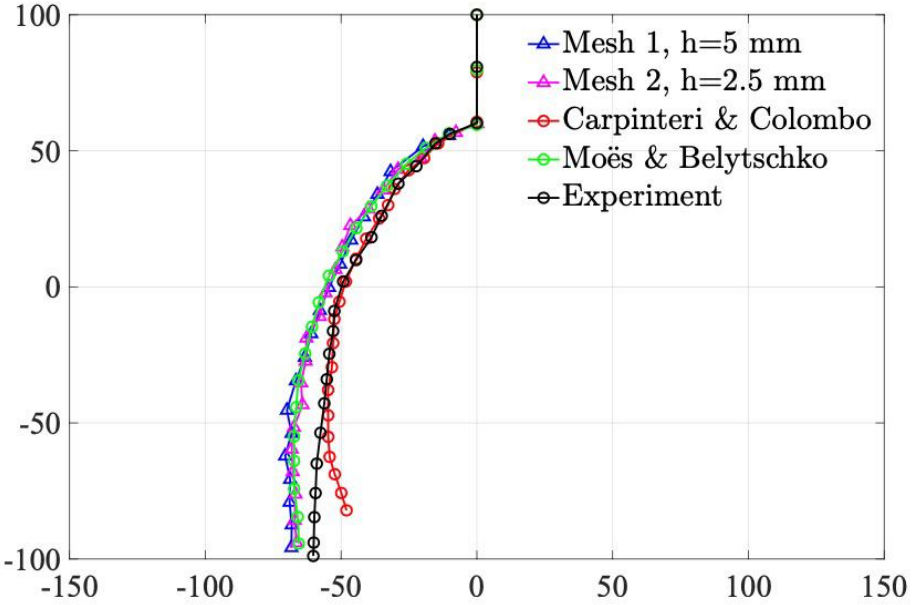

(b) SFM true crack path computed with the stress intensity factor criterion.

Duke UNIVERSITY

Numerical Examples

Four-point bending test:

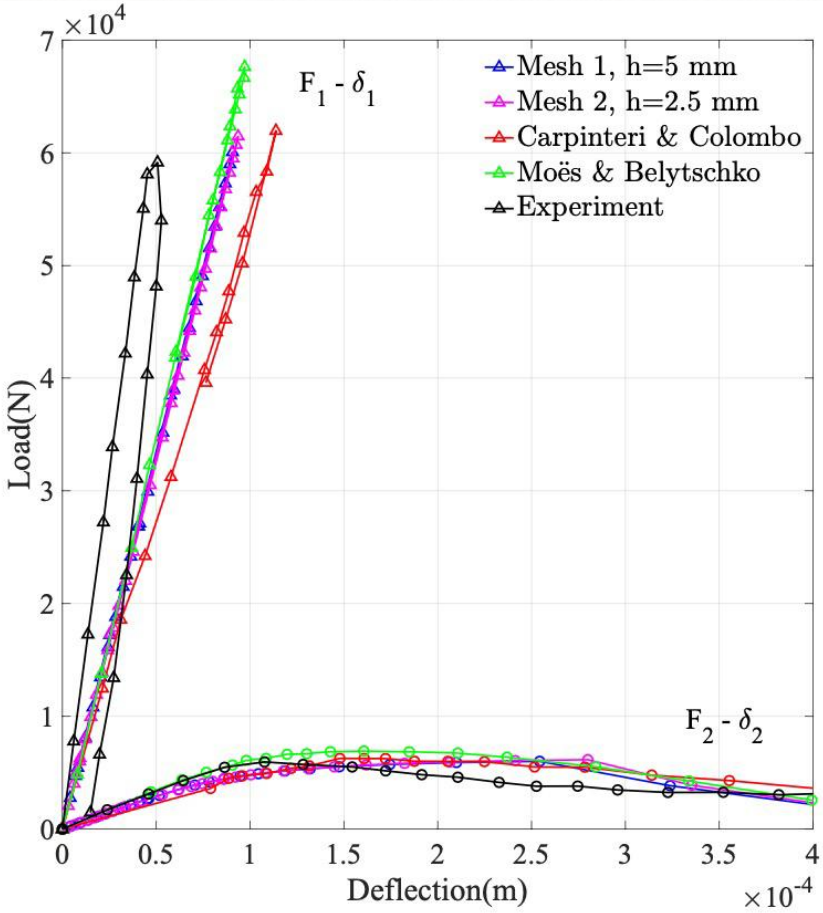

(c) Load-deflection curves for the loads F_1 and F_2 (maximal tensile principal stress criterion).

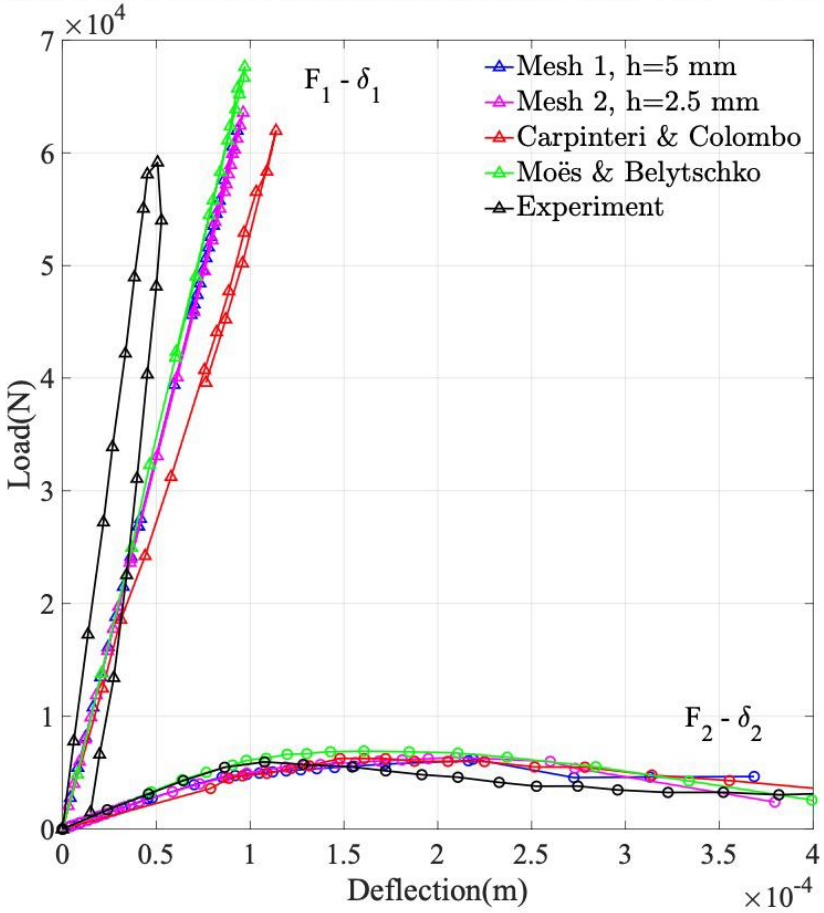

(d) Load-deflection curves for the loads F_1 and F_2 (SIF criterion).

Duke UNIVERSITY

Numerical Examples

Four-point bending test: SFM vs. node-release technique

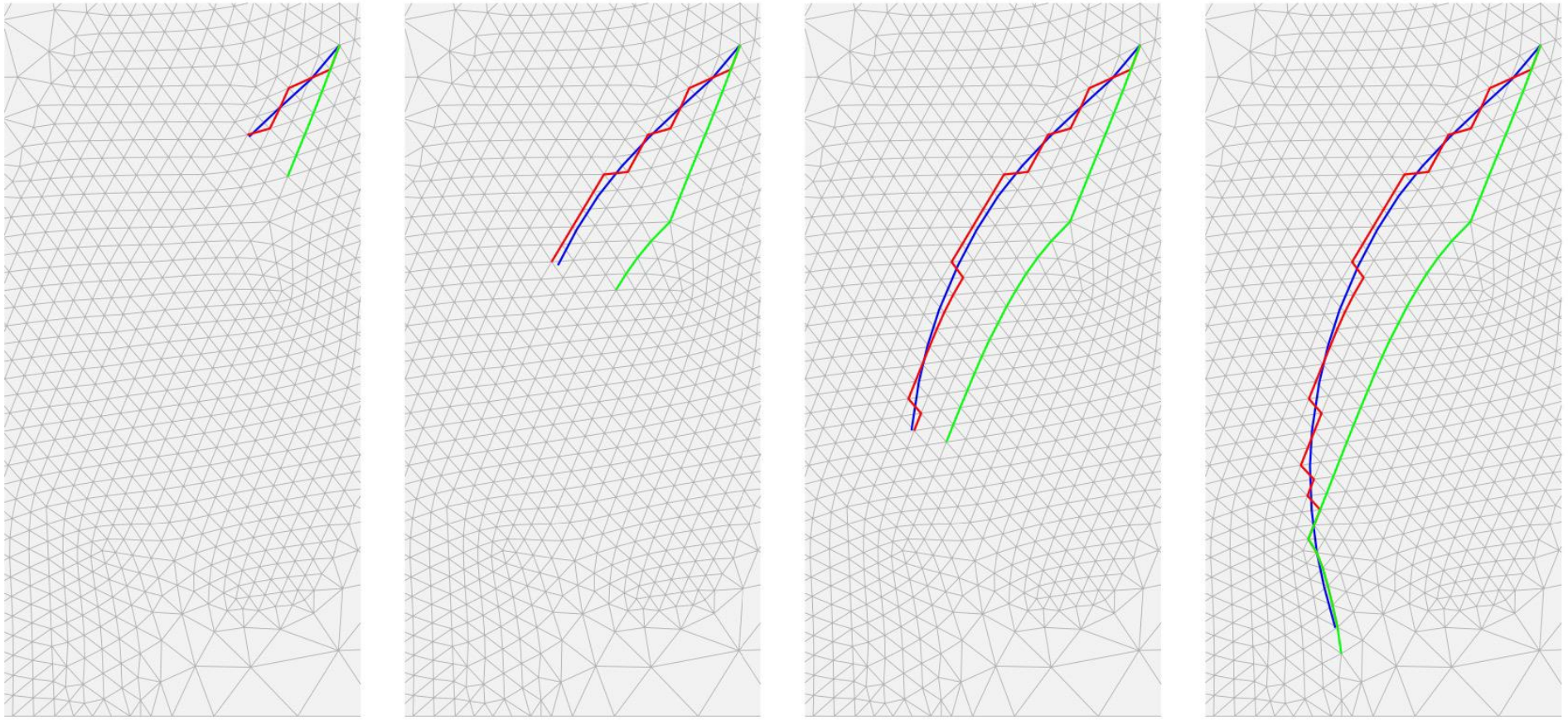

Numerical Examples

Three-dimensional pull-out test

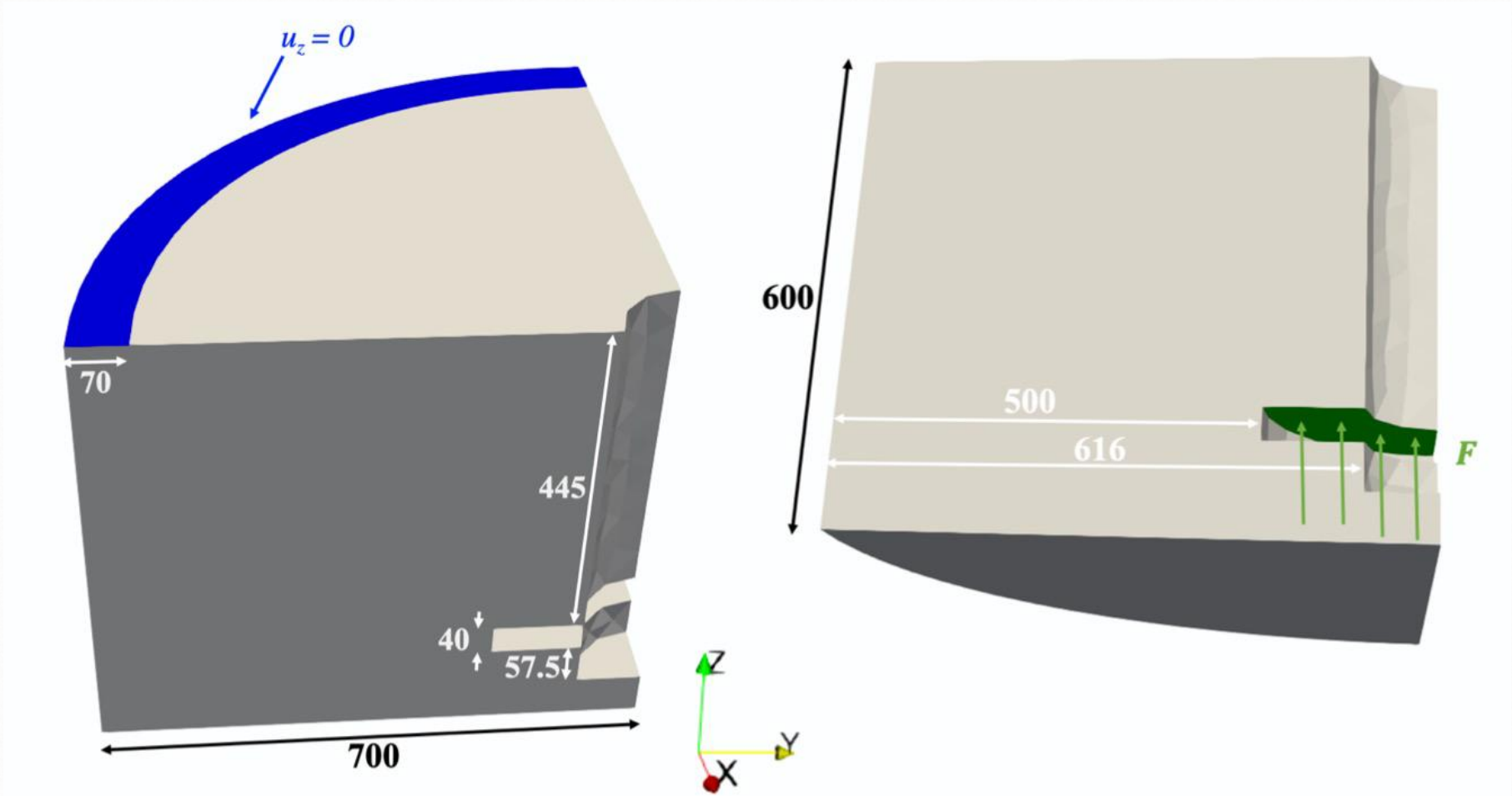

Duke UNIVERSITY

Numerical Examples

Three-dimensional pull-out test

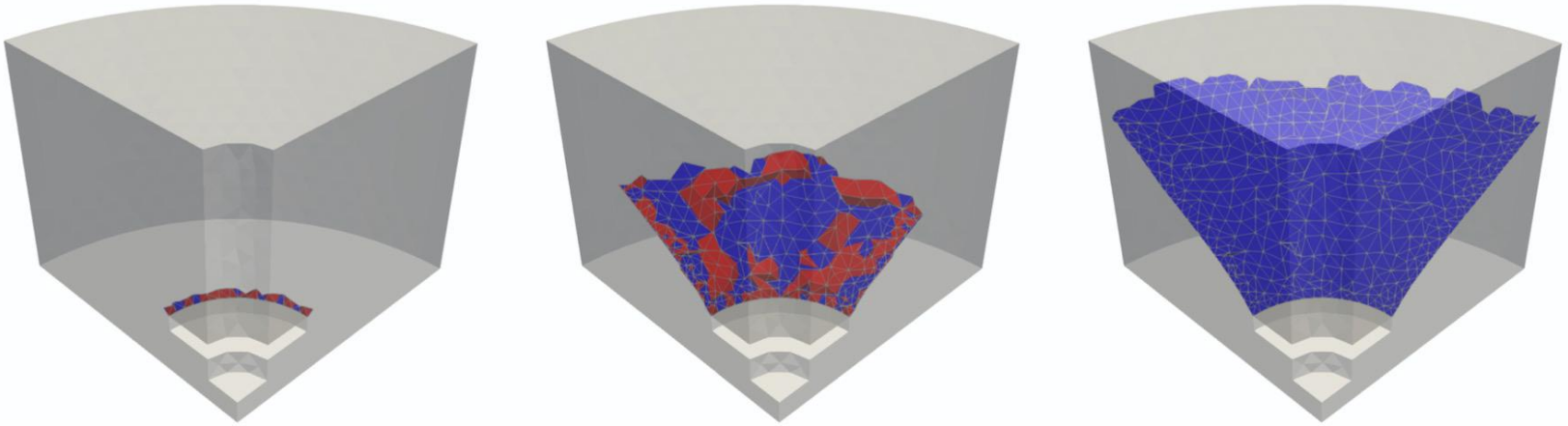

Note: The surrogate and estimate of the true fractures are always continuous

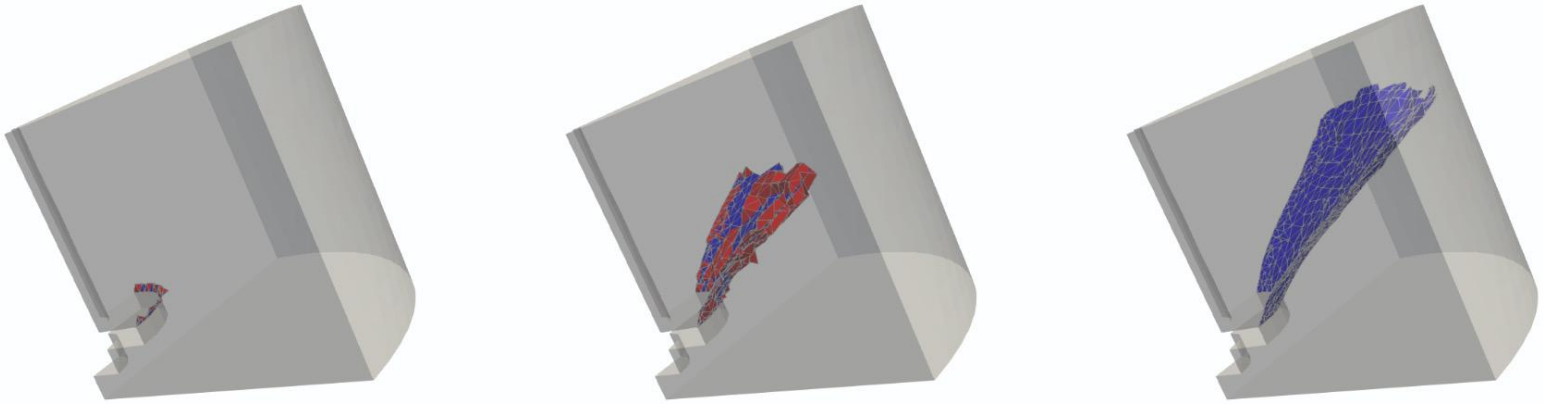

Duke UNIVERSITY

Numerical Examples

Three-dimensional pull-out test

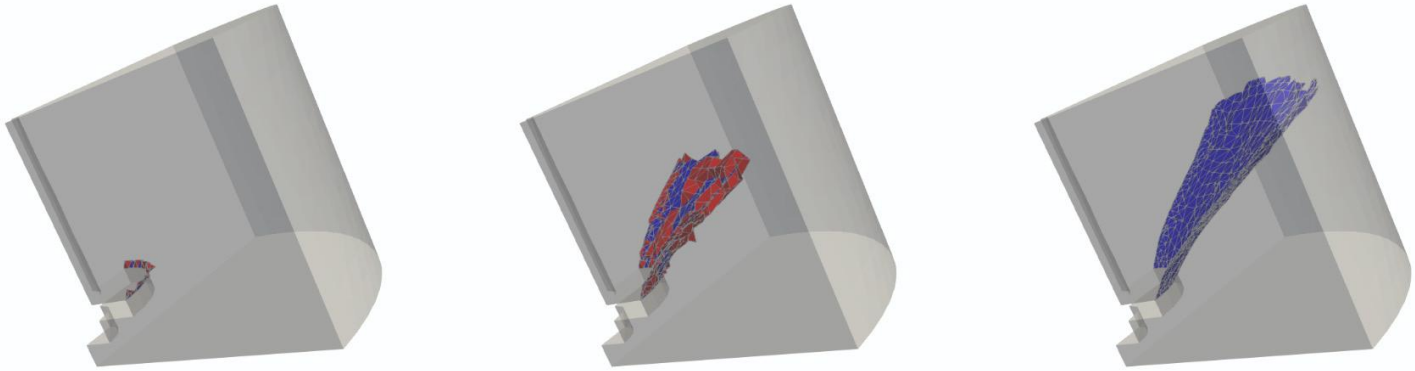

Note: The surrogate and estimate of the true fractures are always continuous

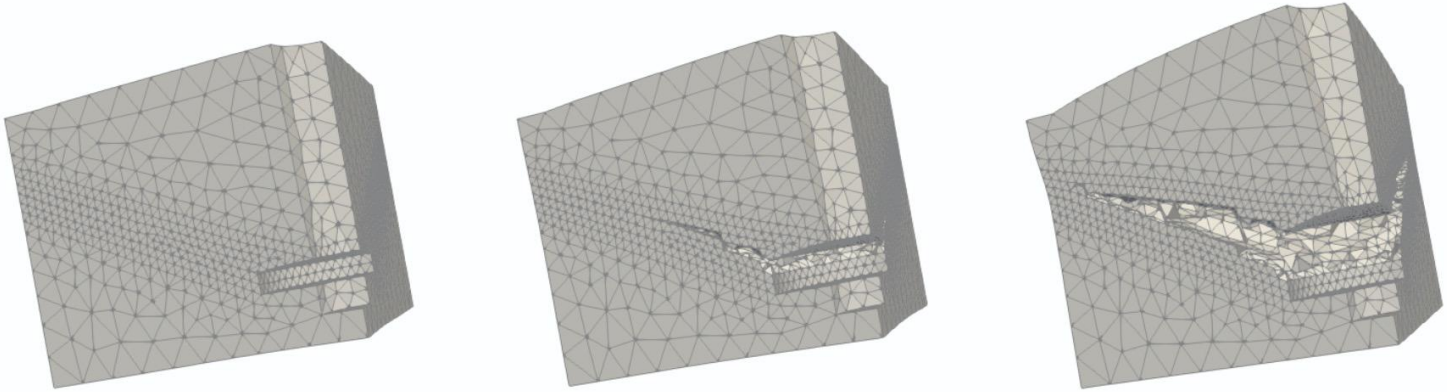

Numerical Examples

Three-dimensional pull-out test

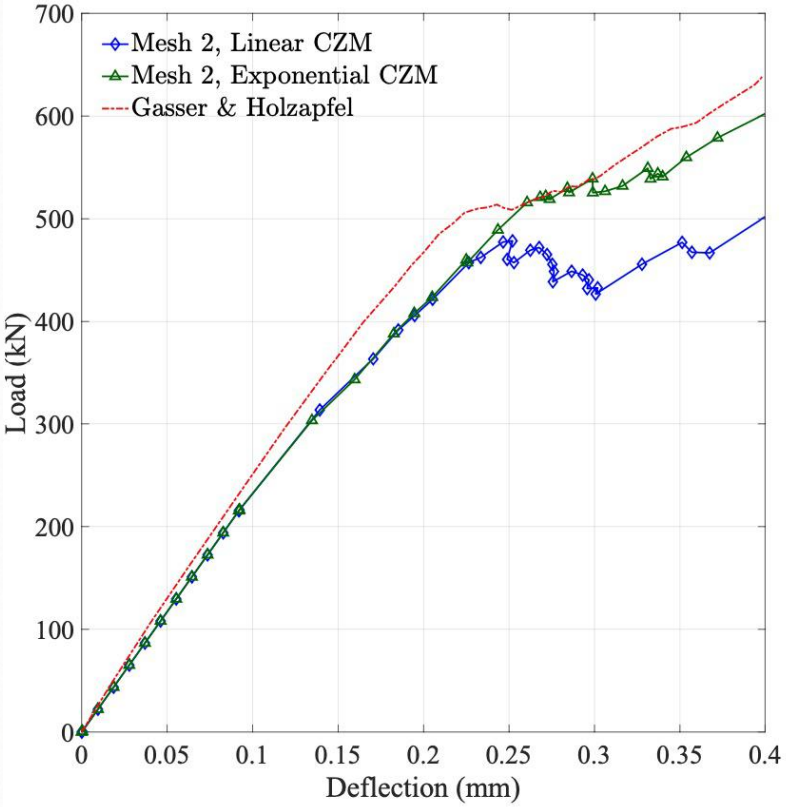

(a) Linear and exponential cohesive zone model.

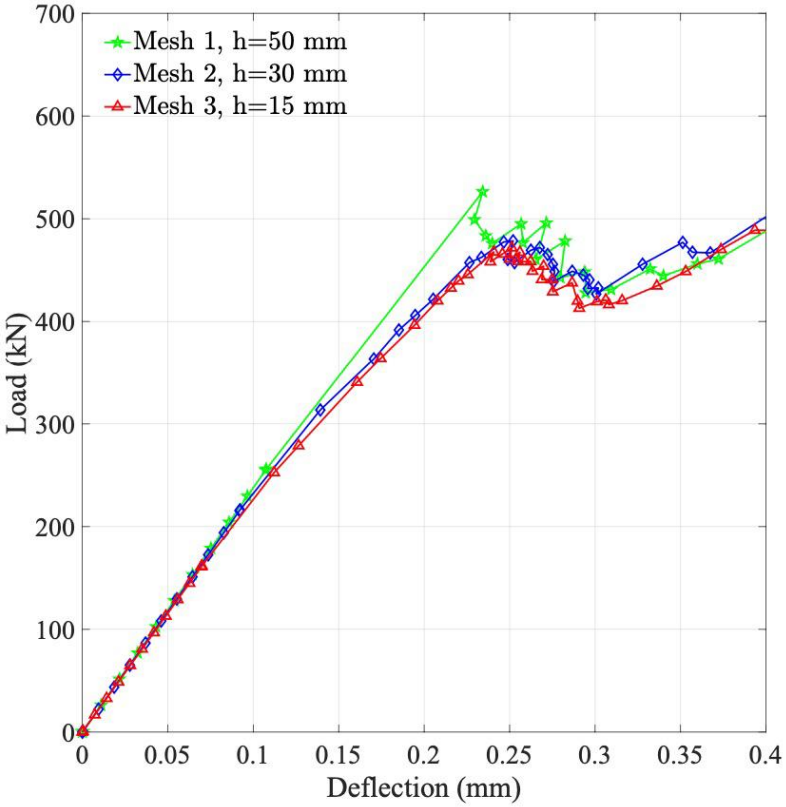

(b) SFM: Linear cohesive zone model.

Meshes	Number of elements	Number of nodes	Average element size around crack path
Mesh 1	10,690	2,176	50 mm
Mesh 2	13,122	2,745	30 mm
Mesh 3	23,443	4,791	15 mm

The Shifted Boundary Method

Theoretical developments for the following equations:

- Poisson (with Alex Main, Nabil Atallah & Claudio Canuto)
- Darcy (with Nabil Atallah & Claudio Canuto)
- Stokes (with Nabil Atallah & Claudio Canuto)
- Advection-diffusion (with Alex Main)
- Linear Elasticity (wih Nabil Atallah)

Computational developments for the following equations:

- Thermo-mechanics (with Kangan Li)
- Navier-Stokes (with Alex Main)
- Free-surface flow (not discussed here, with Alex Main, Léo Nouveau and Oriol Colomés)
- Acoustics and shallow water equations (not discussed here, with Ting Song and Alex Main)
- Fracture mechanics (with Kangan Li, Nabil Atallah, and Antonio Rodriguez-Ferran)

Under development, ongoing work:

- Nonlinear mechanics (with Nabil Atallah, Vladimir Tomov & Bojan Lazarov)
- Shock hydrodynamics (with Nabil Atallah, Vladimir Tomov & Bojan Lazarov)
- Higher-order SBM (with Nabil Atallah, Claudio Canuto, Vladimir Tomov & Bojan Lazarov)
- Moving boundaries (with Danjie Xu, Oriol Colomés, Léo Nouveau, & Vladimir Tomov)